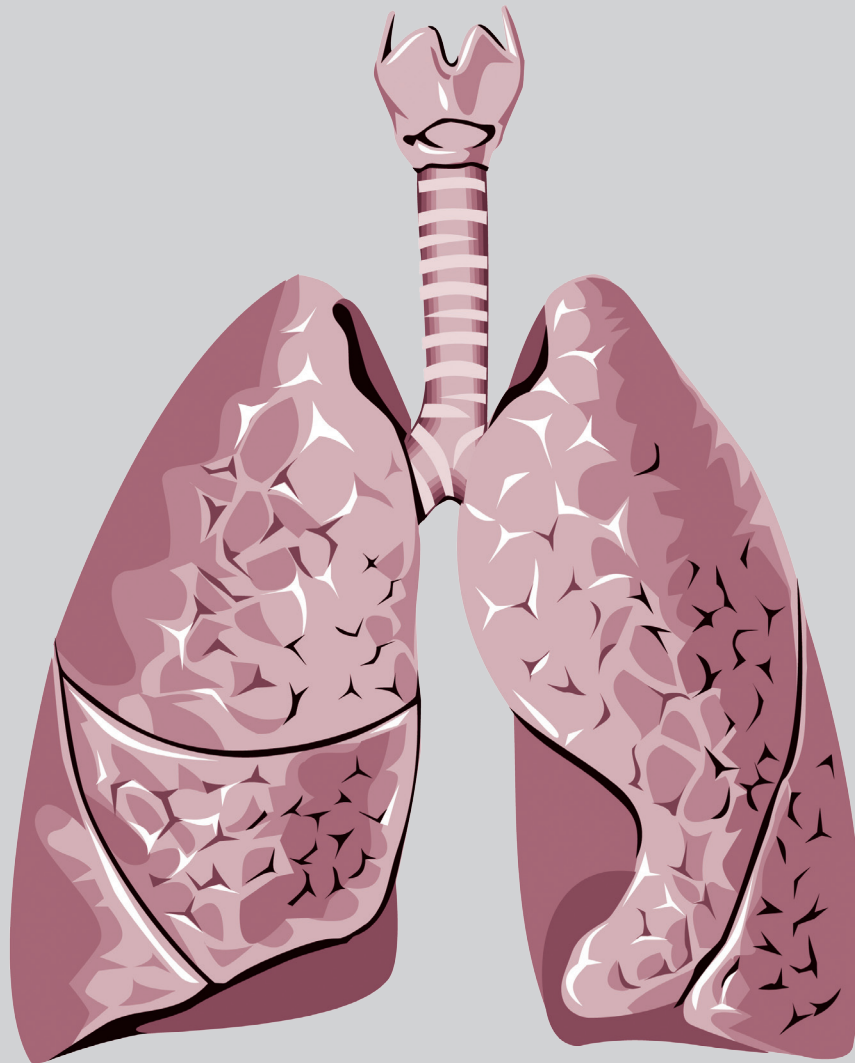


Thoracic Medicine

Volume 37 • Number 2 • June 2022



The Official Journal of



Taiwan Society of
Pulmonary and Critical
Care Medicine



Taiwan Society of Sleep
Medicine



Taiwan Society for
Respiratory Therapy



Taiwan Society of
Tuberculosis and Lung
Diseases

Thoracic Medicine

The Official Journal of
Taiwan Society of Pulmonary and Critical Care Medicine
Taiwan Society for Respiratory Therapy
Taiwan Society of Sleep Medicine
Taiwan Society of Tuberculosis and Lung Diseases

Publisher

Hao-Chien Wang, M.D., Ph.D., President

Taiwan Society of Pulmonary and Critical Care Medicine

Chia-Chen Chu, Ph.D., RRT, FAARC President

Taiwan Society for Respiratory Therapy

Yi-Wen Huang, M.D., President

Taiwan Society of Tuberculosis and Lung Diseases

Hsueh-Yu Li, M.D., President

Taiwan Society of Sleep Medicine

Editor-in-Chief

Kang-Yun Lee, M.D., Ph.D., Professor

Taipei Medical University-Shuang Ho Hospital, Taiwan

Deputy Editors-in-Chief

Shang-Gin Wu, M.D., Ph.D.

National Taiwan University Hospital, Taiwan

Editorial Board

Section of Pulmonary and Critical Care Medicine

Jin-Yuan Shih, M.D., Professor

National Taiwan University Hospital, Taiwan

Gee-Chen Chang, M.D., Professor

Chung Shan Medical University Hospital, Taiwan

Chung-Chi Huang, M.D., Professor

Linkou Chang Gung Memorial Hospital, Taiwan

Kuang-Yao Yang, M.D., Ph.D., Professor

Taipei Veterans General Hospital, Taiwan

Chi-Li Chung, M.D., Ph.D., Associate Professor

Taipei Medical University Hospital, Taiwan

Section of Respiratory Therapy

Hue-Ling Lin, MS, RRT, RN, FAARC, Associate Professor

Chang Gung University, Taiwan

I-Chun Chuang, Ph.D., Assistant Professor

Kaohsiung Medical University College of Medicine, Taiwan

Jia-Jhen Lu, Ph.D., Professor

Fu Jen Catholic University, Taiwan

Shih-Hsing Yang, Ph.D., Associate Professor

Fu Jen Catholic University, Taiwan

Chin Jung, Ph.D., Associate Professor

China Medical University, Taiwan

Section of Tuberculosis and Lung Diseases

Jann-Yuan Wang, M.D., Professor

National Taiwan University Hospital, Taiwan

Chen-Yuan Chiang, M.D., Associate Professor

Taipei Municipal Wanfang Hospital, Taiwan

Ming-Chi Yu, M.D., Professor

Taipei Municipal Wanfang Hospital, Taiwan

Yi-Wen Huang, M.D., Professor

Changhua Hospital, Ministry of Health & Welfare, Taiwan

Wei-Juin Su, M.D., Professor

Taipei Veterans General Hospital, Taiwan

Section of Sleep Medicine

Li-Ang Lee, M.D., Associate Professor

Linkou Chang Gung Memorial Hospital, Taiwan

Pei-Lin Lee, M.D., Assistant Professor

National Taiwan University Hospital, Taiwan

Hsin-Chien Lee, M.D., Associate Professor

Taipei Medical University-Shuang-Ho Hospital, Taiwan

Kun-Ta Chou, M.D., Associate Professor

Taipei Veterans General Hospital, Taiwan

Li-Pang Chuang, M.D., Assistant Professor

Linkou Chang Gung Memorial Hospital, Taiwan

International Editorial Board

Charles L. Daley, M.D., Professor

National Jewish Health Center, Colorado, USA

Chi-Chiu Leung, MBBS, FFPH, FCCP, Professor

Stanley Ho Centre for Emerging Infectious Diseases, Hong Kong, China

Daniel D. Rowley, MSc, RRT-ACCS, RRT-NPS, RPFT, FAARC

University of Virginia Medical Center, Charlottesville, Virginia, U.S.A.

Fang Han, M.D., Professor

Peking University People's Hospital Beijing, China

Huiqing Ge, Ph.D., Chief

Sir Run Run Shaw Hospital, School of Medicine, Zhejiang University Hangzhou, China

J. Brady Scott, MSc, RRT-ACCS, AE-C, FAARC, FCCP, Associate Professor

Rush University, Chicago, Illinois, USA

Kazuhiro Ito, Ph.D., DVM, Honorary Professor

Imperial College London, UK

Kazuo Chin (HWA BOO JIN), M.D., Professor

Graduate School of Medicine, Kyoto University

Masaki Nakane, M.D., Ph.D., Professor

Yamagata University Hospital, Japan

Naricha Chirakalwasan, M.D., FAASM, FAPSR, Associate Professor

Faculty of Medicine, Chulalongkorn University, Thailand

Petros C. Karakousis, M.D., Professor

The Johns Hopkins University School of Medicine, USA

Thoracic Medicine

The Official Journal of
Taiwan Society of Pulmonary and Critical Care Medicine
Taiwan Society for Respiratory Therapy
Taiwan Society of Sleep Medicine
Taiwan Society of Tuberculosis and Lung Diseases

Volume **37**
Number **2**
June 2022

CONTENTS

Original Articles

- Clinical Features and Outcomes of Patients with Interstitial Pneumonia with Autoimmune Features and Acute Respiratory Failure** 58~67
Shan-Yao Yang, Wei-Ling Lain, Kuang-Yao Yang, Wei-Chih Chen
- Effect of Using a Recruitment Maneuver in Morbidly Obese Patients during Weight Reduction Surgery: A Systematic Review and Meta-analysis** 68~79
Yu-Ching Lu, Ching-Yi Chen, Ho-Sheng Lee, Mei-Hua Ceng, Yu-Feng Wei

Case Reports

- Tracheobronchopathia Osteochondroplastica: A Rare Incidental Diagnosis** 80~84
Chun Lin, Kuo-Hsuan Hsu
- Systemic Air Embolism Occurring after Transthoracic Needle Biopsy -- a Rare but Lethal Post-Procedural Complication** 85~89
Yi-Jhih Huang, Chung-Kan Peng, Shih-Chun Lee, Cheng-Kuang Chang, and Kun-Lun Huang
- Diffuse Alveolar Hemorrhage Shortly After Breast Augmentation Surgery: A Case Report** 90~95
Ting-Chia Chang, Hsiu-Nien Shen
- Pulmonary Alveolar Proteinosis with a Rare Presentation: A Case Report** 96~102
Chang-Wei Wu, Yen-Lin, Huang, Ching-Yao Yang
- Fulminant and Fatal Community-Acquired Pneumonia Caused by *Sphingomonas Paucimobilis*** 103~107
Chang-Hung Chen, Chao-Tai Lee
- The First Reported Computed Tomography Scan Images of Remitting-Relapsing Pleural Effusions of Malignant Pleural Mesothelioma** 108~113
Wen-Chi Hsiao, Jen-Wen Hsu, Ming-Hung Chen, Pei-Ru Wu, Tai-Yu Chang
- Hard Metal Lung Disease: A Case Report Using Transbronchial Cryobiopsy in the Diagnosis** 114~119
Chiung-Hung Lin I, Chih-Hao Chang, Jia-Shiuan Ju, Tzu-Hsuan Chiu, Pi-Hung Tung, Shu-Min Lin
- Multiple Nodular Pulmonary Amyloidosis Mimicking Metastatic Lesions: A Case Report** 120~125
Po-Chun Lo, Chi-Lu Chiang
- Chronic Eosinophilic Pneumonia Associated with Heat-Not-Burn Tobacco Cigarette Use** 126~131
Tung-Chi Yeh, Chun-Chieh Wu, Chia-Min Chen, Ming-Ju Tsai, Jen-Yu Hung
- Influenza Pneumonia Associated with Invasive Pulmonary Aspergillosis Requiring Venovenous Extracorporeal Membrane Oxygenation Support: A Case Report and Literature Review** 132~139
Tzu-Hsuan Chiu, Chiung-Hung Lin, Jia-Shiuan Ju, Han-Chung Hu
- Pulmonary Arteriovenous Malformation in a Woman with Chronic Obstructive Pulmonary Disease and Recurrent Stroke: A Case Report** 140~146
Ting-Chia Chang, Shian-Chin Ko
- Bilateral *Cunninghamella Bertholletiae* Empyema and Pneumothorax: A Case Report and Literature Review** 147~153
Wei-Cheng Hong, Chien-Wei Hsu, David-Lin Lee

Clinical Features and Outcomes of Patients with Interstitial Pneumonia with Autoimmune Features and Acute Respiratory Failure

Shan-Yao Yang¹, Wei-Ling Lain¹, Kuang-Yao Yang^{1,2,3,4}, Wei-Chih Chen^{1,2,3}

Introduction: The clinical features and outcomes of patients with interstitial pneumonia with autoimmune features (IPAF) who developed acute respiratory failure (ARF) are not well understood. We aimed to analyze IPAF patients who developed ARF and compare them with patients with connective tissue disease-related interstitial lung disease (CTD-ILD).

Methods: This was a retrospective, observational study conducted in a 24-bed intensive care unit (ICU) of a tertiary medical center in Taiwan during a 3-year period. Patients admitted to the ICU with ARF requiring MV and who had a diagnosis of IPAF or CTD-ILD were included for analysis. Patient characteristics, including demographics, critical illness factors, management and outcome data, were recorded and analyzed.

Results: During the study period, a total of 13 patients with IPAF and 13 patients with CTD-ILD who developed ARF were admitted to the ICU. Overall, 28-day mortality was 50% for the enrolled subjects. Patients with IPAF had significantly lower 28-day mortality than those with CTD-ILD (23.1% vs 76.9%, $p=0.006$). The independent risk factor for 28-day mortality was a diagnosis of CTD-ILD.

Conclusion: High mortality rates were observed among both IPAF and CTD-ILD patients with ARF requiring MV. A diagnosis of IPAF seemed to have a better outcome than that of CTD-ILD. (*Thorac Med* 2022; 37: 58-67)

Key words: acute respiratory failure, intensive care unit, interstitial lung disease, interstitial pneumonia with autoimmune features, connective tissue disease, mechanical ventilation, mortality

Introduction

Interstitial lung disease (ILD) covers a broad spectrum of lung parenchymal diseases

[1], and includes a group of diseases with significant heterogeneity, which leads to differences in their clinical presentation, prognoses and management [2]. Some ILD subgroups, such as

¹Department of Chest Medicine, Taipei Veterans General Hospital, Taipei, Taiwan, ²Faculty of Medicine, School of Medicine, National Yang Ming Chiao Tung University, Taipei, Taiwan, ³Institute of Emergency and Critical Care Medicine, School of Medicine, National Yang Ming Chiao Tung University, Taipei, Taiwan, ⁴Cancer Progression Research Center, National Yang Ming Chiao Tung University, Taipei, Taiwan.

Address reprint requests to: Dr. Wei-Chih Chen, Department of Chest Medicine, Taipei Veterans General Hospital, Taipei, Taiwan, No. 201, Sec. 2, Shih-Pai Road, Taipei 11217, Taiwan

sarcoidosis, idiopathic pulmonary fibrosis (IPF), and hypersensitivity pneumonitis, are known as idiopathic interstitial pneumonias (IIPs). Moreover, connective tissue disease-related interstitial lung disease (CTD-ILD) is also a type of ILD [3]. Some patients exhibit characteristics of both IPF and CTD-ILD, and the term interstitial pneumonia with autoimmune features (IPAF) was coined for them in the European Respiratory Society (ERS)/American Thoracic Society (ATS) consensus published in 2015 [4]. Patients with IIPs other than CTD-ILDs with clinical, serologic and morphologic features of autoimmunity without characteristic connective tissue disease are diagnosed with IPAF [5]. For the diagnosis of IPAF, patients must have interstitial pneumonia without alternative etiologies, must not meet the criteria of certain connective tissue diseases, and must have at least 1 feature from at least 2 of the 3 domains of clinical, serologic and morphologic features [4].

The prevalence and pathophysiology of IPAF remain elusive. The prognosis of IPAF also varies among different study groups. In their prospective cohort, Sambataro *et al.* showed a female predominance of IPAF compared to IPF. The most common findings are nonspecific interstitial pneumonia, antinuclear antibody positivity and Raynaud phenomenon. Compared with IPF, IPAF patients showed a younger age, better performance on pulmonary function tests and a reduced need for O₂ support [6]. The prognosis of IPAF generally lies between that of IPF and CTD-ILD [7]. Despite a growing number of studies on IPAF and CTD-ILD, the prognosis of these patients with ARF is still not well understood. Thus, this study aimed to analyze the characteristics of patients with IPAF and ARF and their prognostic factors compared to those of CTD-ILD patients.

Methods

This was a retrospective observational study conducted in the medical intensive care unit (ICU) of a tertiary medical center in Taiwan. Patients admitted to the ICU with ARF requiring mechanical ventilation (MV) between January 2014 and December 2016 were screened for eligibility. All patients admitted to the ICU with ARF requiring MV during the study period were enrolled if they had a past history or a new diagnosis of IPAF or CTD-ILD during their ICU stay.

We excluded patients based on the following: age less than 20 years, pregnant, repeated ICU admission during the same hospitalization, or MV use for more than 48 hours before ICU admission. Patient characteristics, including demographics, critical illness factors and outcome data, were recorded and analyzed. The study was approved by the institutional review board of Taipei Veterans General Hospital (TPEVGH IRB No. 2017-09-010AC).

Definition of IPAF and CTD-ILD

Two pulmonologists (SYY and WCC) carefully reviewed all medical records, clinical data and images for each study subject whenever available. The confirmation of IPAF was based on the criteria of the latest ERS/ATS task force of ILD. A diagnosis of CTD-ILD was made when the patient had an established autoimmune disease known to cause ILD based on published criteria [8-12].

Data collection and measurement

Data were extracted from the electronic medical record database. These variables included age, sex, smoking status, and comorbidities. We also recorded critical illness

data, such as the cause of respiratory failure, laboratory values, and arterial blood gas at the onset of ARF. Acute exacerbation (AE) of ILD was defined as rapid worsening of respiratory symptoms with increased dyspnea with new radiologic abnormalities within 1 month without evidence of other causes, such as myocardial infarction, pulmonary embolism, or fluid overload. Clinical management, including the type of MV, vasopressor use, sedative use, corticosteroid pulse therapy and steroid dosage, oxygenation, and fluid balance, was recorded. The primary outcomes were 28-day mortality and its risk factors. Secondary outcomes included ICU mortality and overall mortality.

Statistical analysis

The results are presented as the mean \pm standard deviation or number with percentage as appropriate. We used the Kolmogorov-Smirnov and Shapiro-Wilk tests to examine the normality of continuous variables. The independent t test was used to compare normally distributed continuous variables, and the Mann-Whitney U test was used to compare nonnormally distributed continuous variables. We used the Pearson χ^2 test or Fisher's exact test to compare categorical variables. Variables showing significant differences between survivors and non-survivors were entered into univariate and multivariate logistic regression analyses using the enter method to determine factors independently associated with mortality. Odds ratios and 95% confidence intervals were also calculated. A P-value less than 0.05 was considered to be statistically significant. All statistical analyses were performed using IBM SPSS Statistics for Windows/Macintosh, Version 24.0 (IBM Corp., Armonk, NY).

Results

During the study period, 1368 patients were admitted to the ICU with ARF requiring MV. A total of 1286 of the 1368 patients did not have a diagnosis of ILD and were excluded from the study. Patients with a diagnosis of IPAF or CTD-ILD were selected from the remaining 82 patients: 13 patients had IPAF and 13 had CTD-ILD (Figure 1). Twenty-eight-day mortality was 50% for the enrolled subjects, and was statistically higher among patients with CTD-ILD than among those with IPAF (Table 1, Figure 2).

Baseline characteristics are summarized in Table 1. More survivors were diagnosed with IPAF. Data, management and outcomes of critically ill patients are presented in Table 2. Survivors had significantly lower APACHE II scores at the onset of ARF. In addition, survivors had a reduced need for vasopressors. In the outcome analysis, survivors had reduced ICU mortality and longer hospital stays.

We also compared baseline characteristics between patients with IPAF and those with CTD-ILD (Table 3). There were more male patients in the IPAF group. The clinical features during hospitalization were also analyzed (Table 4). The IPAF group had favorable outcomes, including lower ICU mortality, lower 28-day mortality and lower in-hospital mortality.

We used univariate and multivariate logistic regression analyses to further elucidate the clinical predictors of 28-day mortality (Table 5). Significant variables included diagnosis of CTD-ILD, vasopressor use, and APACHE II score. After multivariate logistic regression analysis, diagnosis of CTD-ILD (OR: 22.369, CI: [1.462-342.353]) remained an independent poor prognostic factor.

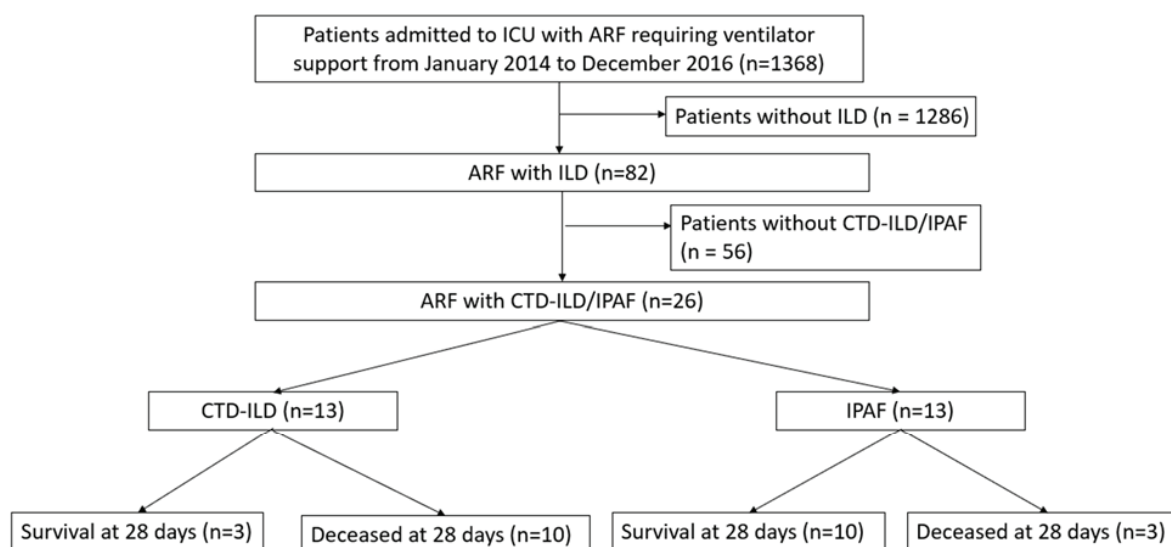


Fig. 1.

Table 1. Baseline Characteristics of Enrolled Subjects

	Survivors (n=13)	Non-survivors (n=13)	<i>P</i> value
Age (years)	84.2 ± 12.2	78.2 ± 11.1	0.197
Males	11 (84.6%)	8 (61.5%)	0.378
Ever-smokers	2 (15.4%)	1 (7.7%)	1.000
Comorbidities			
Hypertension	8 (61.5%)	7 (53.8%)	0.691
Type 2 diabetes	3 (23.1%)	3 (23.1%)	1.000
COPD	3 (23.1%)	1 (7.7%)	0.593
Heart failure	2 (15.4%)	7 (53.8%)	0.097
CKD	2 (15.4%)	2 (15.4%)	1.000
CVA	2 (15.4%)	2 (15.4%)	1.000
Cancer	0 (0)	3 (23.1%)	0.220
ILD classification			
IPAF	10 (76.9%)	3 (23.1%)	
CTD-ILD	3 (23.1%)	10 (76.9%)	

COPD: chronic obstructive pulmonary disease; CKD: chronic kidney disease; CVA: cerebrovascular accident; ILD: interstitial lung disease; IPAF: interstitial pneumonia with autoimmune features; CTD-ILD: connective tissue disease-related interstitial lung disease.

Table 2. Clinical Features of Enrolled Subjects During Hospitalization

	Survivors (n=13)	Non-survivors (n=13)	P value
At the onset of ARF			
APACHE II	12.8 ± 5.3	17.5 ± 5.8	0.039
WBC (cells/mm ³)	9,830.8 ± 4,033.7	10,461.5 ± 3,740.9	0.683
Hemoglobin (g/dl)	11.5 ± 3.3	10.8 ± 3.0	0.548
Platelets (cells/mm ³)	244,538.5 ± 175,942	197,769.2 ± 144,822	0.466
Albumin (g/dl)	2.8 ± 1.1	2.5 ± 0.9	0.552
BUN (mg/dl)	28.5 ± 19.3	32.3 ± 43.6	0.774
Creatinine (mg/dl)	1.2 ± 0.6	1.3 ± 0.9	0.843
Na (mmol/l)	140.9 ± 9.4	134.6 ± 6.6	0.059
K (mmol/l)	4.1 ± 0.6	4.5 ± 1.1	0.255
Total bilirubin (mg/dl)	0.8 ± 0.5	0.6 ± 0.3	0.276
Cancer	0 (0)	3 (23.1%)	0.220
ALT (U/l)	28.9 ± 23.0	22.9 ± 14.5	0.429
AST (U/l)	27.3 ± 17.4	39.8 ± 43.5	0.454
Glucose (mg/dl)	150.8 ± 51.8	164.7 ± 60.2	0.550
LDH (U/l)	516.0 ± 359.2	400.6 ± 210.8	0.427
CK (U/l)	77.5 ± 56.2	47.9 ± 29.8	0.108
CRP (mg/dl)	8.4 ± 8.3	6.3 ± 4.2	0.435
Procalcitonin (ng/dl)	0.9 ± 1.1	0.4 ± 0.5	0.148
Lactate (mg/dl)	43.9 ± 54.2	25.6 ± 17.2	0.265
NT-pro-BNP (pg/ml)	1,685.5 ± 1,816.9	3,352.9 ± 3,439.3	0.167
Arterial blood gas			
pH	7.4 ± 0.2	7.4 ± 0.1	0.184
PaCO ₂ (mmHg)	36.4 ± 12.5	37.9 ± 9.0	0.746
HCO ₃ ⁻ (mmol/l)	21.3 ± 6.9	25.3 ± 4.7	0.097
PaO ₂ /FiO ₂	165.2 ± 85.7	164.3 ± 74.3	0.564
Management and follow-up Type of MV			1.000
Invasive MV	6 (46.2%)	6 (46.2%)	
Noninvasive MV	7 (53.8%)	7 (53.8%)	
Vasopressor	1 (7.7%)	8 (61.5%)	0.011
Sedation	6 (46.2%)	10 (76.9%)	0.107
Muscle relaxant	0 (0)	4 (30.8%)	0.066
Corticosteroid pulse therapy	12 (92.3%)	12 (92.3%)	1.000
Mean daily IO (ml)	141.9 ± 430.0	472.2 ± 399.8	0.054
ICU mortality	2 (15.4%)	7 (53.8%)	0.039
ICU days	14.0 ± 10.0	11.5 ± 6.3	0.447
Hospital days	35.3 ± 21.1	19.0 ± 10.4	0.019
MV days	22.4 ± 17.8	15.0 ± 9.0	0.208

ARF: acute respiratory failure; APACHE II: Acute Physiology and Chronic Health Evaluation II; WBC: white blood cells; BUN: blood urea nitrogen; ALT: alanine aminotransferase; AST: aspartate aminotransferase; LDH: lactate dehydrogenase; CK: creatine kinase; CRP: C-reactive protein; NT-pro-BNP: N-terminal pro-B-type natriuretic peptide; MV: mechanical ventilation; IO: intake and output; ICU: intensive care unit.

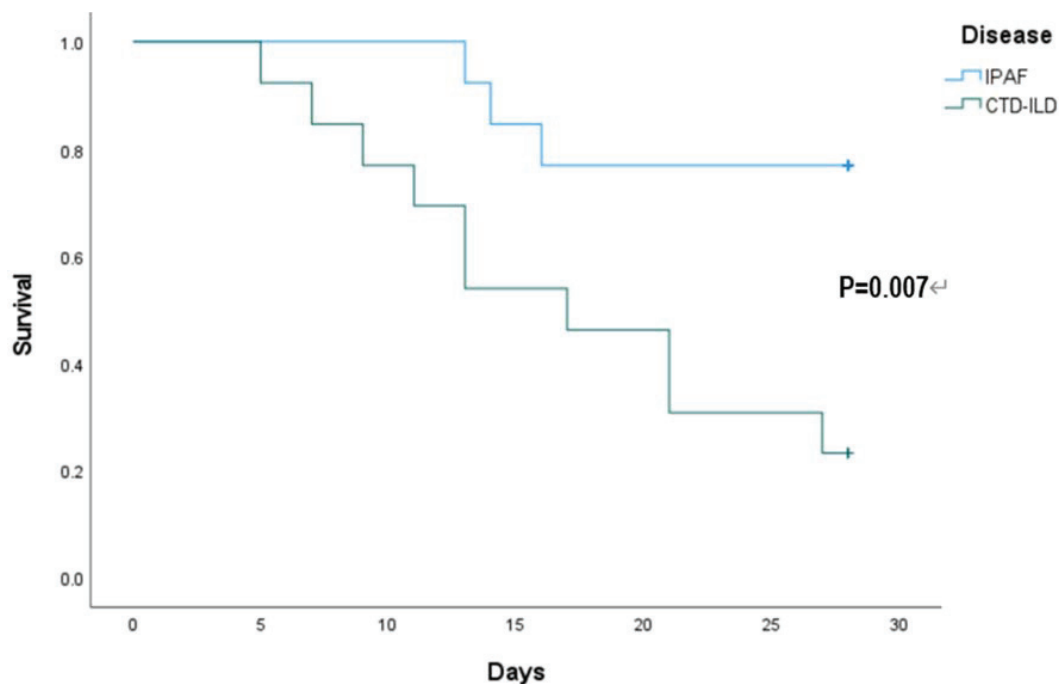


Fig. 2.

Table 3. Baseline Characteristics of IPAF and CTD-ILD Patients

	IPAF (n=13)	CTD-ILD (n=13)	P value
Age (years)	83.5 ± 12.4	78.9 ± 11.3	0.339
Male	12 (92.3%)	7 (53.8%)	0.027
Smoking	2 (15.4%)	1 (7.7%)	0.539
Comorbidities			
Hypertension	8 (61.5%)	7 (53.8%)	0.691
Type 2 diabetes	3 (23.1%)	3 (23.1%)	1.000
COPD	2 (15.4%)	2 (15.4%)	1.000
Heart failure	4 (30.8%)	5 (38.5%)	0.680
CKD	3 (23.1%)	1 (7.7%)	0.277
CVA	1 (7.7%)	3 (23.1%)	0.277
Cancer	0 (0)	3 (23.1%)	0.066

IPAF: interstitial pneumonia with autoimmune features; CTD-ILD: connective tissue disease-related interstitial lung disease; COPD: chronic obstructive pulmonary disease; CKD: chronic kidney disease; CVA: cerebrovascular accident.

Table 4. Clinical Features of IPAF and CTD-ILD Patients During Hospitalization

	IPAF (n=13)	CTD-ILD (n=13)	P value
At the onset of ARF			
APACHE II	14.7 ± 5.7	15.6 ± 6.4	0.703
WBC (cells/mm ³)	10,823.1 ± 4,726.7	9,469.2 ± 2,673.1	0.380
Hemoglobin (g/dl)	11.7 ± 3.8	10.6 ± 2.2	0.371
Platelets (cells/mm ³)	233,692 ± 172,110	208,615 ± 152,157	0.697
Albumin (g/dl)	2.7 ± 1.0	2.6 ± 1.0	0.810
BUN (mg/dl)	30.0 ± 18.7	30.7 ± 44.0	0.961
Creatinine (mg/dl)	1.4 ± 0.8	1.1 ± 0.7	0.481
Na (mmol/l)	140.9 ± 9.6	134.7 ± 6.4	0.066
K (mmol/l)	4.3 ± 0.6	4.2 ± 1.1	0.795
Total bilirubin (mg/dl)	0.8 ± 0.4	0.6 ± 0.3	0.231
ALT (U/l)	28.5 ± 24.0	23.3 ± 13.1	0.503
AST (U/l)	23.2 ± 15.5	47.2 ± 41.0	0.135
Glucose (mg/dl)	155.8 ± 56.4	159.7 ± 56.7	0.867
LDH (U/l)	507.1 ± 345.3	394.7 ± 203.0	0.428
CK (U/l)	76.1 ± 61.8	49.3 ± 19.7	0.158
CRP (mg/dl)	6.1 ± 6.2	8.6 ± 6.8	0.353
Procalcitonin (ng/dl)	0.9 ± 1.0	0.2 ± 0.3	0.090
Lactate (mg/dl)	46.8 ± 53.7	22.4 ± 14.4	0.137
NT-pro-BNP (pg/ml)	1,656.8 ± 1,839.2	3,379.2 ± 3,414.4	0.152
Arterial blood gas			
pH	7.34 ± 0.1	7.4 ± 0.1	0.110
PaCO ₂ (mmHg)	37.2 ± 13.4	37.2 ± 9.2	0.993
HCO ₃ ⁻ (mmol/l)	21.5 ± 7.2	25.1 ± 4.4	0.138
PaO ₂ /FiO ₂	172.2 ± 73.5	147.2 ± 94.0	0.463
Management and follow-up Type of MV			0.431
Invasive MV	7 (53.8%)	5 (38.5%)	
Noninvasive MV	6 (46.2%)	8 (61.5%)	
Vasopressor	3 (23.1%)	6 (46.2%)	0.216
Sedation	7 (53.8%)	9 (69.2%)	0.420
Muscle relaxant	2 (15.4%)	2 (15.4%)	0.592
Corticosteroid pulse therapy	11 (84.6%)	13 (100%)	0.141
Mean daily IO (ml)	159.2 ± 470.5	455.0 ± 367.5	0.087
ICU mortality	1 (7.7%)	8 (61.5%)	0.004
28-day mortality	3 (23.1%)	10 (76.9%)	0.006
In-hospital mortality	5 (38.5%)	11 (84.6%)	0.016
ICU days	11.9 ± 6.2	13.5 ± 10.2	0.629
Hospital days	33.8 ± 20.7	20.5 ± 13.0	0.063
MV days	21.7 ± 17.7	15.8 ± 9.6	0.314

IPAF: interstitial pneumonia with autoimmune features; CTD-ILD: connective tissue disease-related interstitial lung disease; ARF: acute respiratory failure; APACHE II: Acute Physiology and Chronic Health Evaluation II; WBC: white blood cells; BUN: blood urea nitrogen; ALT: alanine aminotransferase; AST: aspartate aminotransferase; LDH: lactate dehydrogenase; CK: creatine kinase; CRP: C-reactive protein; NT-pro-BNP: N-terminal pro-B-type natriuretic peptide; MV: mechanical ventilation; IO: intake and output; ICU: intensive care unit.

Table 5. Risk Factors for 28-Day Mortality Based on Univariate and Multivariate Logistic Regression Analyses

	Univariate			Multivariate		
	Odds ratio	95% confidence interval	<i>p</i> -value	Odds ratio	95% confidence interval	<i>p</i> -value
APACHE II	1.173	0.997-1.380	0.054	1.161	(0.856-1.575)	0.338
Diagnosis of CTD-ILD	11.1	1.792-68.894	0.010	22.369	(1.462-342.353)	0.026
Vasopressor use	19.2	1.876-196.53	0.013	11.495	(0.514-256.83)	0.123

CTD-ILD: connective tissue disease-related interstitial lung disease; APACHE II: Acute Physiology and Chronic Health Evaluation II.

Discussion

The aim of this study was to analyze the clinical features and outcomes of those with IPAF who were admitted to the ICU due to ARF, and to compare them with CTD-ILD patients. Higher APACHE II scores, more CTD-ILD patients and increased vasopressor use were observed among non-survivors. The diagnosis of CTD-ILD was the only risk factor affecting 28-day mortality, based on multivariate logistic regression. IPAF patients had better outcomes than CTD-ILD patients. To our knowledge, this is the first study to describe patients with IPAF who developed ARF and were admitted to the ICU.

To date, the clinical course and prognosis of IPAF with ARF is not completely understood, and optimal management has not been established. For other ILDs, for example, IPF, the use of MV during ARF is debated. Blivet et al. suggested that patients with IPF and ARF should not be intubated with MV support because the prognosis is very poor and is not improved by MV [8]. However, based on a nationwide analysis, the trends in MV use with patients with IPF and ARF have shown no decline, and MV use was associated with higher costs and increased mortality. Those at a younger age and with

fewer chronic medical conditions were likely to receive MV [9]. AE of IPF carries the worst outcome among patients with AE-ILD [10]. The only condition under which MV should be provided is the postsurgical setting, given that patients with MV can be successfully weaned in most cases [11].

In a study from Finland, CTD-ILD was the most prevalent condition among patients with non-IPF ILDs who required hospitalization, and the outcome could be relatively favorable [12]. Another study also confirmed a better prognosis for CTD-ILD than for IPF, regardless of the radiographic patterns [13]. Suda et al. found that age and rheumatoid arthritis were associated with AE of CTD-ILD [14]. The patient characteristics of those with AE of CTD-ILD and AE of IPF were mostly the same, except patients with CTD-ILD were younger. AE of CTD-ILD also had better outcomes than AE of IPF [15]. Patients with AE of CTD-ILD requiring MV had reduced ICU mortality compared to those with AE of IPF [16].

Our study cohort reported a 76% 28-day mortality rate among patients with CTD-ILD who had ARF and needed MV. We did not identify an association between the type of MV and 28-day mortality. Huie et al. reported a cohort of ILD patients with acute respiratory decline,

and the 1-year follow-up mortality was high regardless of the presence of IPF or not, with 100% and 72% mortality, respectively. The use of MV and a higher APACHE score were 2 predictive factors for in-hospital and 1-year mortality [17]. Another study also found that a higher APACHE score predicted the mortality of patients with chronic ILD and ARF needing MV support, as did a high positive end expiratory pressure ventilator setting [18]. A Turkish cohort study reported that an APACHE II score greater than 20 and continuous noninvasive ventilation use indicated a significant risk of NIV failure in patients with ILD admitted to the ICU [19]. In our study, the APACHE II score was not statistically significant after multivariate regression analysis. Thus, the APACHE II score might not truly reflect the disease characteristics of IPAF or CTD-ILD.

Refractory shock has been identified as a risk factor for in-hospital 28-day mortality among patients with acute respiratory distress syndrome (ARDS) [20]. Some authors also found a relationship between the use of vasopressors and 28-day mortality in neutropenic patients with ARDS [21]. However, in our study, the use of vasopressors was not associated with mortality. It seemed that patients with a more severe disease status, such as ARDS with concomitant hemodynamic compromise, would exhibit worse outcomes.

Our study suggested a favorable outcome for IPAF compared to CTD-ILD. However, Oldham *et al.* noted poorer survival in their IPAF cohort than in the CTD-ILD cohort [22]. This finding appeared to be related to the underlying radiographic and histological pattern, as those meeting IPAF criteria with a pattern of typical interstitial pneumonia had survival rates similar to those in the IPF cohort [23].

There are several important limitations to our study. First, it was a retrospective study. Some data might be missing. Second, this study was conducted in a single center with a small number of patients. Further studies enrolling more patients are warranted. Third, the diagnostic rate of IPAF and CTD-ILD might be underestimated due to a lack of clinical and laboratory data. Given that the number of patients with IPAF might be limited within 1 center, a multicenter ILD registry is needed. In addition, prospective research should be considered for a more complete collection of clinical information.

Conclusion

For patients with IPAF or CTD-ILD, 28-day mortality was high in the presence of ARF needing MV. The diagnosis of CTD-ILD was the only prognostic factor predicting 28-day mortality. IPAF patients had better outcomes than CTD-ILD patients.

References

1. Mari PV, Jones MG, Richeldi L. Contemporary Concise Review 2018: Interstitial lung disease. *Respirology* 2019; 24(8): 809-816.
2. Lain WL, Chang SC, Chen WC. Outcome and prognostic factors of interstitial lung disease patients with acute respiratory failure in the intensive care unit. *Ther Adv Respir Dis* 2020; 14:1753466620926956.
3. Gibson GJ, Loddenkemper R, Lundback B, *et al.* European Lung White Book. *Eur Respir J* 2013 Sep; 42(3): 559-63.256-269.
4. Fischer A, Antoniou KM, Brown KK, *et al.* An official European Respiratory Society/American Thoracic Society research statement: interstitial pneumonia with autoimmune features. *Eur Respir J* 2015; 46(4): 976-87.
5. Graney BA, Fischer A. Interstitial pneumonia with

- autoimmune features. *Ann Am Thorac Soc* 2019; 16(5): 525-533.
6. Sambataro G, Sambataro D, Torrisi SE, *et al.* Clinical, serological and radiological features of a prospective cohort of Interstitial Pneumonia with Autoimmune Features (IPAF) patients. *Respir Med* 2019; 150: 154-160.
 7. Fernandes L, Nasser M, Ahmad K, *et al.* Interstitial pneumonia with autoimmune features (IPAF). *Front Med (Lausanne)* 2019; 6:209.
 8. Blivet S, Philit F, Sab JM, *et al.* Outcome of patients with idiopathic pulmonary fibrosis admitted to the ICU for respiratory failure. *Chest* 2001; 120(1): 209-12.
 9. Mooney JJ, Raimundo K, Chang E, *et al.* Mechanical ventilation in idiopathic pulmonary fibrosis: a nationwide analysis of ventilator use, outcomes, and resource burden. *BMC Pulm Med* 2017; 17(1): 84.
 10. Al-Hameed FM, Sharma S. Outcome of patients admitted to the intensive care unit for acute exacerbation of idiopathic pulmonary fibrosis. *Can Respir J* 2004; 11(2): 117-22.
 11. Mallick S. Outcome of patients with idiopathic pulmonary fibrosis (IPF) ventilated in intensive care unit. *Respir Med* 2008; 102(10): 1355-9.
 12. Salonen J, Vahanikkila H, Purokivi M, *et al.* Causes of acute respiratory hospitalizations predict survival in fibrosing interstitial lung diseases. *PLoS One* 2020; 15(11): e0242860.
 13. Park JH, Kim DS, Park IN, *et al.* Prognosis of fibrotic interstitial pneumonia: idiopathic versus collagen vascular disease-related subtypes. *Am J Respir Crit Care Med* 2007; 175(7): 705-11.
 14. Suda T, Kaida Y, Nakamura Y, *et al.* Acute exacerbation of interstitial pneumonia associated with collagen vascular diseases. *Respir Med* 2009; 103(6): 846-53.
 15. Tachikawa R, Tomii K, Ueda H, *et al.* Clinical features and outcome of acute exacerbation of interstitial pneumonia: collagen vascular diseases-related versus idiopathic. *Respiration* 2012; 83(1): 20-7.
 16. Luo Z, Yang L, Liu S, *et al.* Mechanical ventilation for acute respiratory failure due to idiopathic pulmonary fibrosis versus connective tissue disease-associated interstitial lung disease: Effectiveness and risk factors for death. *Clin Respir J* 2020; 14(10): 918-932.
 17. Huie TJ, Olson AL, Cosgrove GP, *et al.* A detailed evaluation of acute respiratory decline in patients with fibrotic lung disease: aetiology and outcomes. *Respirology* 2010; 15(6): 909-17.
 18. Fernandez-Perez ER, Yilmaz M, Jenad H, *et al.* Ventilator settings and outcome of respiratory failure in chronic interstitial lung disease. *Chest* 2008; 133(5): 1113-9.
 19. Gungor G, Tatar D, Salturk C, *et al.*, Why do patients with interstitial lung diseases fail in the ICU? A 2-center cohort study. *Respir Care* 2013; 58(3): 525-31.
 20. Sharif N, Irfan M, Hussain J, *et al.* Factors associated within 28 days in-hospital mortality of patients with acute respiratory distress syndrome. *Biomed Res Int* 2013; 2013: 564547.
 21. Mokart D, van Craenenbroeck T, Lambert J, *et al.* Prognosis of acute respiratory distress syndrome in neutropenic cancer patients. *Eur Respir J* 2012; 40(1): 169-76.
 22. Oldham JM, Adegunsoye A, Valenzi E, *et al.* Characterisation of patients with interstitial pneumonia with autoimmune features. *Eur Respir J* 2016; 47(6): 1767-75.
 23. Lim JU, Gil BM, Kang HS, *et al.* Interstitial pneumonia with autoimmune features show better survival and less exacerbations compared to idiopathic pulmonary fibrosis. *BMC Pulm Med* 2019; 19(1): 120.

Effect of Using a Recruitment Maneuver in Morbidly Obese Patients during Weight Reduction Surgery: A Systematic Review and Meta-analysis

Yu-Ching Lu^{1*}, Ching-Yi Chen^{1,2}, Ho-Sheng Lee^{1,5*}, Mei-Hua Ceng¹, Yu-Feng Wei^{3,4,5}

Introduction: Obese people are prone to develop atelectasis during general anesthesia. Whether the use of an intraoperative recruitment maneuver (RM) during weight reduction surgery is associated with improved intraoperative and postoperative outcomes is unknown.

Methods: We performed comprehensive searches of randomized-controlled trials that investigated the use of RM during weight reduction surgery. The research subjects were morbidly obese patients (BMI >40 kg/m²), and the intervention measures were positive end expiratory pressure (PEEP) combined with RM. The primary outcome was oxygenation capacity during operation.

Results: Eight articles with a total of 359 morbidly obese patients were included. These articles were published between 2006 and 2020, and the average body mass index (BMI) of these patients was 46.6 kg/m². Six studies of them were included for the analysis of oxygenation capacity. We found that the group treated by PEEP combined with RM had higher oxygenation capacity (measured by the ratio of arterial oxygen partial pressure to inspiratory oxygen concentration [PaO₂/FiO₂], P/F ratio) (standard mean difference [SMD] 0.956, 95% confidence interval [CI] 0.680-1.232; *p*<0.001) and better pulmonary compliance (SMD 0.745, 95%CI 0.380-1.110; *p*<0.001) than the control group. The P/F ratio after extubation was similar in both groups (SMD 0.219, 95%CI-0.627-1.065; *p*=0.611).

Conclusion: Intraoperative RM improved gas exchange and pulmonary compliance in morbidly obese patients undergoing weight reduction surgery. There was no difference in oxygenation status after extubation. (*Thorac Med* 2022; 37: 68-79)

Key words: morbid obesity, recruitment maneuver, positive end expiratory pressure, pulmonary mechanics, gas exchange

¹Division of Chest Medicine, Department of Internal Medicine, E-Da Hospital, Kaohsiung, Taiwan, ²School of Medicine, College of Medicine, I-Shou University, Kaohsiung, Taiwan, ³Institute of Biotechnology and Chemical Engineering, I-Shou University, Kaohsiung, Taiwan, ⁴Department of Internal Medicine, E-Da Cancer Hospital, Kaohsiung, Taiwan, ⁵School of Medicine for International Students, College of Medicine, I-Shou University, Kaohsiung, Taiwan.

Address reprint requests to: Dr. Yu-Feng Wei, Department of Internal Medicine, E-Da Cancer Hospital, I-Shou University, No. 21, Yida Road, Jiao-su Village, Yan-chao District, Kaohsiung 824, Taiwan.

*These authors contributed equally to this work.

Introduction

The World Health Organization (WHO) defines obesity as a body mass index (BMI) above 30 kg/m², and morbid obesity as a BMI above 40 kg/m². According to the WHO statistics in 2016, the proportion of obesity throughout the world was more than 39% [1]. There is a significant linear correlation between BMI and lung volume, including functional residual capacity (FRC) and expiratory reserve volume, which will decrease exponentially with the increase in BMI. Hence, morbid obesity causes patients' breath to be close to the residual volume [2]. A large amount of adipose tissue exists in the ribs, abdominal cavity and visceral cavity, which increases the burden on the thoracic cavity and leads to the reduction of the residual volume [3].

Weight loss methods for obese patients include diet adjustments, increased activity, and behavioral therapy. When the BMI is 30 kg/m² or 27–29 kg/m², medications can be initiated for those with existing comorbidities, while for those with a BMI >40 kg/m² or a BMI lower than the operation standard, but with existing comorbidities (e.g., cardiovascular diseases, hypertension, diabetes, etc.), it is recommended to undergo weight reduction surgeries. Common weight reduction surgeries include Roux-en-Y gastric bypass, sleeve gastrectomy, and adjustable gastric banding [4].

More than 11% of obese patients will have postoperative pulmonary complications after weight reduction surgery, and with an increase in weight, the incidence will be higher [5]. Furthermore, about 90% of patients under general anesthesia will develop atelectasis [6]. As such, obese people are more likely to experience atelectasis during anesthesia and mechanical ventilation. In obese patients, the end expiratory

volume may be lower than the residual volume, which can easily cause alveolar collapse, leading to uneven ventilation and perfusion, as well as shunting [7-8].

It has been pointed out that when using a ventilator in morbidly obese patients, a recruitment manoeuvre (RM) can improve lung volume, respiratory system resistance, and oxygenation [9]. RM helps to continuously increase airway pressure to open the collapsed alveoli, and then apply enough positive end expiratory pressure (PEEP) to prevent the alveoli from collapsing again. There are many approaches to this, and continuous positive airway pressure (CPAP), wherein the ventilator is set to the CPAP mode, and the pressure is increased to 30–40 cmH₂O for 30–40 seconds, is the most commonly used. Another way is to gradually decrease the PEEP after applying RM and monitor the dynamic compliance of the lungs at the same time; the pressure point when the dynamic compliance starts to decrease is the best PEEP [10].

Many trials have adopted different ventilation modes under anesthesia during an operation, such as PEEP and RM. However, the ideal ventilation strategy for obese patients has not been established [11]. Souza et al. published a meta-analysis in 2020, which included the literature as of 2015, and proposed that RM could improve oxygenation capacity (measured by the ratio of arterial oxygen partial pressure to inspiratory oxygen concentration [$\text{PaO}_2/\text{FiO}_2$], the P/F ratio) and pulmonary compliance during operation [12]. As of this point, the effect of RM on oxygenation capacity after extubation and hospitalization days has not undergone meta-analysis. Therefore, this study used a systematic review and meta-analysis to integrate the latest literature on randomized-controlled trials

(RCTs), and investigated the effect of applying PEEP combined with RM in morbidly obese patients under anesthesia. The primary outcome was oxygenation capacity during operation. Respiratory compliance and post-extubation oxygenation capacity were also analyzed. Thus, the results could serve as a reference for clinical technical operation to improve quality of care for obese patients receiving bariatric surgery.

Methods

Search strategies and inclusion criteria

In this study, we searched for articles published as of December 31, 2020 from the Cochrane Library, PubMed, Web of Science, Scopus, and Embase databases, and used the keywords “morbid obesity”, “obesity”, “morbidly obese”, “bariatric surgery”, “gastric bypass”, “Roux-en-Y”, “sleeve gastrectomy” “morbidly obese”, “recruitment maneuver”, “positive end expiratory pressure”, “lung mechanics”, “pulmonary mechanics”, “gas exchange”, “PaO₂/FiO₂ ratio”, “P/F ratio,” “gas exchange”, and “oxygenation index” to search the databases using Boolean logic operators.

Inclusion criteria were as follows: (1) RCTs; (2) research subjects with morbid obesity (BMI >30 kg/m²); (3) with PEEP combined with RM used in the experimental group, and PEEP in the control group; (4) measurement results should include gas exchange, pulmonary mechanics, oxygenation index after extubation or hospitalization days. Exclusion criteria included articles irrelevant to the topic, articles in which the research subjects or intervention measures were inconsistent with the inclusion criteria, and duplicate articles. After screening based on the exclusion criteria, the titles or abstracts of the articles were reviewed individu-

ally. If the inclusion criteria were met, the full text would be obtained, resulting in a total of 8 articles.

Evaluation method for research quality

Research quality and risk of bias in the included studies were independently assessed by 2 reviewers (C.-Y.C. and Y.-C.L.), according to the recommendations in the Cochrane Handbook for Systematic Reviews of Interventions 5.1. The following criteria were used: (1) random sequence generation; (2) allocation concealment; (3) blinding of participants and personnel; (4) blinding of outcome assessments; (5) incomplete outcome data; (6) selective reporting; and (7) other bias. Each criterion was marked as “low risk,” “high risk,” or “unclear risk” of bias. Any disagreements were resolved by consensus or assessed by other authors (Y.-F. W.).

Statistical method

Comprehensive Meta-Analysis software 3.0 was used for meta-analysis. Before analyzing and merging the results of the literature, Cochran’s Q test was used to check the heterogeneity of the research results among the collected articles. At the same time, the relative importance of each study and the direction of the research results were marked through a visual presentation of a forest plot. Then, the pooling effect size was calculated using a fixed-effects model or a random-effects model. Sensitivity analyses were performed to assess the impact of each study by excluding one individual study and recalculating the pooled hazard ratio estimates for the remaining studies. Egger’s regression test with the funnel plot was used to evaluate publication bias.

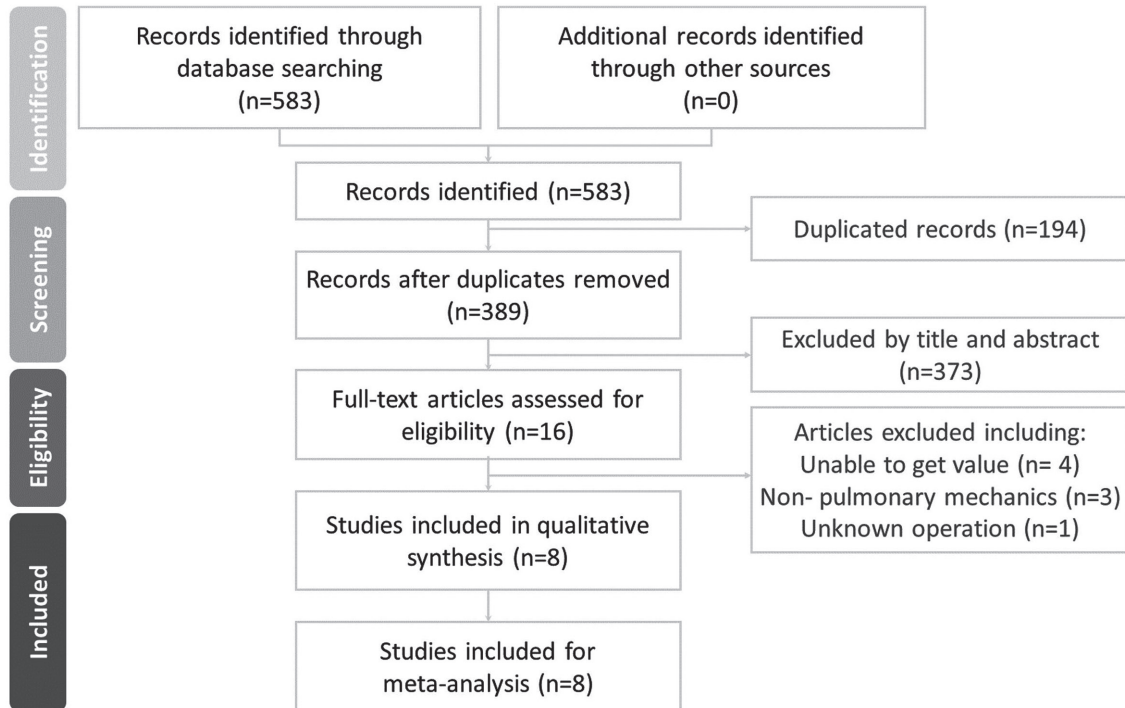


Fig. 1. Flow Diagram of Study Identification -- use "Non-pulmonary" below.

Results

Literature search results and risk of bias assessment

The search of online databases yielded a total of 583 studies (Figure 1). In the end, a total of 8 studies with 359 morbidly obese patients were enrolled. These articles were published between 2006 and 2020, and the average BMI was 46.6 [13-20]. The surgical procedures were gastric bypass, sleeve gastrectomy, and partial gastrectomy. Different ventilator intervention methods were adopted in different articles. The characteristics of the patients enrolled in the studies are detailed in Table 1.

Risk of bias assessments for the included studies were performed independently by the review authors (Figure 2). All the studies had a low risk of bias, since there was sufficient evidence of random sequence generation and

a complete outcome assessment. However, a high risk of performance bias and detection bias were determined in most studies due to the open-label study design.

Evaluation of results

P/F ratio (oxygenation capacity)

A total of 6 articles (289 patients) were included for the P/F ratio assessment (Figure 3). Two of the 8 trials were not included for analysis, since there was only a figure for the P/F ratio but no place value available in 1 study [13], and no assessment of the P/F ratio in the other study [18]. The random-effects model was selected, and the results showed that the P/F ratio of the intervention group was higher than that of the control group (standard mean difference (SMD) 0.956, 95%CI 0.680-1.232; $p < 0.001$). The heterogeneity test was not statistically significant ($p > 0.05$), with a heterogeneity degree (I

Table 1. Characteristics of Patients Enrolled in the Studies

Study	Study patients	Case number	Intervention and Comparators	Surgical approach	RM time point	Measure outcomes
Whalen <i>et al.</i> 2006[13]	BMI > 40 kg/m ²	10	PEEP 4 cmH ₂ O + RM increase from 10 to 15 to 20 cmH ₂ O	bariatric Roux-en-Y	5 minutes after pneumoperitoneum was established	P/F ratio, other variables related to gas exchange, oxygenation, ventilation, respiratory mechanics, and hemodynamics
		10	PEEP 4 cmH ₂ O			
Chalhoub <i>et al.</i> 2007[14]	BMI ≥ 40 kg/m ²	26	PEEP 8 cmH ₂ O + RM 40 cmH ₂ O for 15 seconds	open gastric bypass	10 minutes after laparotomy	Arterial blood gases, ETCO ₂ , PAP, eTV, RR, MAP, and HR
		26	PEEP 8 cmH ₂ O			
Reinius <i>et al.</i> 2009[15]	BMI ≥ 40 kg/m ²	10	PEEP 10 cmH ₂ O + RM 55 cmH ₂ O for 10 seconds	gastric bypass with Y-en-Roux	10 minutes after anesthesia is induced	P/F ratio, ETCO ₂ , MAP, eTV and RR
		10	PEEP 10 cmH ₂ O			
		10	RM 55 cmH ₂ O for 10 seconds			
Souza <i>et al.</i> 2009[16]	BMI ≥ 40 kg/m ²	16	PEEP 5 cmH ₂ O + RM 30 cmH ₂ O for 120 seconds	open gastric bypass	After suturing the aponeurosis	SpO ₂ , PaO ₂ , PaCO ₂ , P/F ratio; Pplateau, and MAP; and intraoperative complications, HR, SBP, DBP
		17	PEEP 5 cmH ₂ O + RM 20 cmH ₂ O for 120 seconds			
		14	PEEP 5 cmH ₂ O			
Futier <i>et al.</i> 2011[17]	BMI ≥ 40 kg/m ²	22	NPPV + PEEP 10 cmH ₂ O + RM 40 cmH ₂ O for 40 seconds	laparoscopic sleeve gastrectomy or Roux-en-Y gastric bypass	5 minutes after anesthesia is induced	Ers; PAP; Pplateau; RR; eTV
		22	NPPV + PEEP 10 cmH ₂ O			
		22	PEEP 10 cmH ₂ O			
Dufresne <i>et al.</i> 2014[18]	BMI ≥ 35 kg/m ²	25	2. PEEP 10 cmH ₂ O + RM 40 cmH ₂ O for 40 seconds	laparoscopic gastric bypass	5 minutes before pneumoperitoneum is established and 5 minutes after pneumoperitoneum is finished	the change in FRC at postoperative day 1 changes in FVC, FEV ₁ and postoperative SaO ₂ and AHI
		25	1. PEEP 10 cmH ₂ O			
Wei <i>et al.</i> 2018[19]	BMI ≥ 40 kg/m ²	11	PEEP 8 cmH ₂ O + RM 40 cmH ₂ O for ten breaths, RM once	laparoscopic sleeve gastrectomy	After pneumoperitoneum is finished	PaO ₂ ; FiO ₂ ; HR; MAP
		11	PEEP 0 cmH ₂ O + RM 40 cmH ₂ O for ten breaths, once every 30 minutes			
		12	PEEP 0 cmH ₂ O			
Sümer <i>et al.</i> 2020[20]	BMI 40-55 kg/m ²	30	2. PEEP 8 cmH ₂ O + RM 40 cmH ₂ O for 40 seconds	Laparoscopic sleeve gastrectomy	5 minutes after pneumoperitoneum is finished	Arterial blood gases (pH, pO ₂ , pCO ₂ , HCO ₃ , lactate) respiratory mechanics of compliance, PIP, Pplateau, and Raw
		30	1. PEEP 8 cmH ₂ O			

*AHI = apnea-hypopnea index; BMI = body mass index; DBP = diastolic blood pressure; ETCO₂ = end tidal carbon dioxide concentration; eTV = expiratory tidal volume; Ers = static elastance of the respiratory system; FVC = forced vital capacity; FEV₁ = forced expiratory volume in the first second; HR = heart rate; MAP = mean arterial pressure; PAP = peak airway pressure; P/F ratio = ratio of arterial oxygen partial pressure (PaO₂) to inspiratory oxygen concentration (FiO₂); PEEP = positive end expiratory pressure; PIP = peak inspiration pressure; Pplateau = plateau airway pressure; Raw = airway resistance; RM = recruitment manoeuvre; RR = respiratory rate; SBP = systolic blood pressure.

	Random sequence generation (selection bias)	Allocation concealment (selection bias)	Blinding of participants and personnel (performance bias)	Blinding of outcome assessment (detection bias)	Incomplete outcome data (attrition bias)	Selective reporting (reporting bias)	Other bias
Chalhoub et al, 2007	+	+	?	?	+	+	+
Defresne et al, 2014	+	+	+	+	+	+	+
Futier et al, 2011	+	+	?	?	+	+	+
Reinius et al, 2009	+	+	?	?	+	+	+
Souza et al, 2009	+	+	●	?	+	+	+
Sümer et al, 2020	+	+	?	?	+	+	+
Wei et al, 2018	+	+	+	?	+	+	+
Whalen et al, 2006	+	+	+	?	+	+	+

Fig. 2. Risk of Bias of Each Item Presented as Percentages across All Included Studies

square) percentage of 39.81%, which indicated low heterogeneity. Sensitivity analyses demonstrated a similar pooling effect size of the included 6 studies (supplementary Figure S1). In addition, no publication bias was detected by funnel test and Egger's regression test ($p>0.05$). (Supplementary Figure S2).

Respiratory compliance

A total of 3 articles that included 140 pa-

tients with evaluated respiratory compliance were analyzed (Figure 4). The fixed-effects model showed that the compliance of the intervention group was better than that of the control group (SMD 0.745, 95%CI 0.380-1.110; $p<0.001$). Similarly, there was a statistically significant difference in the heterogeneity test ($p<0.001$); the percentage of heterogeneity (I square) was 84.91%, which revealed a high degree of heterogeneity.

Post-extubation P/F ratio (oxygenation capacity after extubation)

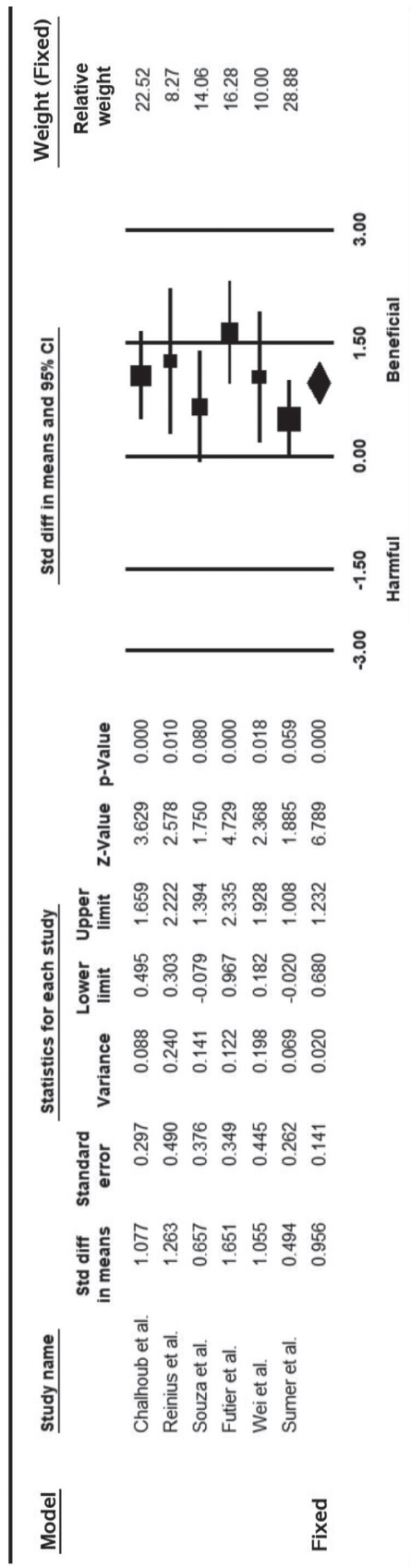
In all, 103 patients from 3 articles were finally included for evaluation of the post-extubation P/F ratio. As shown in Figure 5, the random-effects model indicated that the after-extubation P/F ratio of the intervention group was similar to that of the control group (SMD 0.219, 95%CI-0.627-1.065; $p=0.611$). The heterogeneity test still showed a statistically significant difference ($p=0.0021$), with an I square of 74.06%, which indicated high heterogeneity.

Discussion

The results of this meta-analysis showed that the P/F ratio and pulmonary compliance increased significantly when RM was used in the operation; however, the oxygenation capacity after extubation did not change significantly.

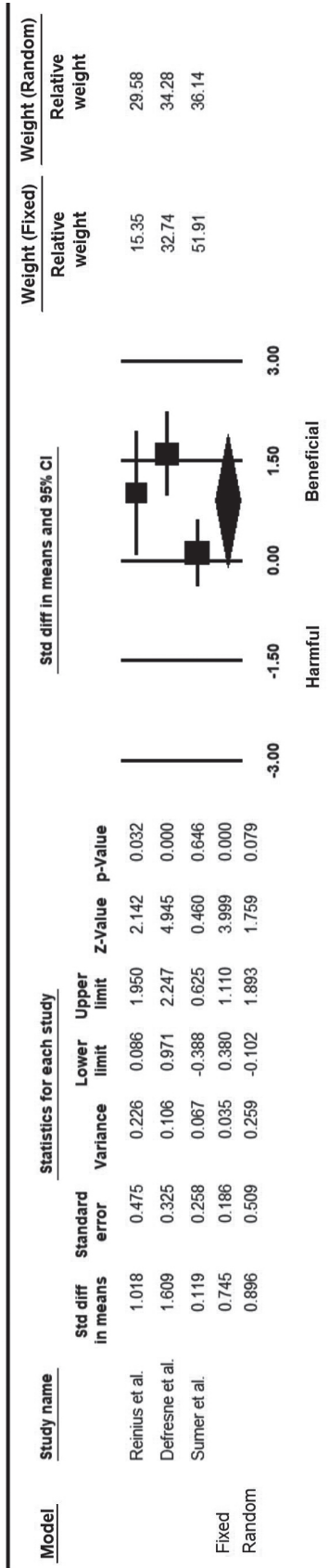
The results of the current study are the same as those published by Aldenkortt et al. (2017) and Souza *et al.* (2020); that is, when morbidly obese patients undergo weight reduction surgery, better oxygenation and pulmonary compliance can be achieved by RM [11-12]. In non-obese patients, the FRC after the induction of anesthesia decreased to about 50% of that before anesthesia, causing insufficient ventila-

Fig. 3. Forrest Plot and Heterogeneity of the Studies for the P/F Ratio of the Intervention and Control Groups – use “standard difference” below



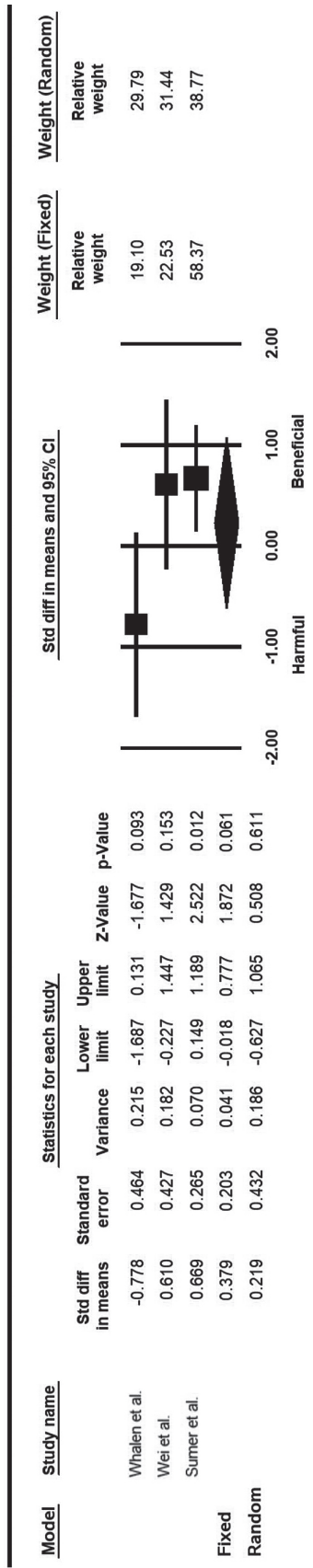
Model	Number Studies	Pooled effect size		Heterogeneity				
		Effect size	95% CI	Q-value	df (Q)	P-value	I-squared	
Fixed	6	0.956	0.141	<0.001	8.307	5	0.140	39.810
Random	6	0.992	0.187	<0.001				

Fig. 4. Forrest Plot and Heterogeneity of the Studies for Compliance of the Intervention and Control Groups – use “standard difference” below



Model		Number Studies		Pooled effect size		Heterogeneity		
Effect size	Standard Error	P-value	Q-value	df	I-squared			
Fixed	3	0.745	0.186	<0.001	13.251	2	0.001	84.907
Random	3	0.896	0.509	0.079				

Fig. 5. Forrest Plot and Heterogeneity of the Studies for the Post-extubation P/F Ratio of the Intervention and Control Groups – use “standard difference” below



Model	Number of Studies	Pooled effect size	Heterogeneity					
			Effect size	95%CI	P-value	Q-value		
Fixed	3	0.379	0.203	0.061	7.711	2	0.021	74.063
Random	3	0.219	0.432	0.611				

tion and perfusion, which resulted in shunting. With an increase in body weight, the decrease in respiratory system compliance is mainly determined by the decrease in pulmonary compliance, rather than the decrease in chest wall compliance. A more important factor regarding the decrease in pulmonary compliance may be the decrease in FRC [21-22]. When morbidly obese patients used a ventilator, RM could improve lung volume, respiratory system resistance and oxygenation.[9]

Pulmonary gas exchange and respiratory mechanics were affected in approximately 90% of patients undergoing general anesthesia. The main cause of gas exchange disorder was atelectasis. Compared with non-obese people, atelectasis was more likely to occur in obese people and persist for 24 hours after the operation [23]. Research has shown that patients with a BMI >40 kg/m² had a higher chance of postoperative pulmonary complications, such as respiratory failure, pneumonia, and use of a ventilator, as well as increased days of hospital stay [5]. Shereen E. *et al.* (2020) performed sleeve gastrectomy on 69 patients with severe obesity, and the RM intervention helped to preserve the diaphragm displacement during operation, improve forced vital capacity (FVC) and forced expiratory volume in the first second (FEV₁) within the 24 hours after the operation, and reduce atelectasis during laparoscopic gastrectomy [24]. A meta-analysis published by Yu Cui *et al.* in 2019 showed that after using RM in patients under general anesthesia, pulmonary complications, including hypoxemia, pulmonary infections, and atelectasis during hospitalization were significantly reduced (RR=0.67; 95%CI, 0.49 to 0.90; *p*<0.05) [25]. In the subgroup analysis, RM could significantly reduce the incidence of postoperative pulmonary com-

plications in non-obese patients, but could not significantly reduce the difference in the obese population (RR = 0.65; 95%CI, 0.46 to 0.91; *P* = 0.01 I² = 76% vs. RR = 1.94, 95%CI, 0.49 to 7.74; *P* = 0.35; I² = 0%). However, only 2 small-sample studies on obese people were included in the analysis, while 8 studies were included in this meta-analysis [25].

As of this time, no meta-analysis has confirmed the postoperative benefit of RM for morbidly obese patients. Therefore, this meta-analysis analyzed the P/F ratio after extubation. The results showed that the standard deviation of the P/F ratio after extubation in the RM group was 0.219 times higher than that in the control group; however, there was no statistically significant difference. According to Wei *et al.* (2018), intraoperative intervention using RM in morbidly obese patients shortened the time for extubation (21.3±9.5 vs 13.7±3.2 minutes; *P*<0.05) [19].

However, this meta-analysis has some limitations. First, the research subjects were mostly non-Asians. The definition of obesity in the Asia-Pacific population and that set by the WHO are different. In Taiwan, the Ministry of Health and Welfare defines BMI ≥27 in adults as being obese. Second, there is no unified RM operation mode, and the modes of RM in the literature are different. The RM mode in 7 articles included continuously providing positive airway pressure with a PEEP value ranging from 0–10 cmH₂O, an airway pressure of 40 cmH₂O lasting for 15–40 seconds, an airway pressure of 30 cmH₂O lasting for 120 seconds, and an airway pressure of 55 cmH₂O lasting for 10 seconds. Only one article adopted a gradual increase in PEEP value, with 10 cmH₂O for 3 breaths, 15 cmH₂O for 3 breaths, 20 cmH₂O for 10 breaths, and 12 cmH₂O for 3 breaths. Third,

this meta-analysis hoped to analyze whether there was any difference in postoperative pulmonary complications and hospitalization days in morbidly obese patients who received RM. As only 2 articles among the RCTs mentioned relevant results, the meta-analysis could not be conducted. However, the results of these 2 articles showed that there was no difference between the 2 groups. Most of the included trials lacked data on long-term results, and the sample sizes were small; therefore, studies on a larger scale are necessary in the future. However, the primary outcome of this study remained unchanged in the sensitivity analysis, which could strengthen the results of this meta-analysis.

In conclusion, when morbidly obese patients undergo weight reduction surgery, intraoperative lung dilatation can improve gas exchange and increase pulmonary compliance, and there is no evidence for significant differences in oxygenation status after extubation. In addition, there is no consensus on the mode of RM or the timing of RM intervention. Although our results show that RM intervention during operation is beneficial to morbid obesity, large-scale RCTs are still required to confirm the best mode of RM in the future for clinical application.

Acknowledgment

This study was supported by research grants from E-Da Hospital (EDA_MA_1090103, EDAH108020).

Conflict of Interest

All authors have no conflict of interest to disclose.

References

1. Hales CM, Carroll MD, Fryar CD, *et al.* Prevalence of obesity among adults and youth: United States, 2015–2016. NCHS data brief, no 288. Hyattsville, MD: National Center for Health Statistics, 2017.
2. Jones RL, Nzekwu MM. The effects of body mass index on lung volumes. *Chest* 2006; 130(3): 827-833.
3. Salome CM, King GG, Berend N. Physiology of obesity and effects on lung function. *J Appl Physiol* (1985) 2010; 108(1): 206-211.
4. Heymsfield SB, Wadden TA. Mechanisms, pathophysiology, and management of obesity. *N Engl J Med* 2017; 376(3): 254-266.
5. Ball L, Hemmes SNT, Serpa Neto A, *et al.* Intraoperative ventilation settings and their associations with postoperative pulmonary complications in obese patients. *Br J Anaesth* 2018; 121(4): 899-908.
6. Hedenstierna G, Edmark L. The effects of anesthesia and muscle paralysis on the respiratory system. *Intensive Care Med* 2005; 31(10): 1327-1335.
7. Bazurro S, Ball L, Pelosi P. Perioperative management of obese patient. *Curr Opin Crit Care* 2018; 24(6): 560-567.
8. Imber DA, Pirrone M, Zhang C, *et al.* Respiratory management of perioperative obese patients. *Respir Care* 2016; 61(12): 1681-1692.
9. Pirrone M, Fisher D, Chipman D, *et al.* Recruitment maneuvers and positive end-expiratory pressure titration in morbidly obese ICU patients. *Crit Care Med* 2016; 44(2): 300-307.
10. HHess DR. Recruitment maneuvers and PEEP titration. *Respir Care* 2015; 60(11): 1688-1704.
11. Aldenkortt M, Lysakowski C, Elia N, *et al.* Ventilation strategies in obese patients undergoing surgery: a quantitative systematic review and meta-analysis. *Br J Anaesth* 2012; 109(4): 493-502.
12. Costa Souza GM, Santos GM, Zimpel SA, *et al.* Intraoperative ventilation strategies for obese patients undergoing bariatric surgery: systematic review and meta-analysis. *BMC Anesthesiol* 2020; 20(1): 36.
13. Whalen FX, Gajic O, Thompson GB, *et al.* The effects of the alveolar recruitment maneuver and positive end-expiratory pressure on arterial oxygenation during laparoscopic bariatric surgery. *Anesth Analg* 2006;

- 102(1): 298-305.
14. Chalhoub V, Yazigi A, Sleilaty G, *et al.* Effect of vital capacity manoeuvres on arterial oxygenation in morbidly obese patients undergoing open bariatric surgery. *Eur J Anaesthesiol* 2007; 24(3): 283-288.
 15. Reinius H, Jonsson L, Gustafsson S, *et al.* Prevention of atelectasis in morbidly obese patients during general anesthesia and paralysis: a computerized tomography study. *Anesthesiology* 2009; 111(5): 979-987.
 16. de Souza AP, Buschpigel M, Mathias LA, *et al.* Analysis of the effects of the alveolar recruitment maneuver on blood oxygenation during bariatric surgery. *Rev Bras Anesthesiol* 2009; 59(2): 177-186.
 17. Futier E, Constantin JM, Pelosi P, *et al.* Noninvasive ventilation and alveolar recruitment maneuver improve respiratory function during and after intubation of morbidly obese patients: a randomized controlled study. *Anesthesiology* 2011; 114(6): 1354-1363.
 18. Defresne AA, Hans GA, Goffin PJ, *et al.* Recruitment of lung volume during surgery neither affects the postoperative spirometry nor the risk of hypoxaemia after laparoscopic gastric bypass in morbidly obese patients: a randomized controlled study. *Br J Anaesth* 2014; 113(3): 501-507.
 19. Wei K, Min S, Cao J, *et al.* Repeated alveolar recruitment maneuvers with and without positive end-expiratory pressure during bariatric surgery: a randomized trial. *Minerva Anesthesiol* 2018; 84(4): 463-472.
 20. Sumer I, Topuz U, Alver S, *et al.* Effect of the "recruitment" maneuver on respiratory mechanics in laparoscopic sleeve gastrectomy surgery. *Obes Surg* 2020; 30(7): 2684-2692.
 21. Pelosi P, Gregoretti C. Perioperative management of obese patients. *Best Pract Res Clin Anaesthesiol* 2010; 24(2): 211-225.
 22. Hodgson LE, Murphy PB, Hart N. Respiratory management of the obese patient undergoing surgery. *J Thorac Dis* 2015; 7(5): 943-952.
 23. LZonneveld B, Vu D, Snelder SM, *et al.* Short-term mortality and postoperative complications of abdominal aortic aneurysm repair in obese versus non-obese patients. *J Obes Metab Syndr* 2021 Dec 30; 30(4):377-385. doi: 10.7570/jomes21057.
 24. Abd Ellatif SE, Mowafy SMS. Ultrasonographic evaluation of the effect of recruitment maneuvers and positive end-expiratory pressure on diaphragmatic functions in obese patients undergoing laparoscopic sleeve gastrectomy: A randomized controlled study. *Egypt J Anaesth* 2020; 36(1): 69-77.
 25. Cui Y, Cao R, Li G, *et al.* The effect of lung recruitment maneuvers on post-operative pulmonary complications for patients undergoing general anesthesia: A meta-analysis. *PLoS One* 2019; 14(5): e0217405.

Tracheobronchopathia Osteochondroplastica: A Rare Incidental Diagnosis

Chun Lin¹, Kuo-Hsuan Hsu^{1,2}

Tracheobronchopathia osteochondroplastica (TO) is a rare disease with a benign nature. The etiology and incidence remain unclear. We present the case of a 67-year-old male with a history of completely treated pulmonary tuberculosis and chronic obstructive pulmonary disease who was admitted due to productive cough. Imaging studies of the thorax, including chest radiography and chest computed tomography, showed partial collapse of the right upper lobe of the lung. Bronchoscopy revealed multiple hard nodular lesions at the anterior tracheal wall, and biopsy was performed. Pathological evaluation of the lesions revealed results compatible with TO. The patient is currently being followed up regularly at our outpatient department. (*Thorac Med* 2022; 37: 80-84)

Key words: tracheobronchopathia osteochondroplastica; bronchoscopic biopsy

Introduction

Tracheobronchopathia osteochondroplastica (TO) is a rare benign disease with an unclear incidence and etiology [1]. Most patients with this disease are asymptomatic and are diagnosed incidentally by bronchoscopic or radiologic examination. According to previous reports, the most common symptoms of TO, such as dyspnea on exertion, chronic cough and sputum production, resemble those of other pulmonary diseases [2-5]. Bronchoscopy remains the gold standard for diagnosis. We herein present a case of TO diagnosed incidentally during bronchos-

copy and provide a review of the literature.

Case Report

The patient was a 67-year-old man who was transferred to our hospital because of intermittent fever and decreased appetite. He had a medical history of completely treated pulmonary tuberculosis, hypertension, and chronic obstructive pulmonary disease. He was a retired sewer cleaner (he had worked for about 20 years), and was a carpenter for 8 years. He did not smoke tobacco, drink alcohol, or use illicit drugs or herbs.

¹Division of Chest Medicine, Department of Internal Medicine, Taichung Veterans General Hospital, Taichung, Taiwan, ²Division of Critical Care and Respiratory Therapy, Department of Internal Medicine, Taichung Veterans General Hospital, Taichung, Taiwan.

Address reprint requests to: Dr. Kuo-Hsuan Hsu, Division of Chest Medicine, Department of Internal Medicine, Taichung Veterans General Hospital, 1650 Taiwan Boulevard Sect. 4, Taichung, Taiwan 40705

Five years before this admission, he underwent 9 months of anti-tuberculosis therapy for pulmonary tuberculosis at another hospital and had completely recovered. His regular medications included inhaled bronchodilators for chronic obstructive pulmonary disease (tiotropium/olodaterol) and an anti-hypertensive agent (valsartan).

Seven days before transfer to this hospital, intermittent fever with temperatures of up to 38°C, chills, and productive cough with yellowish sputum developed. The symptoms were accompanied with sweating, anorexia, mild dyspnea, and general soreness. He had no headache, sore throat, abdominal discomfort, or body weight loss. The symptoms persisted for 4 days, and 3 days before this admission, the patient presented to the outpatient department of another hospital.

On presentation to the other hospital, his body temperature was 39.8°C. Auscultation of the chest revealed bilateral expiratory wheezing. Chest radiograph showed increased radiopacity in the medial aspect of the right upper lung field. Laboratory data showed a white blood cell count of 10680 / μ L with a left shift (neutrophils: 87%), and elevated serum high-sensitivity C-reactive protein (18.68 mg/dL). He was admitted to the general ward at the hospital and intravenous cefuroxime was initiated. Chest computed tomography (CT) scan showed an area of increased opacity extending from the right hilum. Fluid bronchogram and pulmonary vessels were found within the opacity, compatible with right upper lobe collapse. He was hospitalized there for 3 days and subsequently transferred to the emergency department of our hospital.

On examination, his body temperature was 36.8°C, heart rate was 78 beats per minute, and

blood pressure was 204/98 mm Hg. The oxygen saturation was 96% under ambient air. No increased breathing effort was noted. Ampicillin/sulbactam were administered as empiric antibiotics for suspected obstructive pneumonitis. The symptoms subsided after medical treatment. Two sets of cultures from the blood yielded negative results. A review of previous CT scans showed progressive volume reduction of the right upper lobe of the lung, which was suspected to be related to the previous pulmonary tuberculosis. Also, calcified lesions along the tracheal wall were found (Figure 1). Flex-

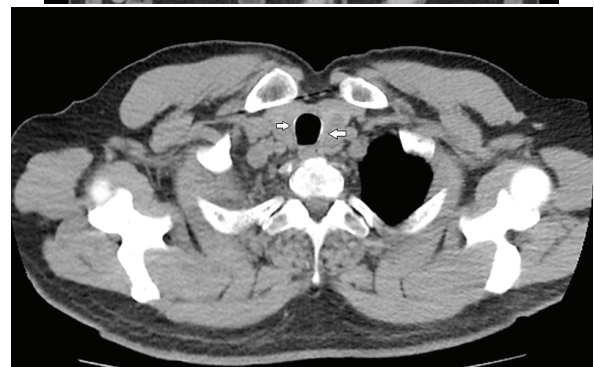


Fig. 1. Chest computed tomography showed calcified lesions (arrows) on the tracheal wall.

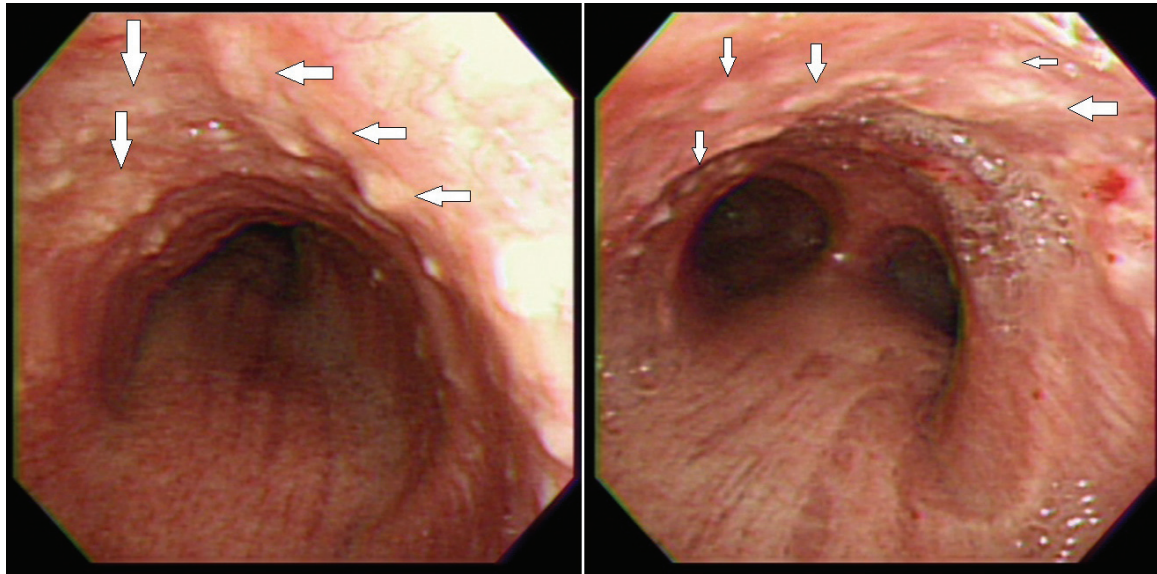


Fig. 2. Bronchoscopy revealed nodular lesions (arrows) on the tracheal wall.

ible bronchoscopy was performed on hospital day 2, but there were no obvious endobronchial lesions nor signs of external compression. However, multiple hard nodular lesions on the anterior and lateral tracheal wall without involvement of the posterior portion were found (Figure 2). Biopsies of these nodular lesions were obtained. The patient was discharged on hospital day 6. Microscopic examination of the specimens revealed blood and tiny fragments of bronchial tissue, as well as some floating epithelial cells, which showed mild cellular atypia. Cultures from the biopsy specimens were negative for mycobacteria and pathogenic fungus.

The patient was readmitted 19 days after discharge for repeated endobronchial biopsy and histopathologic confirmation. Flexible bronchoscopic biopsy of the nodular lesions was performed on hospital day 2 of this admission. The patient was discharged on hospital day 3 without complications related to the procedure. Pathological examination of the specimens revealed bronchial mucosa with

submucosal inflammatory cells infiltration and calcification (Figure 3). The pathological result was compatible with the diagnosis of TO. The patient was seen at our outpatient department 8 days after discharge, and no recurrent symptoms were observed. He is being followed up regularly at our outpatient department.

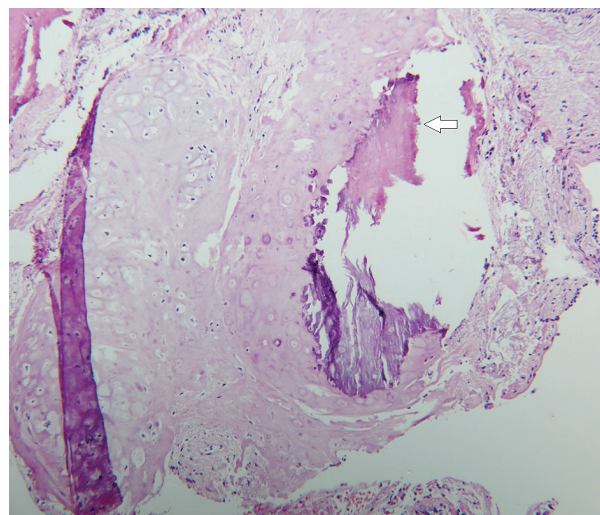


Fig. 3. Pathology showed bronchial mucosa with inflammatory cells infiltrating the submucosal area. Calcification (arrow) was seen.

Discussion

Epidemiology

Tracheobronchopathia osteochondroplastica (TO) is a rare benign disease with an unclear etiology, and was first described by Wilks in 1857 [6]. In previous reports, the detection rate for this disease ranged from 3/1000 autopsies to 0.05% in a single institute cohort of 41,600 patients who had undergone fiberoptic bronchoscopies [1,2]. However, the overall incidence is unknown, as most patients are asymptomatic or have non-specific symptoms. No gender difference was observed in previous studies [1-3], and most cases were diagnosed in the fourth to seventh decade of life [6].

Clinical characteristics

In the literature, the clinical presentations of TO varied greatly. Most patients were asymptomatic and were diagnosed incidentally by bronchoscopy or radiology exam. The most common symptom was chronic cough. Other symptoms included dyspnea on exertion, sputum production, chest pain, hemoptysis, and stridor [2-5]. Central airway obstruction related to TO has been reported, as well [6].

Diagnosis

The diagnosis of TO mainly relied on bronchoscopy. The typical bronchoscopy finding was the presence of hard nodules and ossified lesions arising from the anterior and lateral wall of the airway. This disease involved the cartilaginous portion of the trachea, and usually did not involve the posterior wall [6-7]. In some cases, amyloidosis or papillomatosis was noted, presenting as nodular lesions within the tracheal lumen, and in these patients, the posterior tracheal wall was not spared.

The typical CT finding was calcified nodules in the cartilaginous trachea (with sparing of the posterior membrane). Other clinical conditions such as amyloidosis, warfarin usage, and relapsing polycondritis may also cause tracheal calcification; these characteristics are listed in Table 1 [5]. Biopsy of the lesion for diagnostic confirmation was considered reasonable by some authors. Typical histopathologic findings in TO included inflammatory cell infiltration, squamous metaplasia, submucosal cartilage, submucosal ossification, and calcification. [2,4,6].

In our case, the pathological reports of 2 biopsies were different. We believe that this result may be due to the difficulty of obtaining specimens with biopsy forceps because of the hard nature of these osseous lesions. A previous study had reported a diagnostic yield of 55% after the initial biopsy with flexible bronchoscopy, and 70% after repeated biopsies [6]. Another possible reason for our differing pathological reports may be that various biopsy sites were used, since we biopsied the lesions more randomly during the first exam.

Treatment

In the previous literature, no widely accepted standard therapeutic approach was used, and treatment was mainly with antitussives and expectorants for symptom relief [2,4,6]. Interventional bronchoscopy for symptom relief in affected patients has been reported, either with laser therapy or direct removal of the lesions with biopsy forceps [3,6]. The progression of TO is usually slow and minimal.

In conclusion, TO is a rare and relatively benign disease. The symptoms are non-specific. Bronchoscopy and radiologic examination can help to establish the diagnosis. Treatment is

largely conservative, and intervention bronchoscopy may provide some degree of symptom relief in severe cases. Long-term follow-up is necessary for these patients.

References

1. Lundgren R, Stjernberg NL. Tracheobronchopathia osteochondroplastica. A clinical bronchoscopic and spirometric study. *Chest* 1981; 80: 706-9.
2. Zhu Y, Wu N, Huang HD, *et al.* A clinical study of tracheobronchopathia osteochondroplastica: findings from a large Chinese cohort. *PLoS One* 2014; 9: e102068.
3. Jabbardarjani HR, Radpey B, Kharabian S, *et al.* Tracheobronchopathia osteochondroplastica: presentation of ten cases and review of the literature. *Lung* 2008; 186: 293-7.
4. Luo T, Zhou H, Meng J. Clinical characteristics of tracheobronchopathia osteochondroplastica. *Respir Care* 2019; 64: 196-200.
5. Chung JH, Kanne JP, Gilman MD. CT of diffuse tracheal diseases. *AJR Am J Roentgenol* 2011; 196: W240-6.
6. Abu-Hijleh M, Lee D, Braman SS. Tracheobronchopathia osteochondroplastica: a rare large airway disorder. *Lung* 2008; 186: 353-9.
7. Al-Qadi MO, Artenstein AW, Braman SS. The "forgotten zone": acquired disorders of the trachea in adults. *Respir Med* 2013; 107: 1301-13.
8. Prince JS, Duhamel DR, Levin DL, *et al.* Non-neoplastic lesions of the tracheobronchial wall: radiologic findings with bronchoscopic correlation. *Radiographics* 2002; 22 Spec No: S215-30.
9. Moncada RM, Venta LA, Venta ER, *et al.* Tracheal and bronchial cartilaginous rings: warfarin sodium-induced calcification. *Radiology* 1992; 184: 437-9.

Systemic Air Embolism Occurring after Transthoracic Needle Biopsy -- a Rare but Lethal Post-Procedural Complication

Yi-Jhih Huang^{1,2}, Chung-Kan Peng³, Shih-Chun Lee¹, Cheng-Kuang Chang⁴, and Kun-Lun Huang³

Chest computed tomography (CT)-guided percutaneous core needle biopsy (PCNB) is a well-established, but relatively less invasive procedure than surgical open lung biopsy for the diagnosis of pulmonary lesions. The physician should be aware of possible fatal complications during this procedure, such as massive bleeding, tension pneumothorax, or systemic air embolism (AE). Systemic AE is a rare but critical complication that occurs following CT-guided PCNB. Although the occurrence of systemic AE might be underestimated, the overall incidence rate after performing a CT-guided PCNB is less than 1%. Documented risk factors for AE were positive pressure ventilation, targeting a cavitory lesion, location of the tumor, depth of the targeting lesion, or special position of the patient during the biopsy. The possible mechanisms might be related to the direct puncture of a pulmonary vein, or transient fistula between the airway and a pulmonary vein. Physicians should always keep this complication in mind. The immediate management includes 100% oxygen supplementation, a left lateral decubitus position, and hyperbaric oxygen therapy. (*Thorac Med* 2022; 37: 85-89)

Key words: hyperbaric oxygen therapy, percutaneous core needle biopsy of the chest, systemic air embolism

Introduction

Systemic air embolism (AE) is defined as the air or gas that presents in the pulmonary venous system and flushes into systemic circulation due to the pressure gradient. The overall incidence rate of AE after percutaneous core

needle biopsy (PCNB) has varied enormously between institutions [1-3]. Several factors may also have affected the occurrence rate or the detection rate of systemic AE. An acceptable statement of the incidence rate of life-threatening AE is an estimated 0.01 to 0.89%, but the true incidence of AE after computed tomography

¹Division of Thoracic Surgery, Department of Surgery, Tri-Service General Hospital, ²Department of Oncology, Radiobiology Research Institute, Churchill Hospital, University of Oxford, ³Division of Pulmonary and Critical Care Medicine, Department of Internal Medicine, Tri-Service General Hospital, ⁴Department of Radiology, Tri-Service General Hospital.

Address reprint requests to: Dr. Kun-Lun Huang, Division of Pulmonary and Critical Care Medicine, Department of Internal Medicine, Tri-Service General Hospital, National Defense Medical Center, B1F, No. 325, Sec 2, Cheng-Gong Road, Neihu District, Taipei City 114, Taiwan.

(CT)-guided PCNB may be still underestimated due to asymptomatic or subclinical presentations [1-5]. Systemic AE is a rare disease, but it can be a lethal complication following PCNB. Herein, we report a critical case of systemic AE that presented with synchronous acute coronary syndrome and acute ischemic stroke and was successfully treated by timely hyperbaric oxygen (HBO) therapy.

Case

A 62-year-old male had a history of adenocarcinoma of the sigmoid colon, pT4aN0M0, stage IIB. He underwent laparoscopic resection in July 2000 and finished adjuvant chemotherapy. Chest CT, which was arranged in March 2018, revealed a solitary pulmonary nodule measuring 1.3 cm, peripherally located at the lateral segment of the right middle lobe of the lung. CT-guided PCNB was performed on the left side in a semi-prone position (Figure 1A). After completion of the biopsy process, the patient felt agitated, and had chest pain and cold

sweating. Bradycardia (33 bpm) with hypotension (75/46 mmHg) occurred. He also complained of left-side hemiparalysis at the same time. The post-puncture CT image showed a remarkable air-fluid level at the ascending aorta, and air thrombus at the left anterior descending coronary artery (Figure 1B, arrow and star). The electrocardiogram showed bradycardia, with ST-elevation at leads II, III, aVF, and V1-3 (Figure 2A). Acute ST-elevation myocardial infarction and concurrent ischemic stroke were suspected.

With a diagnosis of systemic pulmonary arterial AE, 100% oxygen was given via a non-rebreathing mask, and emergency HBO was initiated within 1-hour post-PCNB (treatment protocol: 50 ft. depth, 138 minutes). The electrocardiogram showed a return to a normal sinus rhythm immediately after HBO (Figure 2B), and the muscle power of the left-side extremities completely recovered. He underwent chest CT again 2 hours after HBO, and the intravascular air bubble had disappeared. The troponin-I level was <0.010 ng/mL (baseline),

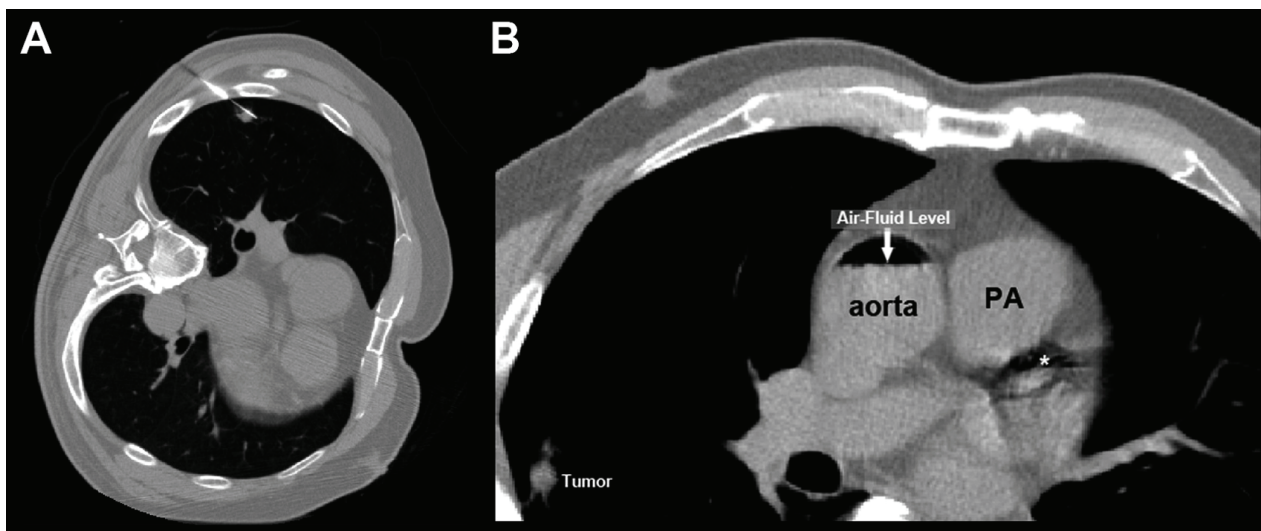


Fig. 1. Chest computed tomography-guided transthoracic needle biopsy (Figure 1A), intra-aortic air-fluid level (Figure 1B, arrow), and air bubble in the left anterior descending coronary artery (Figure 1B, star).

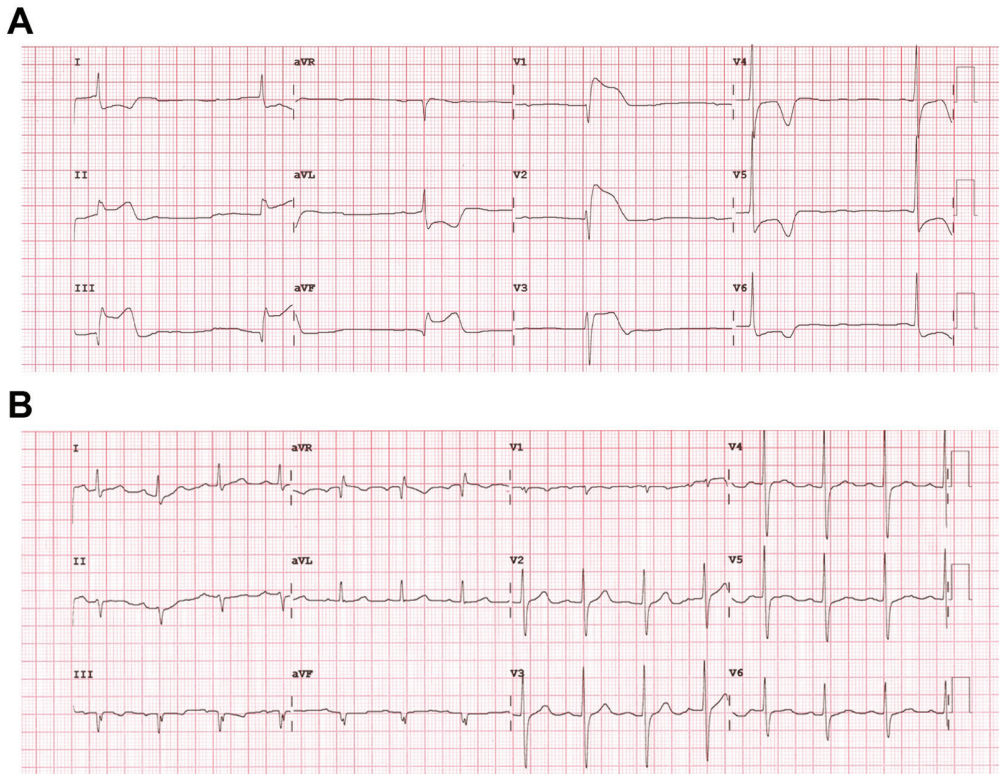


Fig. 2. Electrocardiogram performed before (Figure 2A) and after (Figure 2B) hyperbaric oxygen therapy.

0.224 ng/mL (4 hours later), 0.198 ng/mL (18 hours later), and 0.109 ng/mL (36 hours later). The diffusion-weighted magnetic resonance imaging of the brain showed a small, residual lacunar infarction at the right occipital region. Otherwise, there was no neurologic sequela or associated end-organ damage.

Discussion

The true incidence rate of systemic AE after PCNB is still debated. A recently published cohort study, which enrolled 2,026 CT-guided PCNB procedures, asserted that only 19 patients had been diagnosed as having AE, and the incidence rate was 0.9% [6]. Among all the cases in this cohort, the major distribution of the accumulated air was at the left atrium or

ventricle. All the patients received 100% oxygen. Yet, HBO therapy was given only to those patients who developed low blood pressure or shock. The outcome of these patients was excellent: they all survived and there were no negative sequelae.

There are 3 possible mechanisms that can contribute to this phenomenon. Aside from the direct puncture of a pulmonary vein or transient fistula between the airway (bronchioles or alveoli) and pulmonary veins, direct passage from pulmonary arteries to pulmonary veins is possible [7]. Ibukuro et al. offered a pathological review of an AE case and argued that the air might have entered the large pulmonary vein via the injured vessels [5]. However, since the large pulmonary vein was invisible on the CT scan of this patient, and the radiologist always

plans the puncture path in order not to penetrate large vessels, this point of view is highly questionable. Consequently, risk factors for systemic AE after performing CT-guided PCNB of pulmonary lesions are still controversial.

Reported risk factors for AE were positive pressure ventilation (including intubated general anesthesia), targeting a cavitory lesion, location or depth of the biopsied tumor, or special positioning of the patient, such as in a prone or right lateral decubitus position, during PCNB [3, 7-8]. Monnin-Bares *et al.* recently reported a series of 27 patients that had been reported as having systemic AE. Multivariate analysis of the risk factors associated with systemic AE revealed that the position of the patient during biopsy was a risk factor of utmost importance. Compared to the supine or left lateral decubitus position, the odds ratios for the prone position and right lateral decubitus position were 3.12 and 6.15, respectively [3]. Other contributing risk factors include the number of biopsy samples and the number of pleural passes.

Since the risk factors are known, physicians and radiologists try to make changes in order to prevent systemic AE from happening. Freund *et al.* placed emphasis on the frequency and the risk factors associated with the incidence of systemic AE after CT-guided PCNB. The occurrence rate of systemic AE was 3.8% and the incidence rate of symptomatic systemic AE was 0.49%. Likewise, penetration depth, general intubated anesthesia, prone positioning, and the location of the lesion were proven to be independent risk factors for the entire cohort. In 2017, Glodny *et al.* reexamined the effect of patient positioning on post-procedural systemic AE [7]. They implemented a “protective measurement” by adjusting patient positioning so that the target lung lesion was located below the

horizontal level of the left atrium. Compared with the previous cohort that did not apply the protective measurement, this “ipsilateral-dependent position” significantly reduced the occurrence of systemic AE from 3.77% to 0.16% ($p < 0.001$). However, Fintelmann *et al.* disagreed with the suggestion and contended that the optimal position of the patient is dependent on the relative location of the tumor, pulmonary fissures, and vessels. Furthermore, they also point out that, by applying some normal saline in the needle hub, radiologists can significantly prevent air from filling the pulmonary vessels while removing the stylet of the puncture needle. Apparently, there are several technical issues that have not been completely addressed.

Management of these life-threatening complications includes early recognition, rapid resuscitation, 100% oxygen inhalation by non-rebreathing mask, and prompt HBO [9-10]. The optimal timing of HBO for these systemic AE patients is not conclusive. Previous studies have found that, ideally, it is beneficial to initiate HBO within 1 to 6 hours. Nevertheless, some studies also suggested that HBO still had a beneficial role 30 hours after the episode for these AE patients. For near-fatal AE patients, if HBO is not accessible, 100% oxygen supplementation with or without endotracheal tube intubation may also be helpful [8]. The Trendelenburg position is also reported to be a proper position for patients with systemic AE.

In conclusion, systemic AE after PCNB is a rare but life-threatening complication. Although the true causes and risk factors of AE are still being debated, physicians should be alert for any abnormal clinical manifestation after each thoracic puncture. Post-procedural CT scan should be arranged routinely for early detection of AE.

Conflicts of interest

The authors declare that they have no conflicts of interest.

Patient consent

Consent was obtained from the patient.

References

1. Jang H, Rho JY, Suh YJ, *et al.* Asymptomatic systemic air embolism after CT-guided percutaneous transthoracic needle biopsy. *Clin Imaging* 2019; 53: 49-57.
2. Marchak K, Hong MJ, Schramm KM. Systemic air embolism following CT-guided percutaneous core needle biopsy of the lung: case report and review of the literature. *Semin Intervent Radiol* 2019; 36: 68-71.
3. Monnin-Bares V, Chassagnon G, Vernhet-Kovacsik H, *et al.* Systemic air embolism depicted on systematic whole thoracic CT acquisition after percutaneous lung biopsy: incidence and risk factors. *Eur J Radiol* 2019; 117: 26-32.
4. Pando Sandoval A, Ariza Prota MA, Garcia Clemente M, *et al.* Air embolism: a complication of computed tomography-guided transthoracic needle biopsy. *Respirol Case Rep* 2015; 3: 48-50.
5. Ibukuro K, Tanaka R, Takeguchi T, *et al.* Air embolism and needle track implantation complicating CT-guided percutaneous thoracic biopsy: single-institution experience. *AJR Am J Roentgenol* 2009; 193: W430-6.
6. Liu SH, Fu Q, Yu HL, *et al.* A retrospective analysis of the risk factors associated with systemic air embolism following percutaneous lung biopsy. *Exp Ther Med* 2020; 19: 347-52.
7. Glodny B, Schonherr E, Freund MC, *et al.* Measures to prevent air embolism in transthoracic biopsy of the lung. *AJR Am J Roentgenol* 2017; 208: W184-W91.
8. Cheng HM, Chiang KH, Chang PY, *et al.* Coronary artery air embolism: a potentially fatal complication of CT-guided percutaneous lung biopsy. *Br J Radiol* 2010; 83: e83-5.
9. Kjellberg A, Nystrom H, Soderberg M, *et al.* Massive air embolism as a complication of upper gastrointestinal endoscopy: A case report illustrating a stroke mimic, literature review, and suggested management. *Clin Case Rep* 2018; 6: 1862-7.
10. McCarthy CJ, Behraves S, Naidu SG, *et al.* Air embolism: diagnosis, clinical management and outcomes. *Diagnostics (Basel)* 2017; 7.

Diffuse Alveolar Hemorrhage Shortly After Breast Augmentation Surgery: A Case Report

Ting-Chia Chang¹, Hsiu-Nien Shen²

Diffuse alveolar hemorrhage (DAH) associated with negative-pressure pulmonary edema (NPPE) is a rare cause of acute respiratory failure that occurs after an extreme inspiratory effort against an obstructed airway, such as post-extubation laryngospasm after surgery. Herein, we report a 27-year-old previously healthy woman who underwent breast augmentation surgery in a cosmetic surgery clinic and presented with dyspnea and acute hypoxemic respiratory failure associated with the classic triad of DAH (i.e., hemoptysis, anemia and pulmonary infiltrates) shortly after extubation. A diagnosis of NPPE-related DAH was made based on clinical conditions and the exclusion of other potential causes. After supportive treatment, the patient recovered and was weaned from the ventilator within a few days. (*Thorac Med* 2022; 37: 90-95)

Key words: diffuse alveolar hemorrhage; negative-pressure pulmonary edema; breast augmentation surgery

Introduction

Diffuse alveolar hemorrhage (DAH) associated with negative-pressure pulmonary edema (NPPE) is a rare, potentially fatal condition [1]. NPPE, first reported in 1997 [2], usually occurs shortly after extubation [1], and is caused by postoperative laryngospasm with acute severe upper airway obstruction, which resembles a Müller maneuver, generates extremely negative thoracic pressure, increases pulmonary blood flow and transmural capillary pressure, and eventually leads to alveolar capillary membrane damage with pulmonary edema and hemorrhage

[1]. The classic triad of pulmonary hemorrhage (i.e., hemoptysis, anemia and pulmonary infiltrates) [3] is present in only half of the patients with NPPE-related DAH [1]. Therefore, awareness of the clinical context is of critical importance in the diagnosis of this condition. In this report, we describe a case of DAH associated with NPPE which developed shortly after breast augmentation surgery.

Case Presentation

A 27-year-old previously healthy woman was referred to our emergency department due

¹Department of Internal Medicine, Chi Mei Medical Center,

²Department of Intensive Care Medicine, Chi Mei Medical Center.

Address reprint requests to: Dr. Hsiu-Nien Shen, Department of Intensive Care Medicine, Chi Mei Medical Center, Yong-Kang District, Tainan City, Taiwan

to hemoptysis and acute hypoxemic respiratory failure that developed shortly after breast augmentation surgery in a cosmetic surgery clinic. At that time, she underwent surgery with Motiva® Implants (Establishment Labs Holdings, Inc.) under general anesthesia using a propofol infusion and was extubated in the recovery room. Shortly after extubation, dyspnea, hemoptysis and desaturation developed. She received endotracheal intubation, and then was referred to our hospital, where she was admitted to the intensive care unit. She had been well before the surgery, did not smoke, drink alcohol or take any medication, and had no history of hemoptysis or a bleeding tendency.

On physical examination, she appeared pale and anxious, with copious pink-to-fresh-bloody secretions from the endotracheal tube during coughing episodes. Her body temperature was 37.3°C, pulse rate was 85 (regular) per minute, respiratory rate was 26 per minute, and blood pressure was 144/74 mmHg. Initial pulse oximeter showed a peripheral capillary oxygen saturation (SpO₂) of 100% under mechanical ventilation with a fraction of inspired oxygen (FiO₂) of 45% and a positive end expiratory pressure of 10 cmH₂O. Bilateral lung crackles were noticed. There was no jaundice, jugular vein engorgement, heart murmur, peripheral edema, petechiae or bruises.

The results of laboratory examinations were remarkable, with a white cell count of 20.8 per cubic millimeter (normal range: 3.2-9.2), and a hemoglobin level of 9.6 gm/dL (normal range: 11.6-14.8). However, the results were normal for liver enzymes, creatinine, platelet count, prothrombin and partial thromboplastin time, brain natriuretic peptide, and cardiac enzymes. Arterial blood gas analysis showed a pH of 7.335, a carbon dioxide tension of 31.6 mmHg,

an oxygen tension (PaO₂) of 66.9 mmHg, and bicarbonates of 17.0 mEq per liter (under an FiO₂ of 60%). Electrocardiography showed normal sinus rhythm without a significant ST-T change. The urinalysis result did not show proteinuria or hematuria. Chest radiograph showed a normal heart size and bilateral dense consolidations with a central distribution and almost complete white-out in the right lung (Figure 1). Computed tomography (CT) of the chest revealed that the consolidations were located predominantly in the central and dependent areas, and that septal lines and peribronchial cuffing were present in the background of ground glass opacifications in the peripheral and non-

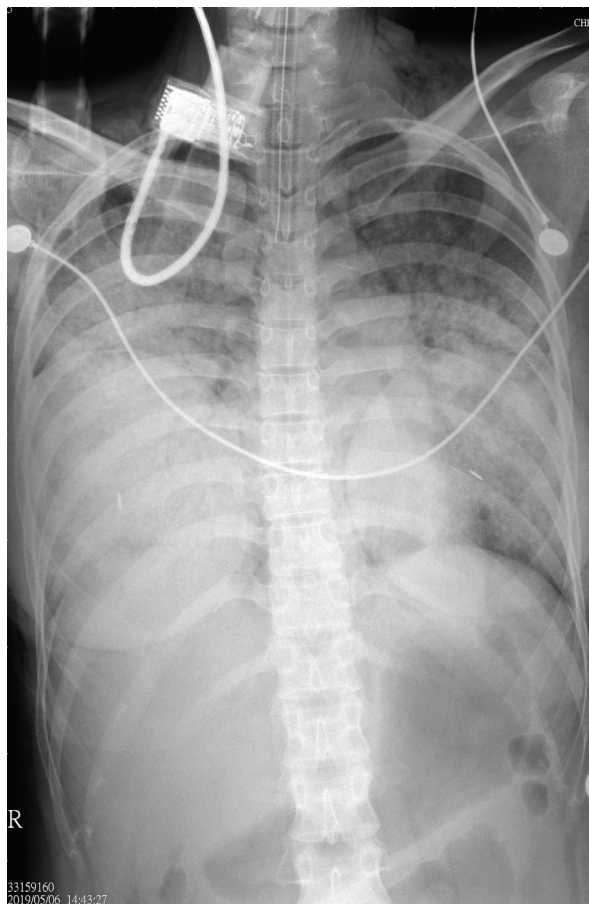


Fig. 1. Chest X-ray showed bilateral dense consolidations with a central distribution and a nearly complete white-out of the right lung.

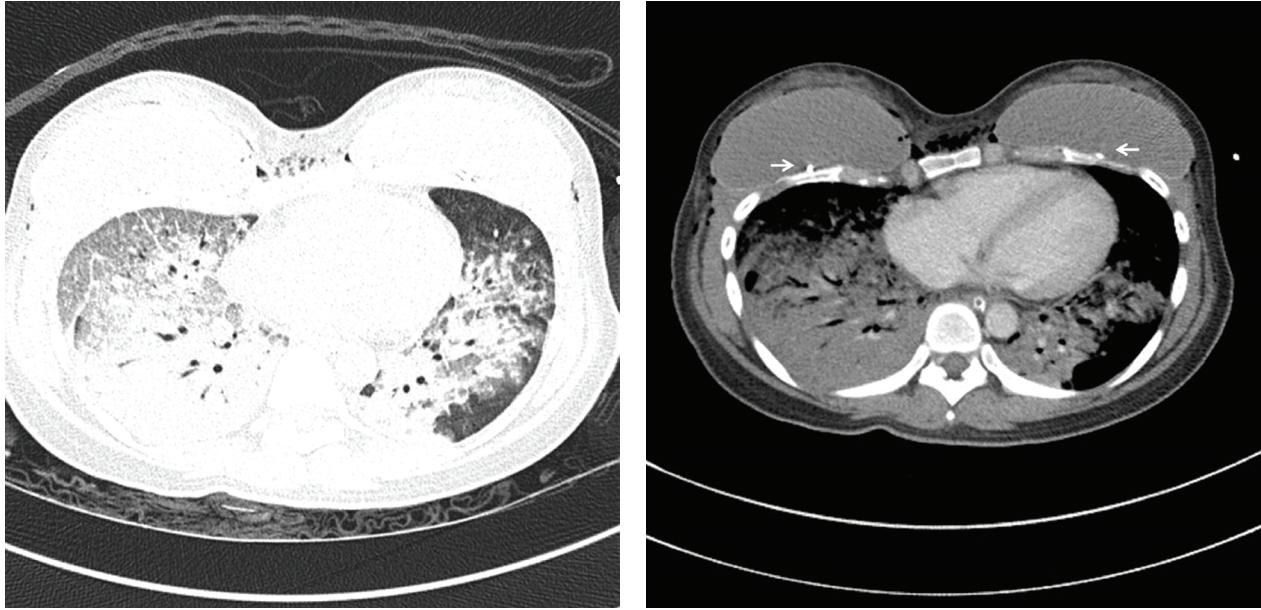


Fig. 2. Computed tomography of the thorax revealed subcutaneous emphysema associated with bilateral breast implants (A), consolidations predominantly in the central/dependent areas and septal lines and peribronchovascular cuffing in the background of ground glass opacifications in the peripheral/non-dependent parts (B). Note: Each Motiva implant® is incorporated with a microtransponder (Qid®) (arrow).

dependent parts (Figure 2A and 2B), a finding suggestive of alveolar edema. There was no CT evidence of pulmonary embolism. Trans-thoracic echocardiography revealed a normal left ventricular function. A diagnosis of DAH was then made. Given the clinical presentation shortly after the surgery, NPPE was considered to be the most likely cause of the DAH. However, other potential causes such as vasculitis or capillaritis and infection could not be excluded.

The patient was empirically treated with tazobactam/piperacillin, methylprednisolone (2mg/kg/day), norepinephrine (10 µg /min), and continuous infusion of midazolam and propofol for protective mechanical ventilation. Bronchoscopy was not performed due to severe hypoxemia ($\text{PaO}_2/\text{FiO}_2$ ratio = 111.5, shown above). The hemoglobin level dropped to 6.6 gm/dL 2 days later. There was no other source of blood loss, except the lungs. In the following days, her oxygenation improved, pulmonary

hemorrhage decreased and lung consolidations resolved gradually (Figure 3). She was successfully weaned off the ventilator on day 5.

Microbiological workups for bacterial, fungal and viral infections were non-revealing. Immunological tests (including antinuclear antibodies, rheumatoid factor, anti-neutrophil cytoplasmic antibodies, and anti-basement membrane antibodies) were normal. The antibiotic and corticosteroid were discontinued after the negative results. The patient was discharged from the hospital on day 8 and had no hemoptysis thereafter.

Discussion

We described a previously healthy woman presenting with dyspnea and acute hypoxemic respiratory failure associated with the classic triad of DAH (i.e., hemoptysis, anemia and pulmonary infiltrates) [1] shortly after breast aug-

mentation surgery. A diagnosis of NPPE-related DAH was made based on the clinical context and the exclusion of other potential causes. Treatment of NPPE-related DAH is mainly supportive. The patient recovered and was weaned from the ventilator within a few days.

Diagnosis of DAH usually requires sequential bronchoscopic alveolar lavage (BAL) to demonstrate progressively hemorrhagic samples, because hemoptysis may be absent in up to one-third of the patients, and the chest

radiographic findings of DAH are non-specific [4]. The causes of DAH are diverse, and can be categorized into 3 histopathologic patterns: pulmonary capillaritis, bland pulmonary hemorrhage (i.e., without vasculitis or capillaritis), and diffuse alveolar damage [4].

Patients with DAH usually present clinically with 1 of 2 scenarios, i.e., DAH associated with or without systemic findings, and with another process or condition [4-5]. Surgical lung biopsy may be needed if serologic testing



Fig. 3. Chest X-ray showed resolution of lung consolidations.

or clinical history is unrevealing [4]. In our patient, the manifestations of hemoptysis, a falling hematocrit, and diffuse pulmonary infiltrates were consistent with the diagnosis of DAH. Due to the patient's poor oxygenation and the development of DAH shortly after breast augmentation surgery, we suspected that NPPE was the most likely cause, and therefore did not perform BAL. Moreover, we performed a series of tests to exclude other potential causes of DAH, including coagulopathy, infection, cardiogenic lung edema, pulmonary embolism and vasculitis or capillaritis. Coagulopathy was excluded specifically by the normal prothrombin time, activated partial thromboplastin time, and platelet count, as well as normal test results for liver and kidney functions. Infection was excluded by the normal level of procalcitonin and the negative results of an influenza test and microbiological studies. Serological testing for vasculitis or capillaritis was negative. Cardiogenic lung edema was ruled out by a normal level of B-type natriuretic peptide and normal electrocardiography and echocardiography. CT pulmonary angiogram revealed no evidence of pulmonary embolism.

Drug-induced DAH should also be considered in patients undergoing general anesthesia [6-7]. For example, sevoflurane, a volatile inhaled halogenated gas, is commonly used for rapid induction during general anesthesia, and has been associated with DAH [6-7]. Other non-anesthetic drugs such as abciximab, amiodarone, carbimazole, crack cocaine, leflunomide, nitrofurantoin, and penicillamine have also been associated with DAH [4-5], but the clinical context was different from that of this case report. Moreover, none of these drugs was used with our patient.

The breast implants used in the patient

were made of silicone. Hematoma is the main complication in the immediate post-operative period of breast augmentation surgery [8]. To our knowledge, there is still no report on the occurrence of DAH after breast augmentation surgery. Although type 1 hypersensitivity reaction to silicone may occur, the reaction primarily causes local pruritus, edema and erythema [9-10].

NPPE, also known as post-obstructive pulmonary edema, occurs in less than 0.1% of patients after surgery [11], and accounted for only 5% of 112 immunocompetent patients with DAH in a published study [12]. However, NPPE-related DAH appears to be an under-recognized condition, because hemoptysis may be absent [1,13]. The pathogenesis of NPPE is mainly hydrostatic edema, which is caused by markedly negative thoracic pressure induced by an inspiratory effort against an obstructed glottis [13]; however, in cases with NPPE-related DAH, high-permeability edema occurs [1,13]. In short, the negative thoracic pressure generates negative interstitial pressure, enhances peripheral venous return to pulmonary circulation, and eventually increases transmural pressures across the cardiac chambers and alveolar capillaries, leading to an increased hydrostatic gradient and alveolar flooding [13].

A hyperadrenergic state and hypertension due to laryngospasm-induced respiratory distress may also contribute to the development of NPPE [13]. In severe cases, an extremely high transmural capillary pressure may induce stress fracture of the capillaries, leading to frank pulmonary alveolar hemorrhage [1,13]. The diagnosis of NPPE-related DAH after extubation relies on physician awareness and recognition of the clinical circumstances. When the diagnosis is made by further exclusion of other potential

causes, the treatment of NPPE-related DAH is mainly supportive. Most patients recover in a few days [1].

In conclusion, NPPE-related DAH may occur after an outpatient surgery such as breast augmentation. Physician awareness and recognition of this rare, potentially fatal condition is key to the diagnosis. The prognosis is generally favorable under supportive treatment.

References

1. Contou D, Voiriot G, Djibré M, *et al.* Clinical features of patients with diffuse alveolar hemorrhage due to negative-pressure pulmonary edema. *Lung* 2017; 195: 477-87.
2. Oswald CE, Gates GA, Holmstrom MG. Pulmonary edema as a complication of acute airway obstruction. *JAMA* 1977; 238(17): 1833-5.
3. Leatherman JW, Davies SF, Hoidal JR. Alveolar hemorrhage syndromes: diffuse microvascular lung hemorrhage in immune and idiopathic disorders. *Medicine (Baltimore)*. 1984; 63(6): 343-61.
4. Lara AR, Schwarz MI. Diffuse alveolar hemorrhage. *Chest* 2010; 137(5): 1164-71.
5. Ioachimescu OC, Stoller JK. Diffuse alveolar hemorrhage: diagnosing it and finding the cause. *Cleve Clin J Med* 2008; 75(4): 258, 260, 264-5.
6. Austin A, Modi A, Judson MA, *et al.* Sevoflurane induced diffuse alveolar hemorrhage in a young patient. *Respir Med Case Rep* 2016; 20: 14-5.
7. Cengiz O, Kivrak A, Yegen M, *et al.* Sevoflurane induced diffuse alveolar haemorrhage in a young patient after orthopedic surgery: A case report. *Niger J Clin Pract* 2020; 23(1): 120-2.
8. Iwuagwu FC, Frame JD. Silicone breast implants: complications. *Br J Plast Surg* 1997; 50(8): 632-6.
9. Stuck BA, Hecksteden K, Klimek L, *et al.* Type I hypersensitivity to a silicone tube after laryngectomy. *HNO* 2004; 52: 255-7.
10. Rubio A, Ponvert C, Goulet O, *et al.* Allergic and nonallergic hypersensitivity reactions to silicone: a report of one case. *Allergy* 2009; 64(10): 1555.
11. Deepika K, Kenaan CA, Barrocas AM, *et al.* Negative pressure pulmonary edema after acute upper airway obstruction. *J Clin Anesth* 1997; 9: 403-8.
12. de Prost N, Parrot A, Cuquemelle E, *et al.* Diffuse alveolar hemorrhage in immunocompetent patients: etiologies and prognosis revisited. *Respir Med* 2012; 106(7): 1021-32.
13. Bhattacharya M, Kallet RH, Ware LB, *et al.* Negative-pressure pulmonary edema. *Chest* 2016 Oct;150(4):927-33.

Pulmonary Alveolar Proteinosis with a Rare Presentation: A Case Report

Chang-Wei Wu¹, Yen-Lin, Huang², Ching-Yao Yang¹

Pulmonary alveolar proteinosis (PAP) is a rare disease characterized by a diffuse accumulation of lipoproteinaceous material in the distal airway and alveolar space that causes shortness of breath, hypoxia, respiratory failure and even death in severe cases. PAP could be a primary or secondary disease, and most PAP patients experienced progressive disease requiring treatment of the underlying disease with whole lung lavage or lung transplant. However, self-resolving PAP has also been described in a few case reports. Here, we reported the case of a 46-year-old man without known systemic disease or symptoms. Abnormal computed tomography imaging studies revealed a bilateral subpleural peribronchial crazy-paving pattern. Organized pneumonia was first suspected, but later, surgical resection confirmed a histological diagnosis of PAP. Partial regression of PAP was noted during the 7-month follow-up. (*Thorac Med* 2022; 37: 96-102)

Key words: pulmonary alveolar proteinosis, crazy-paving pattern, ground glass opacity

Introduction

Pulmonary alveolar proteinosis (PAP) is a rare disease, and was first described in 1958 by Rosen and colleagues [1]. It is characterized by a diffuse filling of amorphous lipoproteinaceous material in the distal airway and alveolar space, resulting in gas exchange impairment. PAP can be classified as autoimmune (previously known as idiopathic), secondary or congenital, based on the underlying etiology [2-3]. According to a

Japanese cohort study, about 90% of PAP cases are autoimmune type, with an incidence of 0.49 per million, and mostly occur in the 30- to 60-year old population, with a men-to-women ratio of around 2:1 [4]. A high proportion of patients are smokers or former smokers (56-64%); however, no causal relationship has been established. The most common presentation is an insidious progression of shortness of breath and hypoxia, which could develop during a period of months to years. Other symptoms include

¹Division of Pulmonary and Critical Care Medicine, Department of Internal Medicine, National Taiwan University Hospital and College of Medicine, National Taiwan University, Taipei, Taiwan, ²Department of Pathology, National Taiwan University Hospital and College of Medicine, National Taiwan University, Taipei, Taiwan.

Address reprint requests to: Dr. Ching-Yao Yang, Division of Pulmonary and Critical Care Medicine, Department of Internal Medicine, National Taiwan University Hospital, No. 7, Chung-Shan South Road, Taipei 100, Taiwan

cough, fatigue, weight loss, arthralgia and fever. If left untreated, PAP cases progress through time and may develop into respiratory failure or even death in severe cases. [3-6]

In this case report, we describe a 46-year-old man with a past history of smoking who developed PAP without any symptoms. Chest computed tomography (CT) revealed an atypical subpleural peri-bronchial distribution of a crazy-paving pattern with spontaneous regression during a 7-month follow-up.

Case Presentation

A 46-year-old male businessman, a smoker (16-pack-years, quit for 10 years) without a known systemic disease, presented to our clinic with an abnormal low-dose CT image as detected from his health examination. CT revealed multiple peri-bronchial subpleural ground glass opacities (GGO) in the bilateral lungs. He denied cough, shortness of breath, chest pain, chest tightness, fever, fatigue, body weight loss, arthralgia, or any other new symptoms. He denied any long-term medication use, contact with metallic dust or fumes, or a travel history in the most recent 3 months. His physical examination was unremarkable, with peripheral oxygen saturation (SpO₂) of 96-100%. His chest radiography revealed multiple subpleural faint opacities in the bilateral lungs. High-resolution CT showed a well-demarcated crazy-paving pattern scattered over the bilateral subpleural region asymmetrically (Figure 1). A blood test revealed no notable findings in the white blood cell count, red blood cell count, platelet cell count, total bilirubin, aspartate aminotransferase, alanine aminotransferase, or creatinine level. Autoimmune profiles revealed a positive antinuclear antibody of 1:40 with a homogenous nuclear

pattern, but no other positive results with regard to rheumatoid arthritis factor, anti-double stranded DNA, complement component 3 and 4, anti-Smith antibody, anti-nuclear ribonucleoprotein antibody, anti-Ro antibody, anti-La antibody, anti-Jo-1 antibody, anti-Scl-70 antibody, anti-centromere antibody, and anti-neutrophil cytoplasmic antibody. The pulmonary function test revealed a forced expiratory volume in 1 second of 4.31L, 118.6% predicted, forced vital capacity of 4.93L, 115.1% predicted, and a normal diffusion capacity for carbon monoxide (105.2%). Due to the peri-bronchial, subpleural radiographic distribution along with no symptoms or signs and a normal SpO₂ level, pulmonary infection, autoimmune disease or heart failure was less likely. Organized pneumonia was suspected, and in order to confirm the diagnosis, wedge-biopsy using video-assisted thoracoscopy was arranged. A whitish elastic-to-firm 2cm tumor was resected from the left lower lung. Under microscopy, the alveolar space was filled with diffuse dense acellular eosinophilic materials with minimal interstitial inflammation and well preserved alveolar architectures. The alveolar space material was positive under periodic acid-Schiff (PAS) and diastase PAS stain. There was no evidence of microbes under PAS and Gomori's methenamine silver stain, including *Pneumocystis jirovecii*. The diagnosis of PAP was then made (Figure 2).

Anti-granulocyte-macrophage colony-stimulating factor (GM-CSF) autoantibody testing was unavailable at our institute. No family member or colleague had been diagnosed with PAP. Autoimmune PAP was the most likely diagnosis. The patient presented no symptoms and had a normal O₂ saturation, hence, observation was favored. The patient followed up at our clinic with a CT scan 7 months later that

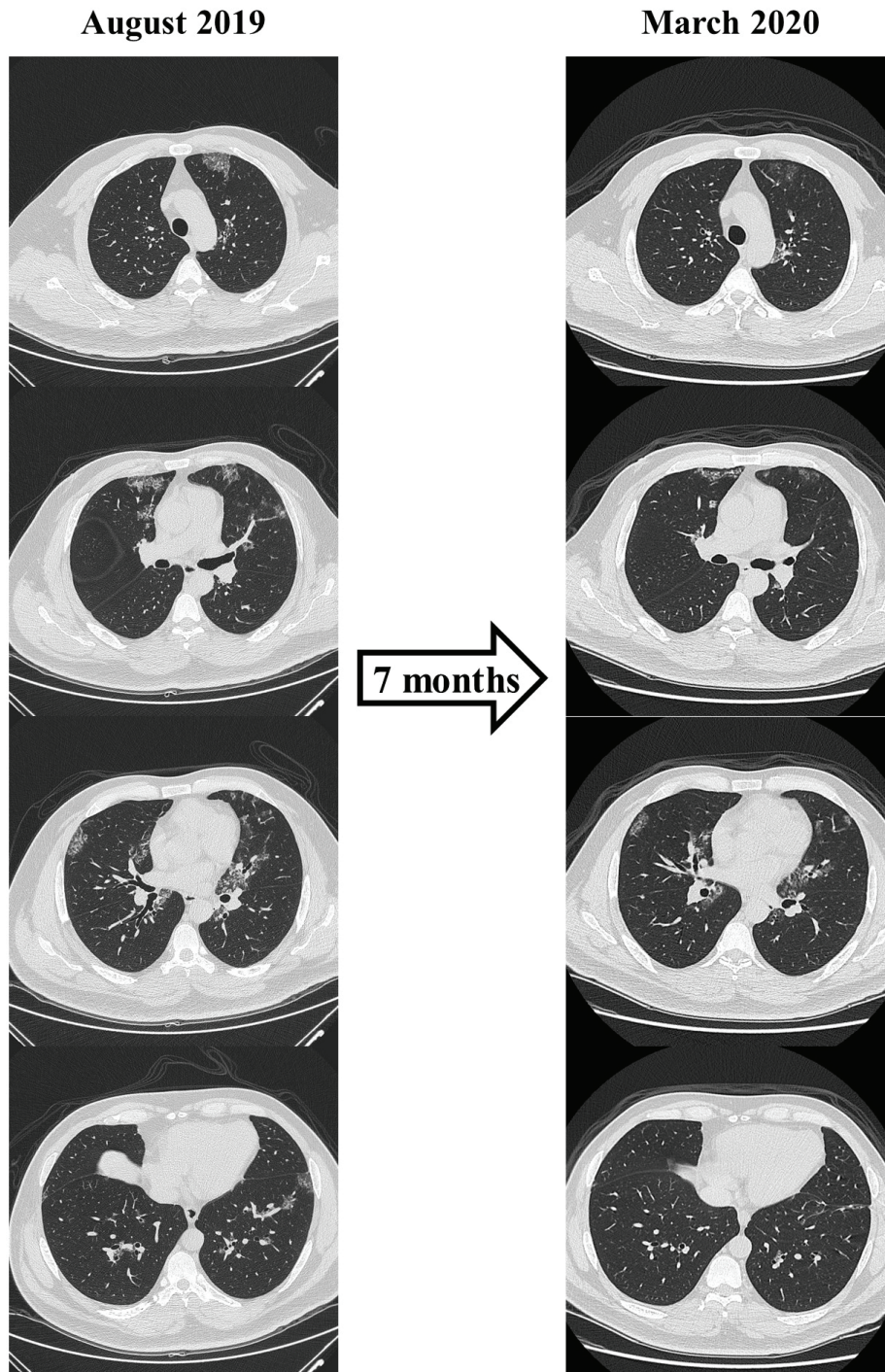


Fig. 1. High-resolution computed tomography revealed a bilateral subpleural peri-bronchial crazy-paving pattern, with spontaneous improvement without treatment after 7 months.

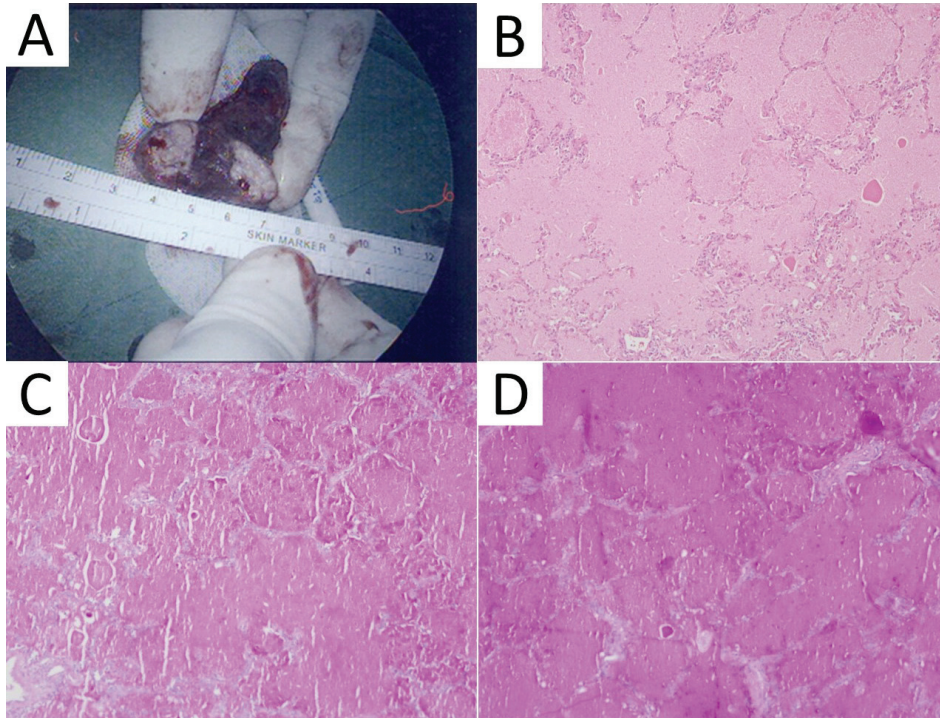


Fig. 2. (A). A whitish elastic-to-firm lesion was resected from the left lower lung; (B). hematoxylin and eosin stain revealed acellular eosinophilic material within the alveolar space with intact airway architecture (100x original magnification); (C). and (D). periodic acid-Schiff (PAS) and diastase PAS stain showed the alveolar space material was positive (100x original magnification).

showed all of the crazy-paving pattern lesions reduced in size without any treatment.

Discussion

PAP is a diffuse lung disease with distal air space filled with lipoproteinaceous content, mainly composed of surfactant phospholipid and apoprotein, along with reduced clearance of the surfactant. Pathogenesis is related to disrupted GM-CSF signaling and disorder or surfactant production. Autoimmune PAP is related to anti-GM-CSF autoantibody causing a disruption in GM-CSF signaling, resulting in alveolar macrophage dysfunction. The gene mutations of GM-CSF receptor or surfactant protein production plays a role in hereditary PAP, and shares a similar clinical course, presentation or

pathologic findings to autoimmune PAP. Secondary PAP is often caused by an underlying hematologic disease (e.g., leukemia, lymphoma, myelodysplastic syndrome, etc.), infection (e.g., *Pneumocystis jirovecii*, *mycobacterium tuberculosis*, etc.), or inhalation exposure (e.g., metallic dust, organic dust, fumes, etc.).

Diagnosis relies on a compatible history of clinical symptoms, CT, bronchoalveolar lavage (BAL) and biopsy. A gradual progression of dyspnea and dyspnea on exertion is the most commonly reported symptom in 50-90% of patients. Other symptoms include cough with or without sputum, fatigue, weight loss, fever, chest tightness and arthralgia. It should be noted that 5-30% of patients are asymptomatic and were detected by health examination [4-5]. Physical examination is unremarkable,

with rales, cyanosis and finger clubbing likely to be observed in severe cases. Typical chest radiography of PAP reveals bilateral symmetric alveolar opacities located centrally with lower lung predominance. High-resolution CT is the main diagnostic approach, and reveals bilateral symmetric GGO. Intralobar and interlobar septal thickening within GGO, known as a crazy-paving pattern, is seen in over 80% of patients [7-8]. To differentiate autoimmune PAP from secondary PAP in image findings, a crazy-paving pattern or subpleural sparing would favor the diagnosis of autoimmune PAP, and a diffuse distribution of GGO would favor secondary PAP [9]. A PAP presentation of a unilateral lesion, peripheral or upper lobe predominance, nodular lesion or air bronchogram is rare and should raise a suspicion of another possible diagnosis.

The BAL specimen has a signature milky appearance with thick sediments. Basophilic acellular oval bodies can be observed with May-Grünwald-Giemsa stain. Biopsy can provide a definite diagnosis, although HRCT and BAL are sufficient for most occasions. Biopsy was performed in only 10-20% of PAP patients and should be considered in cases with an atypical presentation or when there is a suspicion of another diagnosis. Anti-GM-CSF autoantibody is the only disease-specific biomarker with a sensitivity and specificity of 100% in cases of autoimmune PAP and is essential to make the diagnosis [10]. Other serum biomarkers such as lactate dehydrogenase, surfactant protein A, surfactant protein B, surfactant protein D, Krebs von den Lungen 6, and carcinoembryonic antigen are elevated in PAP, but have no role in establishing the diagnosis.

The clinical course varies greatly, from spontaneous recovery to progressive disease de-

veloping into respiratory failure or death. In our case, radiographic spontaneous improvement was observed at the 7-month follow-up (Figure 1), with no alteration in clinical symptoms or SpO₂. Tazawa *et al.* reported a 20% spontaneous improvement in oxygenation, defined as an alveolar-arterial oxygen difference decrease of 10 mmHg or more 12 weeks before starting inhalation of GM-CSF [11]. Other studies reported 5-7% of patients had a spontaneous regression course [3]. In patients with radiographic severity, spontaneous improvement was only reported in cases with as much as a 14-year-follow-up [12-13].

There is no international guideline for PAP management; hence, the treatment strategy is largely based on PAP classification, disease severity, and balancing the benefits against the harm of applied treatment. Whole lung lavage has been the mainstay therapy for PAP since it was first described in 1965. Segmental, single lung or sequential bilateral lavage with or without percussion under general anesthesia has shown improvement in PaO₂, forced vital capacity and diffusing capacity of the lungs for carbon monoxide [14-15]. The procedure is considered safe, with commonly encountered adverse effects being fever, hypoxemia, pneumonia and pneumothorax, with incidences of 18%, 14%, 5%, 0.8%, respectively [16]. Extracorporeal membrane oxygenation support is used in severe PAP cases when single lung ventilation is not feasible due to severe hypoxemia [17]. The relapse rate was 56.25% in a median period of 16.9 months, and required a 2nd lavage or alternative medications [18].

Inhaled GM-CSF has been shown to be effective in autoimmune PAP, with improvements in oxygenation and radiographic severity, a response rate of 48-65.7%, and a duration of

benefit up to 30 months [19-22]. However, only a modest benefit in the alveolar–arterial oxygen gradient and symptoms was noted in the latest randomized controlled trial. This outcome may be due to the exclusion of the most severe PAP ($\text{PaO}_2 < 50$ mmHg) patients, who may benefit the most from inhalation of GM-CSF [22]. Corticosteroid has shown no benefit in treating disease severity and poses an increased risk of infection [23]. Successful treatment with rituximab, plasmapheresis and lung transplantation has been reported, but should be reserved for refractory cases due to the limited cases and evidence in previous studies [24-25].

Secondary PAP requires removal and avoidance of exposure to causative mechanisms (e.g., drugs, silica, metallic dust, fumes, etc.) or treatment of the underlying disease (e.g., infection, hematologic disorder, etc.). It can be potentially reversible after the underlying disease achieves complete remission [26-27]. Congenital PAP lacks effective treatment, and lung lavage has had limited or no success [28]. Lung transplantation should be considered in severe cases; however, PAP recurrence after transplantation has been reported, especially in those with genetic mutations [29]. Smoking cessation and vaccination for pneumococcus and influenza are recommended for all types of PAP cases.

The prognosis of PAP varies among the different types. Recent cohort report suggested a 100% 5-year survival rate with a 5% infection rate [4]. Pulmonary fibrosis, which is present in 7-20% of cases, is a poor prognostic factor, and secondary PAP generally tends to have a worse prognosis due to underlying disease [7, 30].

We reported a case of asymptomatic PAP with an unusual radiographic presentation and spontaneous improvement at follow-up. A thorough evaluation of a lesion with a crazy-paving

pattern, including tissue biopsy, can lead to the correct diagnosis. Close observation with symptomatic control may be considered in asymptomatic or mild PAP, due to possible spontaneous improvement and the possible harm done by unnecessary treatment.

References

1. Rosen SH, Castleman B, Liebow AA. Pulmonary alveolar proteinosis. *N Engl J Med* 1958; 258(23):1123-42.
2. Kumar A, Abdelmalak B, Inoue Y, *et al.* Pulmonary alveolar proteinosis in adults: pathophysiology and clinical approach. *Lancet Respir Med* 2018; 6(7): 554-65.
3. Suzuki T, Trapnell BC. Pulmonary alveolar proteinosis Syndrome. *Clin Chest Med* 2016; 37(3): 431-40.
4. Inoue Y, Trapnell BC, Tazawa R, *et al.* Characteristics of a large cohort of patients with autoimmune pulmonary alveolar proteinosis in Japan. *Am J Respir Crit Care Med* 2008; 177(7): 752-62.
5. Campo I, Mariani F, Rodi G, *et al.* Assessment and management of pulmonary alveolar proteinosis in a reference center. *Orphanet J Rare Dis* 2013; 8: 40.
6. Bonella F, Bauer PC, Griese M, *et al.* Pulmonary alveolar proteinosis: new insights from a single-center cohort of 70 patients. *Respir Med* 2011; 105(12): 1908-16.
7. Holbert JM, Costello P, Li W, *et al.* CT features of pulmonary alveolar proteinosis. *AJR Am J Roentgenol* 2001; 176(5): 1287-94.
8. Mehrian P, Homayounfar N, Karimi MA, *et al.* Features of idiopathic pulmonary alveolar proteinosis in high resolution computed tomography. *Pol J Radiol* 2014; 79: 65-9.
9. Ishii H, Trapnell BC, Tazawa R, *et al.* Comparative study of high-resolution CT findings between autoimmune and secondary pulmonary alveolar proteinosis. *Chest* 2009; 136(5): 1348-55.
10. R Uchida K, Nakata K, Carey B, *et al.* Standardized serum GM-CSF autoantibody testing for the routine clinical diagnosis of autoimmune pulmonary alveolar proteinosis. *J Immunol Method* 2014; 402(1): 57-70.
11. Tazawa R, Trapnell BC, Inoue Y, *et al.* Inhaled granulocyte/macrophage-colony stimulating factor as therapy for pulmonary alveolar proteinosis. *Am J Respir*

- Crit Care Med 2010; 181(12): 1345-54.
12. Amin A, Chow M-Y. Primary autoimmune pulmonary alveolar proteinosis: A case of spontaneous resolution. *Chest* 2019; 156(4): A2186.
 13. Martínez-López MA, Gómez-Cerezo G, Villasante C, *et al.* Pulmonary alveolar proteinosis: prolonged spontaneous remission in two patients. *Eur Respir J* 1991; 4(3): 377-9.
 14. Beccaria M, Luisetti M, Rodi G, *et al.* Long-term durable benefit after whole lung lavage in pulmonary alveolar proteinosis. *Eur Respir J* 2004; 23(4): 526-31.
 15. Cheng SL, Chang HT, Lau HP, *et al.* Pulmonary alveolar proteinosis: treatment by bronchofiberscopic lobar lavage. *Chest* 2002; 122(4): 1480-5.
 16. Campo I, Luisetti M, Griese M, *et al.* Whole lung lavage therapy for pulmonary alveolar proteinosis: a global survey of current practices and procedures. *Orphanet J Rare Dis* 2016; 11(1): 115.
 17. Krecmerova M, Mosna F, Bicek V, *et al.* Extracorporeal membrane oxygenation to support repeated whole-lung lavage in a patient with pulmonary alveolar proteinosis in life-threatening dyspnoe – a case report. *BMC Anesthesiol* 2015; 15(1): 173.
 18. Gay P, Wallaert B, Nowak S, *et al.* Efficacy of whole-lung lavage in pulmonary alveolar proteinosis: a multicenter international study of GELF. *Respiration* 2017; 93(3): 198-206.
 19. Seymour JF, Dunn AR, Vincent JM, *et al.* Efficacy of granulocyte-macrophage colony-stimulating factor in acquired alveolar proteinosis. *N Engl J Med* 1996; 335(25): 1924-5.
 20. Venkateshiah SB, Yan TD, Bonfield TL, *et al.* An open-label trial of granulocyte macrophage colony stimulating factor therapy for moderate symptomatic pulmonary alveolar proteinosis. *Chest* 2006; 130(1): 227-37.
 21. Tazawa R, Inoue Y, Arai T, *et al.* Duration of benefit in patients with autoimmune pulmonary alveolar proteinosis after inhaled granulocyte-macrophage colony-stimulating factor therapy. *Chest* 2014; 145(4): 729-37.
 22. Tazawa R, Ueda T, Abe M, *et al.* Inhaled GM-CSF for pulmonary alveolar proteinosis. *New Engl J Med* 2019; 381(10): 923-32.
 23. Akasaka K, Tanaka T, Kitamura N, *et al.* Outcome of corticosteroid administration in autoimmune pulmonary alveolar proteinosis: a retrospective cohort study. *BMC Pulm Med* 2015; 15(1): 88.
 24. Kavuru MS, Malur A, Marshall I, *et al.* An open-label trial of rituximab therapy in pulmonary alveolar proteinosis. *Eur Respir J* 2011; 38(6): 1361-7.
 25. Luisetti M, Rodi G, Perotti C, *et al.* Plasmapheresis for treatment of pulmonary alveolar proteinosis. *Eur Respir J* 2009; 33(5): 1220-2.
 26. Cordonnier C, Fleury-Feith J, Escudier E, *et al.* Secondary alveolar proteinosis is a reversible cause of respiratory failure in leukemic patients. *Am J Respir Crit Care Med* 1994; 149(3): 788-94.
 27. Lin KP, Sheng WH, Wang CP, *et al.* Resolution of secondary pulmonary alveolar proteinosis following treatment of rhinocerebral aspergillosis. *Int J Infect Dis* 2010; 14 Suppl 3: e246-9.
 28. Seymour JF, Presneill JJ. Pulmonary alveolar proteinosis: progress in the first 44 years. *Am J Respir Crit Care Med* 2002; 166(2): 215-35.
 29. Takaki M, Tanaka T, Komohara Y, *et al.* Recurrence of pulmonary alveolar proteinosis after bilateral lung transplantation in a patient with a nonsense mutation in CSF2RB. *Respir Med Case Rep* 2016; 19: 89-93.
 30. Akira M, Inoue Y, Arai T, *et al.* Pulmonary fibrosis on high-resolution CT of patients with pulmonary alveolar proteinosis. *AJR Am J Roentgenol* 2016; 207(3): 544-51.

Fulminant and Fatal Community-Acquired Pneumonia Caused by *Sphingomonas Paucimobilis*

Chang-Hung Chen¹, Chao-Tai Lee²

Sphingomonas paucimobilis is a gram-negative bacillus that is omnipresent in both environmental and hospital settings. *S. paucimobilis* is considered to have limited virulence, probably due to the lack of lipopolysaccharide in its cell wall. We described an immunocompromised patient with community-acquired pneumonia caused by *S. paucimobilis* that was both fulminant and fatal, even though the initial antibiotic treatment was appropriate. Chest X-ray examination revealed rapidly progressive bilateral diffuse alveolar consolidation. (*Thorac Med* 2022; 37: 103-107)

Key words: *Sphingomonas paucimobilis*, community-acquired pneumonia, fatal

Introduction

Sphingomonas paucimobilis is a gram-negative bacillus that is omnipresent in both environmental and hospital settings. It is well known as a waterborne organism, with its infections attributable to contaminated water sources. Most *S. paucimobilis* infections reported in the literature are nosocomial, and include ventilator-associated pneumonia or indwelling intravascular device-related infection. Community-acquired *S. paucimobilis* infections are

sporadic, and primary bacteremia is the main presentation [1,2]. The virulence of *S. paucimobilis* is considered limited. In this report, we describe the case of an immunocompromised patient with fulminant and fatal community-acquired pneumonia caused by *S. paucimobilis*.

Case presentation

A 78-year-old woman with type 2 diabetes mellitus presented to our emergency department with progressive dyspnea after falling

¹Department of Internal Medicine, Chest Division, Tainan Municipal Hospital (Managed by Show Chwan Medical Care Corporation), ²Department of Clinical Laboratory, Tainan Municipal Hospital (Managed by Show Chwan Medical Care Corporation).

Address reprint requests to: Dr. Chang-Hung Chen, Department of Internal Medicine, Chest Division, Tainan Municipal Hospital (Managed by Show Chwan Medical Care Corporation), No. 670, Chongde Rd., East Dist., Tainan City 701033, Taiwan (R.O.C.)

into a ditch and choking on several mouthfuls of water about 3 hours prior to her presentation. Physical examination revealed a body temperature of 36.5°C, pulse rate of 104 beats/min, respiratory rate of 26 breaths/min, and blood pressure of 185/95 mmHg. The oximeter revealed oxygen saturation under 94% with a non-rebreather mask. Laboratory examination yielded a white blood cell count of 18,000 cells/mm³ with 84% neutrophils, a platelet cell count of 234,000/mm³, C-reactive protein level of 36.2 mg/dL (reference range: <0.3 mg/dL), blood glucose level of 264 mg/dL, and a glycosylated hemoglobin level of 7.7%. Chest X-ray

examination revealed bilateral diffuse alveolar consolidation (Figure 1). Aspiration pneumonia was indicated. Due to progressive respiratory distress, intubation with ventilator support was performed, and the patient was sent to the intensive care unit for further care and treatment. Antimicrobial therapy with piperacillin with tazobactam was initiated. Antibiotics were shifted to meropenem due to a deteriorated disease condition after 3 days of initial treatment (Figure 2). Blood culture and sputum (tracheal aspirate) both revealed *S. paucimobilis*, which was susceptible to cabapenem, piperacillin with tazobactam, third-generation cephalosporin, and

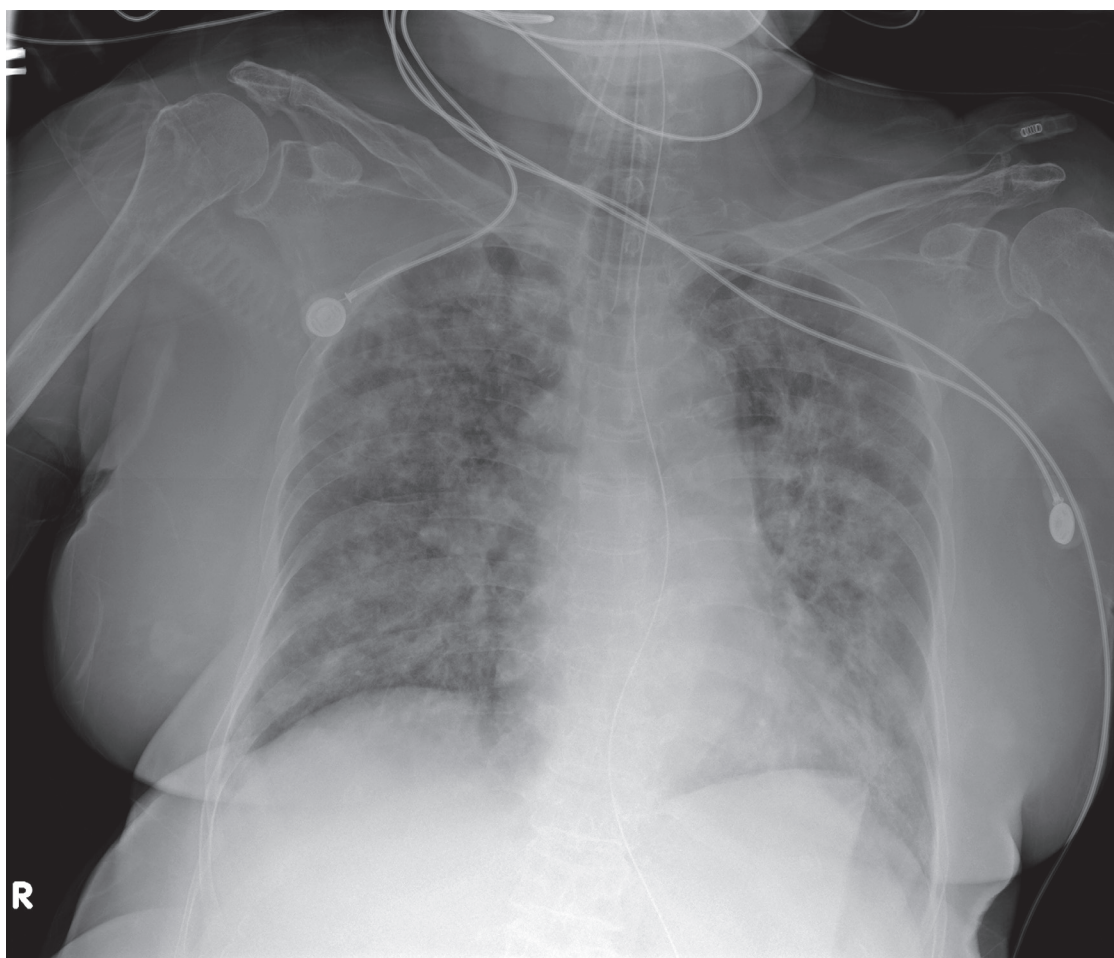


Fig. 1. Bilateral diffuse alveolar consolidation noted on the day of admission.



Fig. 2. Rapidly deteriorating bilateral pneumonia 3 days after admission.

levofloxacin. Rapid progression of pneumonia and multiple organ failure were noted thereafter. Unfortunately, our patient died on day 11 after admission.

Discussion

S. paucimobilis is an omnipresent gram-negative bacillus in both environmental and hospital settings. It is well known as a water-borne organism, with its infections being attributable to contaminated water sources. Clinical syndromes, such as primary bacteremia, intra-

vascular catheter infection, peritoneal dialysis-associated peritonitis, urinary tract infection, biliary tract infection, cutaneous infection, pneumonia, meningitis, myositis, osteomyelitis, septic arthritis, endophthalmitis, cervical adenitis, keratitis and diarrheal disease, are associated with *S. paucimobilis* [1-11]. Most *S. paucimobilis* infections reported in the literature, such as ventilator-associated pneumonia, or those associated with the presence of indwelling intravascular devices or systemic immunosuppressant use, are nosocomial [1-3,7,12]. Community-acquired *S. paucimobilis* infections are sporadic,

Table 1. Cases of Community-acquired *Sphingomonas paucimobilis* infection in recent 20 years literatures

Reference	Case numbers Average age	Infection foci	Underlying conditions	Outcomes
Toh <i>et al.</i> [1]	29 44 y/o	Primary bacteremia (13/29) Pneumonia/empyema (2/29) Soft tissue infection (7/29) CNS infection (1/29) Head and neck infection (6/29)	Diabetes mellitus Malignancy Chronic heart disease Cirrhosis Steroid usage Alcoholism	1 mortality 28 recovery
Lin <i>et al.</i> [2]	6 40 y/o	Primary bacteremia (2/6) Pneumonia (1/6) Soft tissue infection (2/6) Urinary tract infection (1/6)	Malignancy Chronic kidney disease	Recovery
Bayram <i>et al.</i> [4]	13 5 y/o	Primary bacteremia (12/13) Urinary tract infection (1/13)	Down's syndrome Premature birth PSAGN (Post-streptococcal acute glomerulonephritis)	Recovery
Nandy <i>et al.</i> [5]	2 55 y/o, 2 y/o	Primary bacteremia (2/2)	Malignancy	Recovery
Saboor <i>et al.</i> [6]	1 10 y/o	Primary bacteremia	None	Recovery

and primary bacteremia is the main presentation (Table 1) [1,2,4-6]. No standard method currently exists to determine the antibiotic susceptibility of *S. paucimobilis*, and data vary in the literature [2]. *S. paucimobilis* has been reported to be susceptible to aminoglycosides, carbapenem, third-generation cephalosporin, fluoroquinolones, β -lactam/ β -lactamase inhibitor combinations, and trimethoprim/sulfamethoxazole [1-3,12]. Risk factors for *S. paucimobilis* infection include malignancy, hematopoietic stem cell transplantation, immunosuppressant use, diabetes mellitus, and alcoholism in adults [1]. In children, prematurity also plays a key role in *S. paucimobilis* infection [4]. The difference between *S. paucimobilis* and other gram-negative bacteria is the presence of glycosphingolipid as the component of cellular lipids, and the ab-

sence of lipopolysaccharides [9,13]. A limited number of fatal cases has been reported. Glycosphingolipids bound to the outer membrane of *S. paucimobilis* have been proposed to be the reason for its low virulence [12]. Even when the antibiotic treatment initiated is inappropriate, most patients infected with *S. paucimobilis* survive [1,4,12]. The majority of patients with favorable outcomes are middle-aged adults and children. In our opinion, since community-acquired pneumonia due to *S. paucimobilis* occurs infrequently, the association of this organism with a patient is not always initially considered. Our patient, according to the family's statements, did not have regular and effective diabetes control. Furthermore, she fell into a ditch and swallowed several mouthfuls of water, and the pathogen load was enormous. As a result,

the combined effect of her age, her diabetes-related compromised immunity, and the bacterial load probably contributed to the rapid progression of pneumonia and sepsis. The drug sensitivity test for the initial antibiotic revealed it was effective, but the final patient outcome was compromised; we consider the *in vitro* activity of antibiotics with this rare type of infection to be probably unreliable. Toh *et al.* reported the antimicrobial susceptibility to imipenem–cilastatin of community-acquired and hospital-acquired strains to be 96.9% and 92.3%, respectively [1]. If we had initially used antibiotics belonging to the carbapenem category, perhaps the result would have been different. Our experience with this case shows that even though *S. paucimobilis* is an environmental pathogen and has low virulence, it can cause life-threatening pneumonia and septic shock, especially in immunocompromised and older hosts, and initial aggressive antibiotic treatment is necessary.

References

- Toh HS, Tay HT, Kuar WK, *et al.* Risk factors associated with *Sphingomonas paucimobilis* infection. *J Microbiol Immunol Infect* 2011; 44(4): 289-95.
- Lin JN, Lai CH, Chen YH, *et al.* *Sphingomonas paucimobilis* bacteremia in humans: 16 case reports and a literature review. *J Microbiol Immunol Infect* 2010; 43(1): 35-42.
- Hsueh PR, Teng LJ, Yang PC, *et al.* Nosocomial infections caused by *Sphingomonas paucimobilis*: clinical features and microbiological characteristics. *Clin Infect Dis* 1998; 26(3): 676-81.
- Bayram N, Devrim I, Apa H, *et al.* *Sphingomonas paucimobilis* infections in children: 24 case reports. *Mediterr J Hematol Infect Dis* 2013; 5(1): e2013040.
- Nandy S, Dudeja M, Das AK, *et al.* Community-acquired bacteremia by *Sphingomonas paucimobilis*: two rare case reports. *J Clin Diagn Res* 2013; 7(12): 2947-2949.
- Saboor F, Amin F, Nadeem S. Community-acquired *Sphingomonas paucimobilis* in a child - a rare case. *J Pak Med Assoc* 2018; 68(11): 1714-1716.
- Yozgat Y, Kilic A, Karadeniz C, *et al.* *Sphingomonas paucimobilis* bacteraemia and shock in a patient with rheumatic carditis. *Indian J Med Microbiol* 2014; 32(4): 451-454.
- Göker T, Aşık RZ, Yılmaz MB, *et al.* *Sphingomonas paucimobilis*: a rare infectious agent found in cerebrospinal fluid. *J Korean Neurosurg Soc* 2017; 60(4): 481-483.
- El Beaino M, Fares J, Malek A, *et al.* *Sphingomonas paucimobilis*-related bone and soft-tissue infections: a systematic review. *Int J Infect Dis* 2018; 77: 68-73.
- Agarwal R, Gagrani M, Mahajan A, *et al.* Fulminant *Sphingomonas paucimobilis* keratitis: case study and review of literature. *BMJ Case Rep* 2019; 12(12): e231642.
- Wasiura J, Segal BH, Mullin KM. Cluster of *Sphingomonas paucimobilis* bacteremias linked to diversion of intravenous hydromorphone. *N Engl J Med* 2019; 381(6): 584-585.
- Cheong HS, Wi YM, Moon SY, *et al.* Clinical features and treatment outcomes of infections caused by *Sphingomonas paucimobilis*. *Infect Control Hosp Epidemiol* 2008; 29(10): 990-2.
- Kawasaki S, Moriguchi R, Sekiya K, *et al.* The cell envelope structure of the lipopolysaccharide-lacking gram-negative bacterium *Sphingomonas paucimobilis*. *J Bacteriol* 1994; 176(2): 284-90.

The First Reported Computed Tomography Scan Images of Remitting-Relapsing Pleural Effusions of Malignant Pleural Mesothelioma

Wen-Chi Hsiao¹, Jen-Wen Hsu², Ming-Hung Chen¹, Pei-Ru Wu³, Tai-Yu Chang⁴

Malignant pleural effusions usually accumulate progressively unless they have been treated. Spontaneous remitting of malignant pleural effusions without therapy and remitting-relapsing malignant pleural effusions are rare. Until now, there have been no computed tomography (CT) scan images that reveal these specific conditions and only 2 chest X-rays have been reported. We report a 59-year-old man who was a boiler worker with asbestos exposure for 20 years. He suffered persistent right chest pain for 18 months, and his pleural effusions remitted and relapsed during this period. Video-assisted thoracoscopic surgery was arranged and the pathological reports showed malignant mesothelioma. The serial changes of the pleural effusions were clearly shown first by the CT scan. When treating these patients, clinicians should maintain follow-up even if the pleural effusions remit spontaneously. These are the first CT scan images of remitting-relapsing malignant pleural effusions caused by malignant pleural mesothelioma in the literature. (*Thorac Med* 2022; 37: 108-113)

Key words: asbestos; mesothelioma; pleural effusion

Introduction

Pleural effusions may occur in many common diseases, and malignant pleural effusions account for 22% of cases [1]. The majority of the malignant pleural effusions are due to metastasis of lung cancer in men and breast cancer in women [2]. Mesothelioma is the most common primary pleural tumor, and over 95% of these patients have malignant pleural effusions [3]. The mechanisms of malignant pleural ef-

fusions remain poorly understood, but blocked lymphatic drainage due to a tumor or altered vascular permeability may play a role [2,4].

Malignant pleural effusions continue to accumulate unless they receive effective cancer treatment, or pigtail catheter drainage and pleurodesis [2,4]. Spontaneous remitting of malignant pleural effusions without therapy and remitting-relapsing malignant pleural effusions are rare. Only 2 chest X-rays (CXR) of remitting-relapsing malignant pleural effusions

¹Division of Family Medicine, Cheng Ching Hospital, Taichung, Taiwan, ROC, ²Division of Chest Medicine, Department of Internal Medicine, Cheng Ching Hospital, Taichung, Taiwan, ROC, ³Division of Pathology, Cheng Ching Hospital, Taichung, Taiwan, ROC, ⁴Division of Radiology, Cheng Ching Hospital, Taichung, Taiwan, ROC. Address reprint requests to: Dr. Jen-Wen Hsu, Department of Internal Medicine, Cheng Ching Hospital, No.139 Ping Tien Street, Taichung, Taiwan, ROC

been published [5]. Here, we present the first computed tomography (CT) scan images of remitting-relapsing malignant pleural effusions caused by malignant pleural mesothelioma.

Case Report

A 59-year-old man had chronic hepatitis B and smoked 1 pack of cigarettes per day for 40 years. He was a boiler worker with asbestos exposure for 20 years.

He was admitted in October 2016 due to persistent right chest pain for 1 month. Associated symptoms included right upper abdominal pain and fever once. Physical examination showed no edema in the 4 limbs. Laboratory evaluation revealed normal renal functioning, and serum albumin within a normal range. CXR demonstrated no cardiomegaly but blunting of the right costophrenic angle, which suggested

right-side pleural effusion (Figure 1a). The sputum acid-fast stain was negative. An abdominal ultrasound examination revealed gallstones, but no cholecystitis finding. CT scan showed normal lung parenchyma, and no lesions such as tumors, tuberculosis or pneumonia, but right-side pleural effusion (Figure 1e). The pleural effusion was too small for aspiration. A Tc99m methylene diphosphonate whole-body bone scan showed negative findings. After symptomatic and analgesic treatment, the abdominal pain improved, and he was discharged without a definite diagnosis of pleural effusion.

One month later, he suffered from intermittent right upper abdominal pain. CXR showed no more blunting of the right costophrenic angle and suggested resolution of the right-side pleural effusion (Figure 1b). CT scan also revealed remission of the right-side pleural effusion (Figure 1f). Laparoscopic cholecystectomy

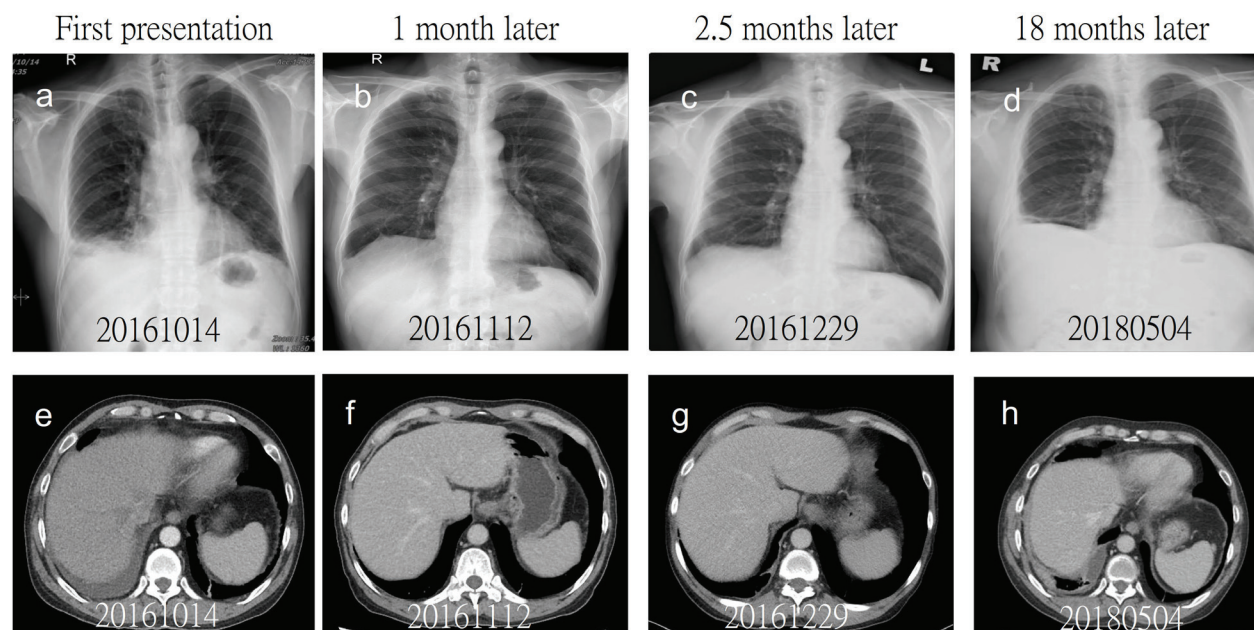


Fig. 1. Chest X-ray (CXR) (a) demonstrated the right-side pleural effusion and computed tomography (CT) (e) revealed right-side pleural effusion at the first presentation on October 14, 2016. One month later, CXR (b) and CT (f) showed spontaneous remission of the right-side pleural effusion before laparoscopic cholecystectomy. Two and a half months post-operation, CXR (c) and CT (g) revealed only pleural thickening, and no pleural effusion. Eighteen months later, CXR (d) showed blunting of the right costophrenic angle and CT (h) revealed recurrence of the right-side pleural effusion, pleural thickening and multiple subpleural nodules.

was arranged due to the above symptoms and multiple gallstones in the images.

Two and a half months post-operation, the patient still felt right chest and right abdominal pain. Both CXR and CT scan were performed again (Figure 1c and g), but the images revealed only pleural thickening, and no pleural effusion was found. The patient maintained follow-up at the chest medicine outpatient department.

Eighteen months later, right upper abdominal pain was noted again. The CXR showed blunting of the right costophrenic angle and CT scan revealed recurrence of the right-side pleural effusion, pleural thickening and multiple subpleural nodules (Figure 1d and h). Diagnostic video-assisted thoracoscopic surgery then was performed. Dense adhesions in the pleural cavity and subpleural nodules with firm content were found. It was decided in a multi-disciplinary discussion that the multiple pleural

masses found by CT scan could not be totally removed by decortication. The tissues that were removed were sent for histopathological diagnosis. Hematoxylin and eosin stain showed epithelioid tumor cells in the stroma. Immunohistochemical stains of the tumor cells were positive for calretinin, CK5/6, and WT-1, and negative for TTF-1 (Figure 2). This confirmed the diagnosis of malignant epithelioid mesothelioma [6]. There were no significant mediastinal lymph nodes and no obvious other distant metastasis. According to the 8th TNM classification for malignant pleural mesothelioma published by the International Association for the Study of Lung Cancer (IASLC), the staging was cT4N0M0, stage IV [7].

Thus, the patient first received 6 cycles of Alimta (pemetrexed) and cisplatin-based combination chemotherapy for stable disease [3]. Since the pleural masses showed mild shrink-

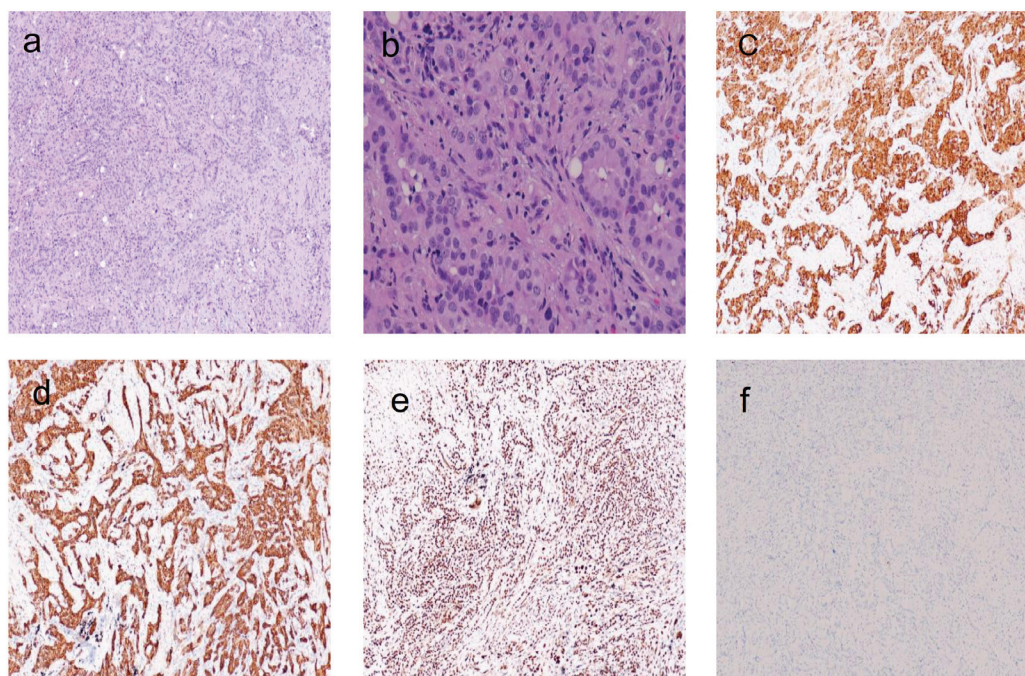


Fig. 2. Histopathological specimens with hematoxylin and eosin stain showed epithelioid tumor cells in the stroma (a, magnification X 100) (b, magnification X 400). Immunohistochemical stains of the tumor cells were positive for calretinin (c), CK5/6 (d), and WT-1 (e), and negative for TTF-1 (f).

age, we continued the combination therapy to a total of 11 cycles. Another re-staging with a CT scan also showed stable disease. After that, we shifted to maintenance therapy with single Alimta (pemetrexed) with bevacizumab for another 4 cycles. However, the tumors showed a gradual mild increase in size. He has survived up to this writing (over 20 months).

Discussion

The estimated prevalence of pleural effusion is 320 cases per 100,000 people in industrialized countries [8]. The most common etiologies are heart failure, pneumonia, and cancer [9]. There are 2 types of pleural effusion: transudate and exudate. Transudate effusion is caused by high hydrostatic pressure in the blood vessel, such as in cases of heart failure. Exudate effusion results from damage to the vascular endothelium caused by inflammation, infection or malignancy. Pleural effusions can be divided into benign and malignant. Benign pleural effusion can spontaneously resolve or improve by treating the underlying disease, or can recur multiple times, such as in cases of benign asbestos pleural effusion (BAPE) [6,9].

There are about 50,000 new cases of malignant pleural effusion in the United Kingdom each year [2]. Metastatic diseases (lung cancer in men and breast cancer in women) cause the majority of malignant pleural effusions [2]. Mesothelioma is the most common type of primary pleural tumor and is associated with malignant pleural effusions in more than 95% of mesothelioma cases [3]. The most common symptom of malignant mesothelioma is dyspnea caused by pleural effusion [10]. CXR often reveals unilateral pleural effusions. CT scan images demonstrate the changes in the pleura, including

pleural nodules or pleural thickening, and the amount of pleural effusions [2,6,10], but these findings have had low sensitivity in confirming cancer [2].

The American Thoracic Society has stated that annual screening of mesothelioma is not suggested [11]. Malignant pleural mesothelioma screening is not practical [12]. But our case indicates that if pleural effusions present in a remitting and relapsing manner, mesothelioma must be taken into consideration. Pleural effusions accompanied with pleuritic pain may be a manifestation of malignant mesothelioma [10]. Impaired lymphatic outflow caused by the tumor or increased fluid production due to fluid extravasation from a hyper-permeable pleura leads to the accumulation of pleural effusion [2,4]. So, management of malignant pleural effusions involves treatment of the cancer or obstruction of the pleural cavity (pleurodesis) [2-4]. Spontaneous remitting of malignant pleural effusions without therapy and remitting-relapsing malignant pleural effusions are rare: only 2 CXR images have been reported [5]. The CT scan images presented herein are the first to appear in the literature.

Our patient had an asbestos exposure history, which made BAPE a possible differential diagnosis. The mean interval between exposure and presentation of BAPE was 16.3 years [13]. BAPE may present with fever or asymptotically. Spontaneous resolution is a characteristic of BAPE, but it may recur several times [9,13]. To diagnose BAPE is to exclude tuberculosis and malignancy [9-10]. The serial images for our patient did not reveal pneumonia, tuberculosis, or malignancy. Sputum acid-fast stain and culture showed negative findings.

Considering the symptoms of right upper abdominal pain and gall bladder stone find-

ings in CT scan images, cholecystitis could be another cause of pleural effusions. However, pleural effusion occurred in the early stage of chest pain in our patient, and spontaneously remitted before laparoscopic cholecystectomy, which could exclude cholecystitis as the cause of his pleural effusion. After the operation, the pleural pain continued for nearly 1 year, with recurrent pleural effusion, so malignant pleural mesothelioma was suspected and confirmed by thoracoscopic surgery.

We decided to arrange video-assisted thoracoscopic surgery biopsy for the patient because there were pleural masses with a small amount of pleural effusion. We first arranged chest echography and thoracentesis, but there was too little pleural effusion for a definite cytological diagnosis of malignant mesothelioma. However, mesothelioma should be suspected in any person with an unexplained exudative pleural effusion [3]. After excluding a transudate cause and tuberculosis, malignancy was the possible diagnosis. The patient was a boiler worker and had an asbestos exposure history which raised a suspicion of mesothelioma.

A previous report described 2 cases of remitting-relapsing pleural effusions of malignant pleural mesothelioma [5]. But, the images were only CXR films, and there were no further CT scan images to clarify the differences [5]. Our report adds CT scan films, which are the first in the literature showing changes in pleural effusions at critical moments to better understand the changes in pleural membranes, pleural tumors, and pleural thickening. Mesothelioma has 3 cell types: epithelioid, sarcomatoid, and mixed [6]. Our pathological type was epithelioid, the same as in the other 2 cases [5]. Thus, we assumed the epithelioid type of malignant pleural mesothelioma is associated with recur-

rent malignant pleural effusions. The pathogenesis of recurrent malignant pleural effusion is still unknown, and requires more cases to reach an understanding.

In conclusion, remitting-relapsing pleural effusions are rare, and when they are encountered, mesothelioma should be considered. History-taking for mesothelioma, such as asbestos exposure, should be done, even though it may not be part of the regular procedure. Further studies such as a CT scan, thoracoscopic surgery, and pleural biopsy also should be arranged. An earlier diagnosis would lead to the best treatment results.

Conflicts of interest

The authors declare that they have no conflicts of interest related to the subject matter or materials discussed in this article.

References

1. Marel M, Zrustova M, Stasny B, *et al.* The incidence of pleural effusion in a well-defined region. *Epidemiologic study in central Bohemia.* *Chest* 1993; 104(5): 1486-9.
2. Psallidas I, Kalomenidis I, Porcel JM, *et al.* Malignant pleural effusion: from bench to bedside. *Eur Respir Rev* 2016; 25(140): 189-98.
3. West SD, Lee YC. Management of malignant pleural mesothelioma. *Clin Chest Med* 2006; 27(2): 335-54.
4. Davies HE, Lee YC. Management of malignant pleural effusions: questions that need answers. *Curr Opin Pulm Med* 2013; 19(4): 374-9.
5. Muruganandan S, Fitzgerald DB, Lee YCG. Malignant pleural mesothelioma presenting with remitting-relapsing pleural effusions: report of two cases. *Respir Case Rep* 2018; 6(3), e00306.
6. Porcel JM, Light RW. Pleural effusions. *Diseases-a-month* 2013; 59(2): 29-57.
7. Berzenji L, Van Schil PE, Carp L. The eighth TNM classification for malignant pleural mesothelioma. *Transl*

- Lung Cancer Res 2018 Oct; 7(5):543–9.
8. Adeoye PO, Johnson WR, Desalu OO, *et al.* Etiology, clinical characteristics, and management of pleural effusion in Ilorin, Nigeria. *Niger Med J* 2017; 58(2): 76-80.
 9. Thomas R, Lee YC. Causes and management of common benign pleural effusions. *Thorac Surg Clin* 2013; 23(1): 25-42.
 10. O'Reilly KM, McLaughlin AM, Beckett WS, *et al.* Asbestos-related lung disease. *Am Fam Physician* 2007; 75(5): 683-8.
 11. American Thoracic Society. Diagnosis and initial management of nonmalignant diseases related to asbestos. *Am J Respir Crit Care Med* 2004; 170: 691-715.
 12. Falaschi F, Romei C, Fiorini S, *et al.* Imaging of malignant pleural mesothelioma: it is possibly a screening or early diagnosis program? —a systematic review about the use of screening programs in a population of asbestos-exposed workers. *J Thorac Dis* 2018; 10(Suppl 2): S262-8.
 13. Robinson BW, Musk AW. Benign asbestos pleural effusion: diagnosis and course. *Thorax* 1981; 36(12): 896-900.

Hard Metal Lung Disease: A Case Report Using Transbronchial Cryobiopsy in the Diagnosis

Chiung-Hung Lin¹, Chih-Hao Chang¹, Jia-Shiuan Ju¹, Tzu-Hsuan Chiu¹,
Pi-Hung Tung¹, Shu-Min Lin⁴

Hard metal lung disease (HMLD) is a rare disease diagnosed pathologically by the presence of multinucleated giant cells in the alveoli with interstitial pneumonitis and centrilobular fibrosis. In the past, surgical lung biopsy and transbronchial lung biopsy (TBLB) were the only means of obtaining a tissue specimen. Transbronchial cryobiopsy (TBC) is an emerging and excellent technique in the diagnosis of diffuse parenchymal lung disease, but it has never been used in the diagnosis of HMLD. We reported the case of a 41-year-old female turner who presented with progressive dyspnea on exertion for 3 years. Tissues from TBLB failed to yield a specific diagnosis, while those from TBC confirmed the diagnosis of HMLD. Cryobiopsy offers diagnostic advantages compared with conventional techniques and appears to be a useful diagnostic tool for diagnosing HMLD. (*Thorac Med* 2022; 37: 114-119)

Key words: cryobiopsy, hard metal lung disease, bronchoscopy

Introduction

Hard metal lung disease (HMLD) is a rare occupation-related pulmonary disease (1). The hard metal is produced by pressurizing and heating powders, including tungsten carbide powder (often additionally mixed with tantalum carbide or titanium carbide) and cobalt. The hard metal has a diamond-like hardness and extreme strength, and is resistant to heat, so it has a wide variety of applications in industry as

drill tips, cutting and tunneling tools, and grinding wheels (2). Hard-metal workers are exposed in hard-metal dust, which may lead to asthma, rhinitis, hypersensitivity pneumonitis and interstitial fibrosis (3). The characteristic feature of HMLD is interstitial fibrosis combined with the presence of multinucleated giant cells, resulting in a pathologic pattern called giant cell interstitial pneumonia (GIP) (4). In diagnosing interstitial lung disease (ILD), surgical lung biopsy (SLB) is the most frequently used tool for ob-

¹Department of Thoracic Medicine, Chang Gung Memorial Hospital, Chang Gung University, School of Medicine, Taipei, Taiwan, ²Department of Respiratory Therapy, Chang Gung Memorial Hospital, Chang Gung University, School of Medicine, Taipei, Taiwan.

Address reprint requests to: Dr. Shu-Min Lin, Department of Thoracic Medicine, Chang Gung Memorial Hospital, 199 Tun-Hwa N. Rd., Taipei, Taiwan

taining adequate tissue samples for pathologic diagnosis. Compared with SLB, transbronchial lung biopsy (TBLB) by flexible forceps may not provide an adequate tissue sample for diagnosis of diffuse parenchymal lung diseases (DPLDs). Emerging evidence shows that cryobiopsy via flexible bronchoscopy may be more able to obtain an adequate specimen than SLB for diagnosis of DPLDs (5). Here, we present a case of HMLD diagnosed by cryobiopsy via flexible bronchoscopy.

Case Presentation

A 41-year-old female nonsmoker came to our chest outpatient clinic due to progressive dyspnea on exertion for 3 years. She denied any systemic disease. She had worked as a turner, mainly using a drill grinder, for 10 years. She also had a dry cough for 1 year. The cough usually developed at night, and physical examination showed an injected throat with a cobblestone appearance. The pulmonary function test results were as follows: Pre-bronchodilator forced vital capacity (FVC): 1.76L (55% of predicted value); forced expiratory volume in 1 s (FEV_1): 1.47L (55% of predicted value); FEV_1/FVC : 83.5%; maximal mid-expiratory flow (MMEF): 1.50L/s (48% of predicted value); post-bronchodilator FVC: 2.32L (73% of predicted value); FEV_1 : 1.84L (69% of predicted value); FEV_1/FVC : 79.3%, MMEF: 1.74L/s (56% of predicted value); and FEV_1 change ratio: 25%. There was reversibility on the bronchodilator. Chest X-ray showed increased interstitial infiltrations in the bilateral lower lung fields. Inhaled corticosteroid and a long-acting bronchodilator were given due to a suspicion of asthma, and an anti-histamine was given due to a suspicion of allergic rhinitis.



Fig. 1. Chest X-ray showing increased interstitial infiltrations in bilateral lung fields.

However, she was lost to follow-up for 3 years and the dyspnea gradually aggravated. So, she went to a pulmonologist at a local clinic. Chest X-ray showed increased interstitial infiltrations in bilateral lung fields (Figure 1). Chest high-resolution CT (HRCT) was arranged and showed diffuse and symmetric ground-glass opacities and interstitial infiltrations in bilateral lungs (Figure 2). So, she came back to our outpatient clinic in September 2018 for further evaluation and treatment. Hemogram showed a normal white blood cell count and no left shift. Biochemistry profile showed normal renal and liver function. Autoimmune surveys, including antinuclear antibody, rheumatoid factor, anti-Smith antibody, anti-histone antibody, anti-ribonucleoprotein antibody, anti-Jo-1 antibody, anti-SSA, anti-SSB, and anti-Scl-70, were all nega-

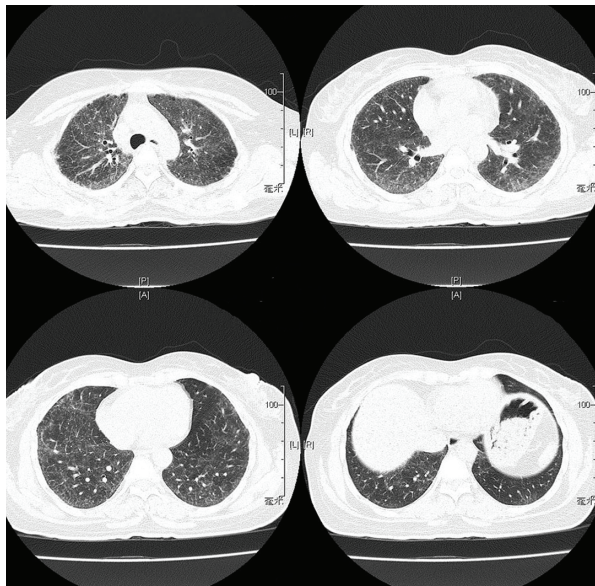


Fig. 2. HRCT showing diffuse and symmetric ground-glass opacities and interstitial infiltrations in bilateral lungs.

tive. The pulmonary function test showed FVC: 1.20 L (38% of predicted value), FEV₁: 0.86 L (32% of predicted value), FEV₁/FVC: 72%, MMEF: 0.55 L/s (18% of predicted value), total lung capacity: 2.48 L (51% of predicted value), residual volume: 0.92 L (57% of predicted value), and carbon monoxide diffusion capacity (DLCO) of the lung: 3.8 mL/mmHg/min (18% of predicted value) (Figure 3).

Due to ILD, we arranged bronchoscopy for survey. The patient was fiberoptically intubated with a 7.5-mm endotracheal tube under midazolam sedation in the bronchoscopy suite. A radial probe endobronchial ultrasound was used and no peribronchial mass lesion was found in the right upper lobe apical and anterior segments, right lower lobe superior segment, left upper lobe apico-posterior segment, or left lower lobe superior segment. Bronchoalveolar lavage (BAL) was done through the upper lobe apico-posterior segment. TBLB by forceps and transbronchial cryobiopsy (TBC) by a 1.9-mm

cryoprobe were performed at the left lower lobe superior segment. Minor bleeding from the biopsy site was noted during the procedure, but was controlled by scope tamponade. No pneumothorax developed after the procedure.

The BAL fluid was whitish-cloudy in appearance. The microbiologic study showed negative for bacteria, fungi, *Mycobacterium tuberculosis*, virus, and *Pneumocystis jiroveci*. Cell analysis revealed 155 cells/ μ L in total cell count, with a differential count of 2.7% eosinophils, 32% neutrophils, 21.8% lymphocytes, and 43.5% macrophages. The lymphocyte subset analysis showed the CD4/CD8 T cell ratio was 1.1. The BAL fluid cytology was negative for malignancy, but multinucleated giant cells were

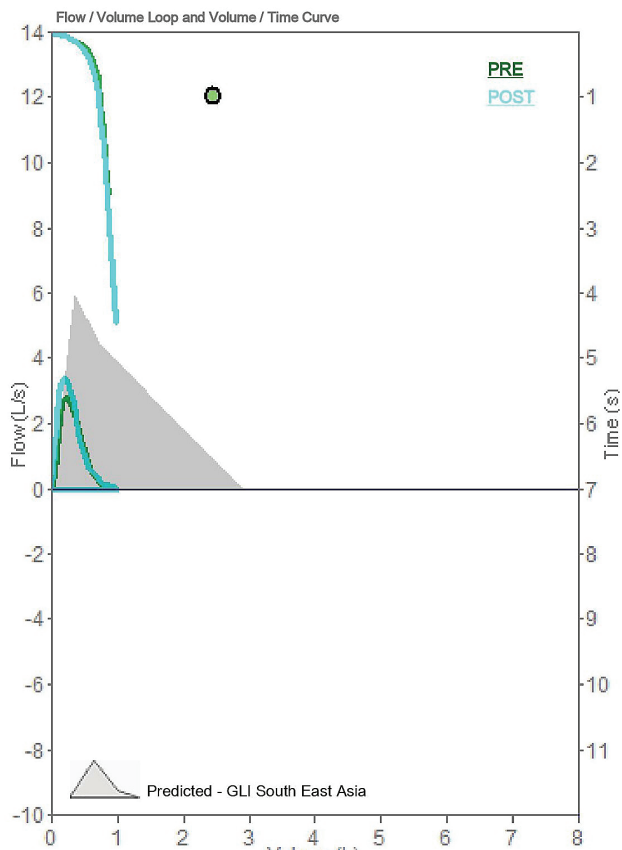


Fig. 3. Pulmonary function test showed severe restrictive lung disease.

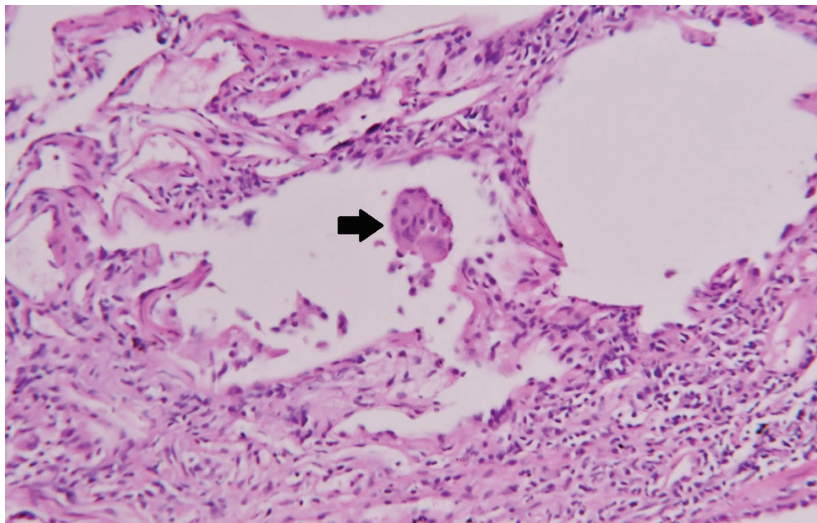


Fig. 4. Specimen of cryobiopsy showed centrilobular chronic inflammation and multinucleated giant cells (black arrow) within the airspace (hematoxylin and eosin stain, 200x).

found. The pathology of the TBLB specimen revealed bronchioalveolar tissue with chronic inflammatory cells infiltrations and fibrosis. The pathology of the TBC specimen revealed centrilobular chronic inflammation and multinucleated giant cells within the airspace, consistent with HMLD (Figure 4).

For HMLD, we prescribed systemic corticosteroid with prednisolone 10 mg per day. We also advised her to change her working environment, but she refused. Her symptoms were partially improved and she maintained outpatient clinical follow-up.

Case Discussion

HMLD was first reported by Jobs and Ballhausen in 1940 in Germany, as a type of pneumoconiosis caused by occupational exposure to hard metals (6). In 1971, Coates and Watson brought out a diagnostic framework for HMLD, including occupational exposure, characteristic radiographic, clinical, and pathologic findings, and the presence of hard metal in lung tissue

specimens (7). The clinical presentation usually includes dyspnea, cough, wheezing, hypoxia, body weight loss, and clubbing fingers. Either restrictive lung disease or obstructive lung disease is found by pulmonary function tests. The DLCO test usually shows a decreased value. Ground-glass opacities and irregular linear opacities are the most common findings on HRCT. Other CT scan findings include consolidations, and centrilobular nodules. In advanced disease, there is a presence of parenchymal distortion, traction bronchiectasis and honeycombing (8). BAL fluid analysis often shows an increased proportion of lymphocytes, eosinophils, and giant cells.

The most common and specific pathology pattern is known as GIP. It is characterized as multinucleated giant cells in the alveoli with interstitial pneumonitis and centrilobular fibrosis. In the older literature, GIP is considered a chance finding in HMLD. But studies have discovered the correlation between GIP and HMLD (9). Ohori et al. reviewed the published literature and concluded that GIP is indeed

highly specific for HMLD (10). In advanced disease, a fibrotic lung pattern such as usual interstitial pneumonitis (UIP) is more frequently seen. Elemental analysis combined with electron microscopy and energy-dispersive X-ray fluorescence spectrometry are essential for the diagnosis when the histological pattern is inconsistent with GIP. Proper prevention of exposure to dust is the mainstay of treatment for HMLD. Withdrawal from exposure to dust can stabilize or even improve pulmonary function. Most HMLD patients respond well to corticosteroid treatment. However, in advanced fibrotic lung cases, there seems to be more resistance to corticosteroid (6). Immunosuppressants are occasionally used in severe cases, but the evidence is not well established. In cases with the most advanced disease, lung transplantation may be the only treatment option (1).

BAL is commonly used in the evaluation of ILD. An abnormal proportion of immune cell types may help to differentiate different types of ILD. A BAL fluid cell differential count with greater than 3% neutrophils is called neutrophilia, and greater than 15% lymphocytes is called lymphocytosis (11). Idiopathic pulmonary fibrosis tends to show a neutrophilic pattern instead of a lymphocytic pattern in BAL studies (12). The cellular distribution of BAL in HMLD has shown diverse patterns of inflammation. For most patients, a normal cellular distribution, like a high number of macrophages, is usually found. For others, there may be an increased number of neutrophils, lymphocytes, or eosinophils (9). Moriyama *et al.* reported the presence of CD163+ macrophages surrounded by CD8+ lymphocytes in the centrilobular fibrosis and peribronchioles (13). Other than the inflammatory cell distribution, the finding of multinucleated giant cells in the BAL is more

specific and pathognomonic for HMLD (9). In our case, there were multinucleated giant cells in the BAL, and the cellular distribution revealed neutrophilic and lymphocytic cellular patterns, which are compatible with the findings reported in the above literature.

In the present case, HMLD was diagnosed by TBC via bronchoscopy. TBC via bronchoscopy was initially used to diagnose and manage central airway lesions. In recent years, there has been an increasing role for TBC in the diagnosis of DPLD, even though SLB remains the gold standard. Compared to SLB, TBC has the advantages of an avoidance of operative and anesthesia risks, shorter hospitalization duration, less mortality, and adequate diagnostic accuracy (14). TBLB by flexible forceps usually yields a small sample size with significant crush artifacts, which is usually inadequate for DPLD diagnosis. In comparison to traditional TBLB, TBC has the advantages of a larger sample size and more preserved tissue architecture (5). TBC has higher rates of bleeding complications than forceps TBLB, but they were generally manageable. Higher pneumothorax rate (1.4% to 33%) is also found, and chest tube drainage is usually needed if pneumothorax develops (15). HMLD is grouped as DPLD based on its histopathologic entity. To the best of our knowledge, there is currently no case report on the diagnosis of HMLD through TBC. Our case shows that cryobiopsy is a useful tool in the diagnosis of HMLD.

In conclusion, we present the first case report using cryobiopsy for diagnosis of HMLD. HMLD is rare, but it should be evaluated carefully once the exposure history and typical radiographic findings are presented. Performing cryobiopsy to obtain a tissue specimen should be taken into consideration when HMLD is

suspected. Further study is needed to clarify the role of cryobiopsy in diagnosing HMLD.

References

- Mizutani RF, Terra-Filho M, Lima E, *et al.* Hard metal lung disease: a case series. *J Bras Pneumol* 2016; 42(6): 447-452.
- Cowie RL, Becklake MR. Pneumoconioses. In: Broaddus VC, Murray JF, Mason RJ. *Murray and Nadel's Textbook of Respiratory Medicine*. 6th ed. Philadelphia: Elsevier Saunders, 2015: 1307-30.e12.
- Balmes JR. Respiratory effects of hard-metal dust exposure. *Occup Med* 1987; 2(2): 327-44.
- Tanaka J, Moriyama H, Terada M, *et al.* An observational study of giant cell interstitial pneumonia and lung fibrosis in hard metal lung disease. *BMJ Open* 2014; 4(3): e004407.
- Lentz RJ, Argento AC, Colby TV, *et al.* Transbronchial cryobiopsy for diffuse parenchymal lung disease: a state-of-the-art review of procedural techniques, current evidence, and future challenges. *J Thorac Dis* 2017; 9(7): 2186-203.
- Chiba Y, Kido T, Tahara M, *et al.* Hard metal lung disease with favorable response to corticosteroid treatment: a case report and literature review. *Tohoku J Exp Med* 2019; 247(1): 51-8.
- Coates EO Jr, Watson JH. Diffuse interstitial lung disease in tungsten carbide workers. *Ann Intern Med* 1971; 75(5): 709-716.
- Sergio P CM, Manotti L, Manuguerra R, *et al.* Hard metal lung disease: unexpected CT findings. *Indian J Radiol Imaging* 2017; 27: 258-9.
- Nemery B, Verbeken EK, Demedts M. Giant cell interstitial pneumonia (hard metal lung disease, cobalt lung). *Semin Respir Crit Care Med* 2001; 22(4): 435-448.
- Ohori NP, Scieurba FC, Owens GR, *et al.* Giant-cell interstitial pneumonia and hard-metal pneumoconiosis. A clinicopathologic study of four cases and review of the literature. *Am J Surg Pathol* 1989; 13(7): 581-7.
- Meyer KC, Raghu G, Baughman RP, *et al.* An official American Thoracic Society clinical practice guideline: the clinical utility of bronchoalveolar lavage cellular analysis in interstitial lung disease. *Am J Respir Crit Care Med* 2012; 185(9): 1004-14.
- Meyer KC, Raghu G. Bronchoalveolar lavage for the evaluation of interstitial lung disease: is it clinically useful? *Eur Respir J* 2011; 38(4): 761-769.
- Moriyama H, Kobayashi M, Takada T, *et al.* Two-dimensional analysis of elements and mononuclear cells in hard metal lung disease. *Am J Respir Crit Care Med* 2007; 176(1): 70-7.
- Iftikhar IH, Alghothani L, Sardi A, *et al.* Transbronchial lung cryobiopsy and video-assisted thoracoscopic lung biopsy in the diagnosis of diffuse parenchymal lung disease. A meta-analysis of diagnostic test accuracy. *Ann Am Thorac Soc* 2017; 14(7): 1197-211.
- Ussavarungsi K, Kern RM, Roden AC, *et al.* Transbronchial cryobiopsy in diffuse parenchymal lung disease: retrospective analysis of 74 cases. *Chest* 2017; 151(2): 400-8.

Multiple Nodular Pulmonary Amyloidosis Mimicking Metastatic Lesions: A Case Report

Po-Chun Lo¹, Chi-Lu Chiang¹

Amyloidosis is a group of diseases caused by extracellular tissue deposition of insoluble fibrils. Pulmonary amyloidosis may present as a nodular form, a diffuse interstitial disease or as localized to the transbronchial tree. Nodular pulmonary amyloidosis that is not associated with primary systemic amyloidosis is rare. We reported a 48-year-old female who was initially suspected of having metastatic lung cancer with bilateral multiple pulmonary nodules on chest computed tomography (CT). CT-guided needle biopsy of the pulmonary nodules revealed nodular pulmonary amyloidosis. (*Thorac Med* 2022; 37: 120-125)

Key words: pulmonary amyloidosis, lung nodule, CT-guided needle biopsy

Introduction

Amyloidosis is a group of diseases caused by extracellular tissue deposition of insoluble fibrils [1]. It could be localized or systemic in nature, resulting in a wide range of clinical manifestations. Pulmonary amyloidosis is more often a localized process and may present as a nodular form, a diffuse interstitial disease, or as localized to the transbronchial tree [2]. Although the presence of amyloidosis may be suggested by the history and clinical manifestations, definitive diagnosis of amyloidosis is made by tissue biopsy. Patients should undergo complete assessment and amyloid typing to determine their optimal treatment. Nodular

pulmonary amyloidosis that is not associated with primary systemic amyloidosis is rare [3]. Here, we describe a case of nodular pulmonary amyloidosis without systemic involvement that resembled metastatic lung cancer.

Case Report

A 48-year-old female presented to our chest clinic with a complaint of dry cough for 2 months. There were no other respiratory symptoms. There was no history of fever, dry eye, night sweats, anorexia or unintentional weight loss. She denied a history of smoking, chronic lung disease, malignancy, or connective tissue disorders. She was not taking any regular medi-

¹Department of Chest Medicine, Taipei Veterans General Hospital, Taipei, Taiwan.

Address reprint requests to: Dr. Chi-Lu Chiang, Division of Thoracic Oncology, Department of Chest Medicine, Taipei Veterans General Hospital, Taipei, Taiwan

cations. Recent travel or exposure to individuals with infectious diseases was denied. There was no apparent history of alcohol consumption, or usage of illicit drugs, herbs, or immunosuppressants. Physical examination was unremarkable. There was no palpable lymphadenopathy, purpura, clubbing finger, or other signs of connective tissue disease. Blood test showed a normal peripheral blood count. Baseline serum chemistry screening tests and urinalysis were also within normal values. Chest radiograph showed bilaterally distributed multiple pulmonary nodules of varying sizes (Figure 1). A computed tomography (CT) scan of the chest was performed, and revealed multiple nodules diffused in bilateral lungs and varying in shape and size. The distribution of amyloid nodules was in the lower lobe with a subpleural predominance. (Figure 2). There was no evidence of interstitial



Fig. 1. Chest radiograph showing bilaterally distributed multiple pulmonary nodules of varying size.

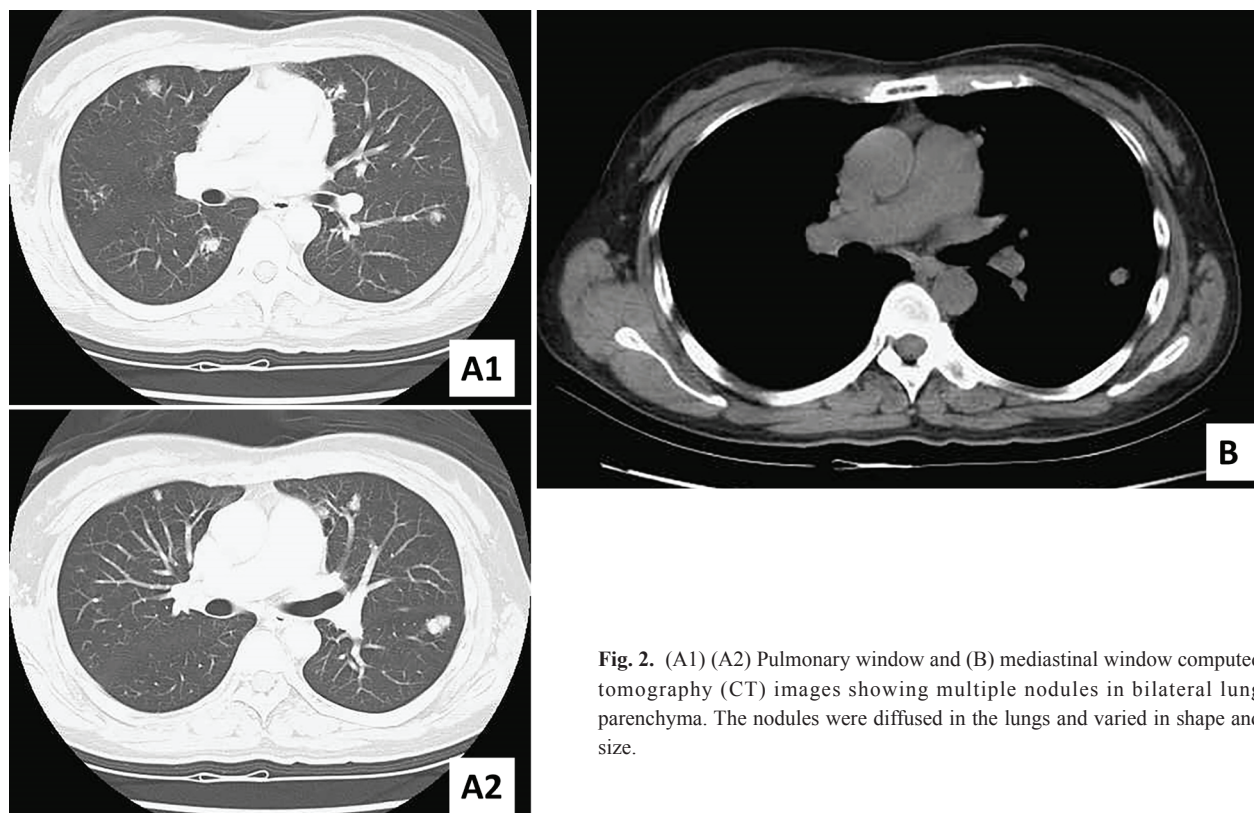


Fig. 2. (A1) (A2) Pulmonary window and (B) mediastinal window computed tomography (CT) images showing multiple nodules in bilateral lung parenchyma. The nodules were diffused in the lungs and varied in shape and size.

lung disease, cystic lung disease, or mediastinal lymphadenopathy. The differential diagnosis of the patient included primary or metastatic malignant nodules, granulomatous disease, and benign pulmonary hamartomas. Sputum cytology revealed negative malignant cells. Neither acid-fast bacilli staining, nor mycobacterial culture were positive. We carried out shared decision-making with the patient for pulmonary nodule management. CT-guided biopsy was suggested because of the small nodules and subpleural distribution. Biopsy of the lung nodules revealed a deposition of fragments of amorphous pink materials, which showed an apple-green birefringence in polarized light after Congo red staining (Figure 3). The immunostains for kappa and lambda were non-contributory. The diagnosis of nodular pulmonary amyloidosis then was established. To exclude other underlying disease, NT-proBNP, echocardiogram, serum-free kappa, serum-free lambda, electrophoresis of serum and urine, immunoelectrophoresis of serum, cryptococcal antigen, anti-nuclear antibody (ANA) titer, and extractable nuclear antigen (ENA) were evaluated and all showed

normal findings. Her symptoms resolved after the use of antitussive agents. The prognosis of pulmonary nodular amyloidosis was excellent, so we decided that further treatment was not required, and the patient could be regularly followed up in our clinic. Follow-up chest CT revealed there was no interval change compared with the image 6 months previous (Figure 4). She is still under active follow-up in our chest clinic.

Discussion

Pulmonary amyloidosis is a disorder that is more often localized than systemically involved. Pulmonary amyloidosis can be divided in 3 different forms: nodular pulmonary amyloidosis, diffuse alveolar-septal amyloidosis, and tracheobronchial amyloidosis. Chronic lung disease (such as bronchiectasis) can lead to systemic AA (apolipoprotein serum amyloid A) amyloidosis [2]. Nodular pulmonary amyloidosis is most often localized and is an incidental finding on chest radiography. It is defined as solitary or multiple nodular amyloid deposits,

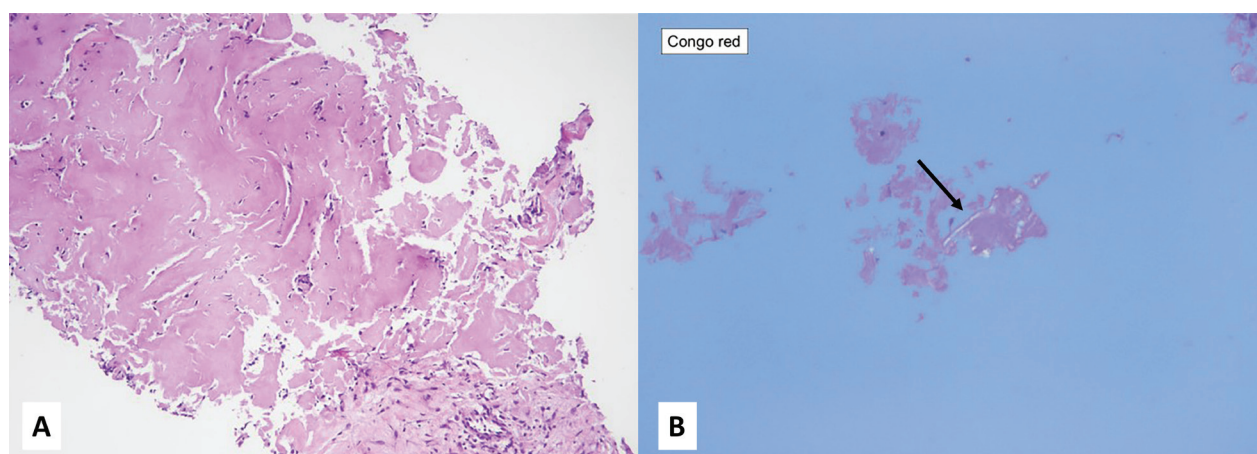


Fig. 3. Histology of nodular pulmonary amyloidosis (A) showing amorphous acidophilic homogeneous material; (B) (arrowhead) showing a positive result of Congo red staining.

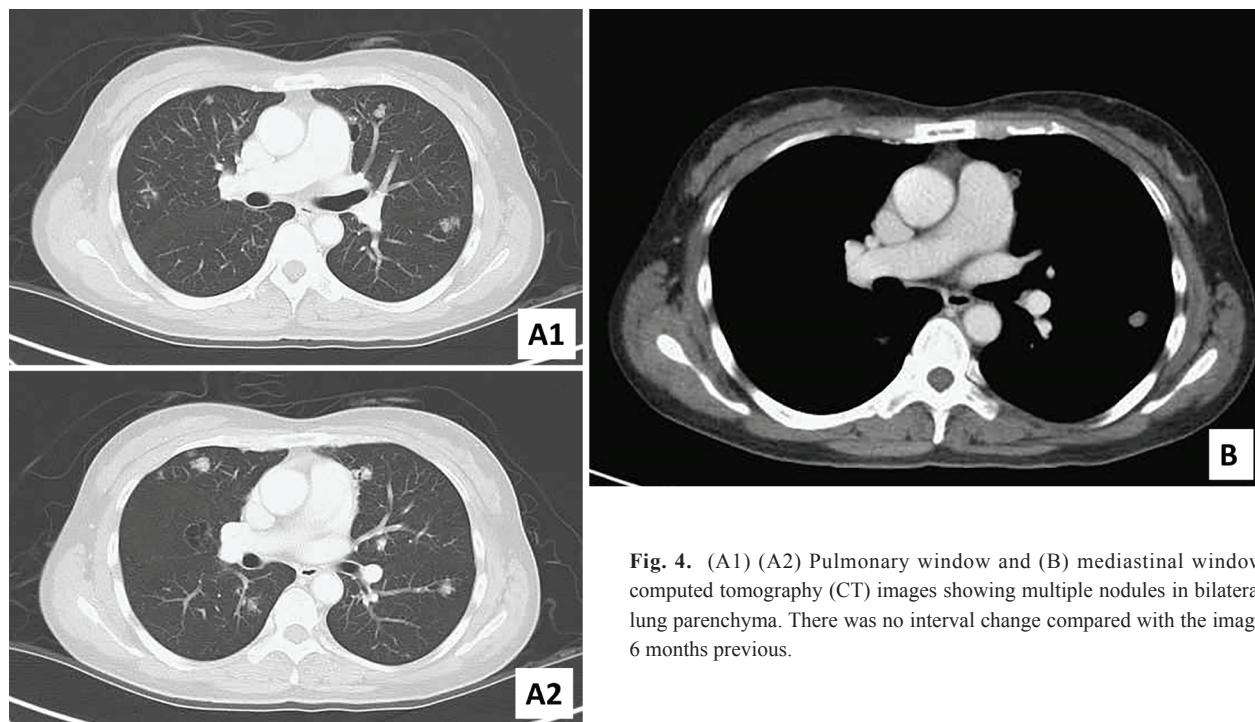


Fig. 4. (A1) (A2) Pulmonary window and (B) mediastinal window computed tomography (CT) images showing multiple nodules in bilateral lung parenchyma. There was no interval change compared with the image 6 months previous.

and is usually associated with immunoglobulin light chains (AL type) or AL/AH (mixed immunoglobulin light chain/heavy chain) amyloidosis [4-5]. In some reports, localized AL amyloidosis could be found not only in the lung but also in the urinary tract, larynx, skin, and eyelids [6-7].

A single center case series of pulmonary amyloidosis found that the mean age of patients is 67 years, and the male:female ratio is 3:2 [9]. Clinical manifestations were determined by the type of precursor protein, the tissue distribution, and the amount of amyloid deposition. Almost all patients with tracheobronchial and diffuse interstitial amyloidosis had respiratory symptoms. Dyspnea was the symptom most often presented. Patients with nodular pulmonary amyloidosis are usually asymptomatic. Some may rarely present with shortness of breath, hemoptysis, or cough, as in our case [7-8]. About

60% of patients exhibit a solitary nodular deposit [10]. Multiple pulmonary nodular deposits in varying sizes are common and may present smooth, lobulated, or spiculated margins and occasional central or punctate calcification [11-13]. Cavitated lesions are rare. Larger masses measuring up to 15 cm at their greatest dimensions have been reported [8]. Amyloid nodules usually tend to be localized to the lower lobes and towards the peripheral and subpleural areas. A nodular lesion associated with a thin-wall cyst may be most common in patients with Sjogren's syndrome [11, 14-15]. The imaging features of our case included multiple nodules with smooth margins distributed peripherally in different sizes. It is difficult to reliably differentiate nodular amyloidosis from metastasis since they have a similar appearance, as demonstrated in our case. Amyloid lung deposits can also have positron emission tomography (PET)

uptake. Increased uptake of 18F-FDG, particularly with a SUVmax greater than 3, increases suspicion about an associated lymphoma or plasmacytoma [16].

Due to the varying imaging appearances, diagnosis cannot be made by image evaluation alone. Diagnosis may be suggested if complete clinical information is available, but biopsy is often required for a definite diagnosis. Amyloid deposits appear as amorphous hyaline material on light microscopy. The fibrils bind Congo red, leading to green birefringence under polarized light and thioflavin T, producing an intense yellow-green fluorescence [17-18]. An association between nodular pulmonary amyloidosis and cancer has been reported recently. A previous report described extranodal marginal zone lymphoma of mucosa-associated lymphoid tissue (MALT lymphoma) with localized amyloid deposition in the lung tissue [4]. Sjogren's disease was also found to be associated with nodular pulmonary amyloidosis [19].

In general, the natural history of nodular pulmonary amyloidosis is benign. Lesions may slowly grow in size and numbers, but the long-term prognosis is excellent. The outcome of 606 cases of localized amyloidosis was reported in a recent series [7]. The estimated 5-year overall survival was 90.6% (95% CI 87.7–92.9), and 10-year overall survival was 80.3% (75.1–84.1). Nodular pulmonary amyloidosis was identified in 47 patients. Median (range) age was 65.5 (36–80) years and 13 cases were male. Surgical intervention was required for 4 patients and only 2 received chemotherapy due to symptomatic pulmonary amyloid deposits. The dearth of controlled clinical studies shows that management decisions must be made on an individual empirical basis. Complete evaluation of pulmonary amyloidosis is required to determine

the treatment. Nodular pulmonary amyloidosis rarely requires intervention, based on the literature.

The differential diagnosis of nodular amyloidosis includes both malignant and benign granulomatous disease. For this patient, metastatic tumor was considered before biopsy. Thorough assessment was done to exclude systemic amyloidosis, lymphoproliferative disorders, or autoimmune disease. The outcome of nodular pulmonary amyloidosis was excellent in our patient and the symptoms resolved. She did not receive aggressive treatment, but choose to be closely followed up in our clinic.

In conclusion, we presented a rare case of nodular pulmonary amyloidosis without systemic involvement, in which the radiographic features mimicked metastatic tumor. An adequate classification of pulmonary amyloidosis helps in assessing its natural course and prognosis, and differentiating patients with or without systemic involvement is necessary. Systemic involvement indicates a poor prognosis and requires more aggressive management. A comprehensive examination is necessary to determine optimal treatment and prognosis.

References

1. Merlini G, Bellotti V. Molecular mechanisms of amyloidosis. *N Engl J Med* 2003; 349: 583-596.
2. Milani P, Basset M, Russo F, *et al.* The lung in amyloidosis. *Eur Respir Rev* 2017; 26(145).
3. Berk JL, O'Regan A, Skinner M. Pulmonary and tracheobronchial amyloidosis. *Semin Respir Crit Care Med* 2002; 23(2): 155-165.
4. Grogg KL, Aubry MC, Vrana JA, *et al.* Nodular pulmonary amyloidosis is characterized by localized immunoglobulin deposition and is frequently associated with an indolent B-cell lymphoproliferative disorder. *Am J Surg Pathol* 2013; 37: 406-412.

5. Kaplan B, Martin BM, Boykov O, *et al.* Co-deposition of amyloidogenic immunoglobulin light and heavy chains in localized pulmonary amyloidosis. *Virchows Arch* 2005; 447: 756-761.
6. Westermark P, Benson MD, Buxbaum JN, *et al.* A primer of amyloid nomenclature. *Amyloid* 2007; 14: 179-183.
7. Mahmood S, Bridoux F, Venner CP, *et al.* Natural history and outcomes in localised immunoglobulin light-chain amyloidosis: a long-term observational study. *Lancet Haematol* 2015; 2: e241-e250.
8. Hui AN, Koss MN, Hochholzer L, *et al.* Amyloidosis presenting in the lower respiratory tract. Clinicopathologic, radiologic, immunohistochemical, and histochemical studies on 48 cases. *Arch Pathol Lab Med* 1986; 110(3): 212-218.
9. Utz JP, Swensen SJ, Gertz MA. Pulmonary amyloidosis. The Mayo Clinic experience from 1980 to 1993. *Ann Intern Med* 1996; 124: 407-413.
10. Pickford HA, Swensen SJ, Utz JP. Thoracic cross-sectional imaging of amyloidosis. *AJR Am J Roentgenol* 1997; 168(2): 351-355.
11. Aylwin AC, Gishen P, Copley SJ. Imaging appearance of thoracic amyloidosis. *J Thorac Imaging* 2005; 20(1): 41-46.
12. Urban BA, Fishman EK, Goldman SM, *et al.* CT evaluation of amyloidosis: spectrum of disease. *RadioGraphics* 1993; 13(6): 1295-1308.
13. Marchiori E, Franquet T, Gasparetto TD, *et al.* Consolidation with diffuse or focal high attenuation: computed tomography findings. *J Thorac Imaging* 2008; 23(4): 298-304.
14. Kim HY, Im JC, Song KS, *et al.* Localized amyloidosis of the respiratory system: CT features. *J Comput Assist Tomogr* 1999; 23: 627-31.
15. Desai SR, Nicholson AG, Stewart S, *et al.* Benign pulmonary lymphocytic infiltration and amyloidosis: computed tomographic and pathologic features in three cases. *J Thorac Imaging* 1997; 12: 215-20.
16. Baqir M, Lowe V, Yi ES, *et al.* 18F-FDG PET scanning in pulmonary amyloidosis. *J Nucl Med* 2014; 55: 565-8.
17. Kyle RA. Amyloidosis: a convoluted story. *Br J Haematol* 2001; 114(3): 529-538.
18. Biancalana M, Koide S. Molecular mechanism of thioflavin-T binding to amyloid fibrils. *Biochim Biophys Acta* 2010; 18.
19. Kobayashi H, Matsuoka R, Kitamura S, *et al.* Sjögren's syndrome with multiple bullae and pulmonary nodular amyloidosis. *Chest* 1988; 94: 438-440.

Chronic Eosinophilic Pneumonia Associated with Heat-Not-Burn Tobacco Cigarette Use

Tung-Chi Yeh¹, Chun-Chieh Wu^{2,3}, Chia-Min Chen¹, Ming-Ju Tsai^{1,4}, Jen-Yu Hung^{1,4}

Heat-not-burn (HNB) tobacco cigarettes are devices that heat tobacco below the temperature at which traditional tobacco burns, producing fewer toxic chemical compounds. However, the potential health risk of HNB tobacco cigarette use remains unclear. We reported the case of a 25-year-old healthy male who suffered from afebrile cough with whitish sputum for 4 months after switching from conventional cigarettes to smuggled HNB tobacco cigarettes for 1 year. Chest computed tomography showed bilateral consolidation patches and ground-glass patches. Peripheral and bronchoalveolar lavage fluid eosinophilia were noted. After steroid treatment for chronic eosinophilic pneumonia (CEP), his symptoms improved rapidly. CEP is a rare disease. Diagnosis of CEP is made by exclusion of other possible causes of eosinophilic pneumonia. E-cigarettes, or vaping product use-associated lung injury has been widely reported recently, so smokers may choose HNB instead. Thus, we elucidate the risk to health of HNB cigarette use. (*Thorac Med* 2022; 37: 126-131)

Key words: heat-not-burn tobacco, chronic eosinophilic pneumonia

Introduction

Heat-not-burn (HNB) tobacco cigarettes are devices that heat tobacco to a temperature of 250-350°C, below the temperature at which normal tobacco burns (about 600°C) [1]. HNB tobacco cigarettes are different from e-cigarettes, another form of battery-operated device, which heats liquid or wax to produce vapor. By heat-

ing tobacco only, aerosol and vapor containing lower levels of nicotine and fewer toxic chemical compounds than conventional cigarettes will be generated. The chemical compounds include volatile organic compounds, polycyclic aromatic hydrocarbons, and carbon monoxide [2-3]. IQOS (an acronym for “I Quit Ordinary Smoking”) is 1 of the HNB tobacco cigarettes designed by Philip Morris International, and

¹Division of Pulmonary and Critical Care Medicine, Department of Internal Medicine, Kaohsiung Medical University Hospital, Kaohsiung, Taiwan, ²Department of Pathology, School of Medicine, College of Medicine, Kaohsiung Medical University, Kaohsiung, Taiwan, ³Department of Pathology, Kaohsiung Medical University Hospital, Kaohsiung, Taiwan, ⁴Department of Internal Medicine, School of Medicine, College of Medicine, Kaohsiung Medical University, Kaohsiung, Taiwan.

Address reprint requests to: Dr. Jen-Yu Hung, Division of Pulmonary and Critical Care Medicine, Department of Internal Medicine, Kaohsiung Medical University Hospital, Kaohsiung Medical University No.100, Tzyou 1st Road, Kaohsiung 807, Taiwan

includes a battery charger, a holder and tobacco sticks, plugs or capsules. Tobacco sticks are heated with an electronically controlled heating element by insertion into the holder. This device has been on the market in Japan since 2014 and in the United States since 2019 [4]. However, the potential risk of using HNB tobacco cigarettes remains unclear.

Case Report

This 25-year-old male had no underlying disease. He had smoked 0.2 pack-per-day for 6 years. He switched from conventional cigarettes to smuggled HNB tobacco cigarettes (brand name: IQOS) 1 year previous to this presentation. He suffered from afebrile cough with whitish sputum for 4 months. Progressive dyspnea on exertion and recent body weight loss were noted 1 month before admission. He denied any recent contact with sick persons or a travel history. Family history was also unremarkable. Lung auscultation revealed mild wheezing in the left lower lobe. Examination of other systems was unremarkable. Chest posteroanterior radiograph showed infiltrations and opacities

in bilateral lung fields (Figure 1A). Pulmonary tuberculosis (TB) was first suspected. Complete blood count showed no leukocytosis (10690/ μL) with 36% neutrophils, 21% lymphocytes, and 34% eosinophils. C-reactive protein (52.42 mg/L) and erythrocyte sedimentation rate (43 mm/h) were both elevated. Sputum acid-fast stain study yielded negative results. Chest high-resolution computed tomography (CT) showed consolidation patches and ground-glass patches at bilateral lung fields (Figure 1B). Lung function test showed a reduced forced vital capacity (FVC) (51%) and forced expiratory volume in 1 second (FEV_1) (52%), but normal FEV_1/FVC (86.6%), and an increased diffusing capacity of the lungs for carbon monoxide (DLCO) (128%). We performed a bronchoscopic examination, but there was only scanty sputum in the airways, and no endobronchial lesion was found. The cells recovered from the bronchoalveolar lavage (BAL) fluid (BALF) were 765/ μL , which included 68% eosinophils, 12% lymphocytes, 18% macrophages, and 2% neutrophils (Figure 2). Microorganisms, including bacteria, fungi and TB, were not identified in the BALF study. The histopathologic assess-

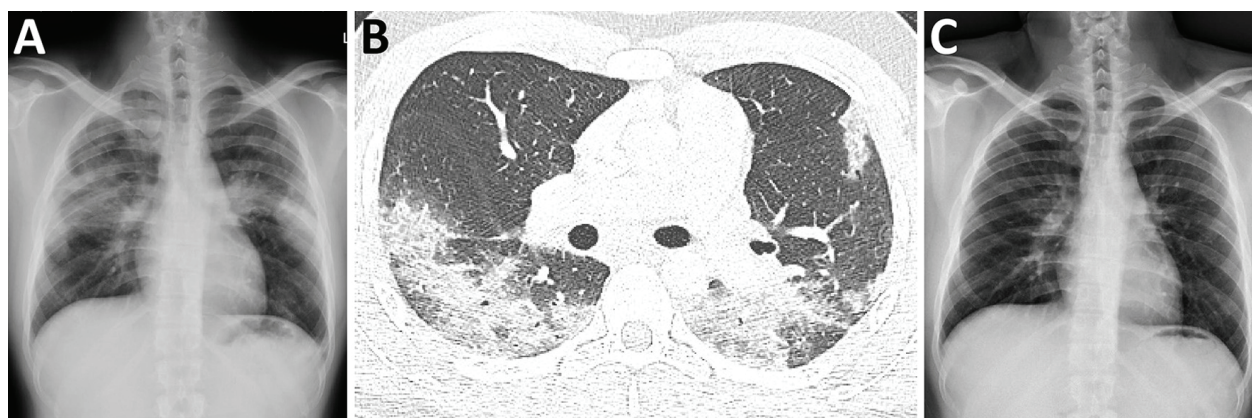


Fig. 1. (A) Chest posteroanterior radiograph showing infiltration and opacity in bilateral lungs; (B) High-resolution computed tomography axial and reformatted coronal view revealed consolidation patches and ground-glass opacities in both lungs; (C) Chest posteroanterior radiograph after 16 days of systemic steroid treatment.

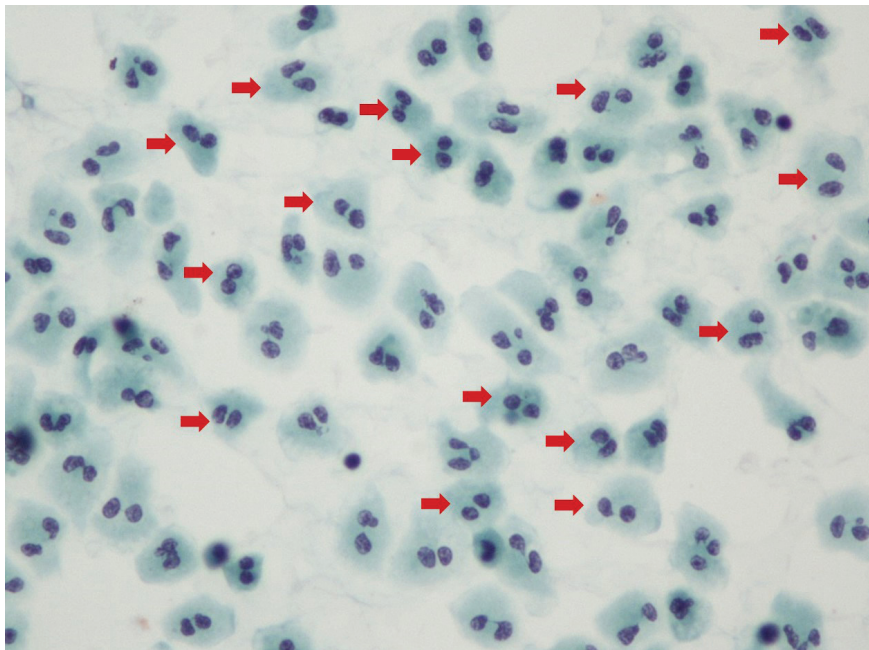


Fig. 2. Papanicolaou stain of bronchoalveolar lavage fluid showed numerous eosinophils (some labeled with red arrows).

ment performed using transbronchial forceps biopsies showed numerous eosinophils aggregations within alveolar spaces with some lipid-laden macrophages and fibrinopurulent materials (Figure 3). Under the impression of chronic eosinophilic pneumonia (CEP), we prescribed prednisolone 30 mg daily for 17 days. The pa-

tient responded well, with complete resolution of symptoms. Chest radiograph findings at the outpatient department (OPD) on day 17 of steroid therapy showed a clearing of the bilateral lung infiltration and opacities (Figure 1C). We then gradually tapered the prednisolone dosage. The total duration of steroid use was about 3

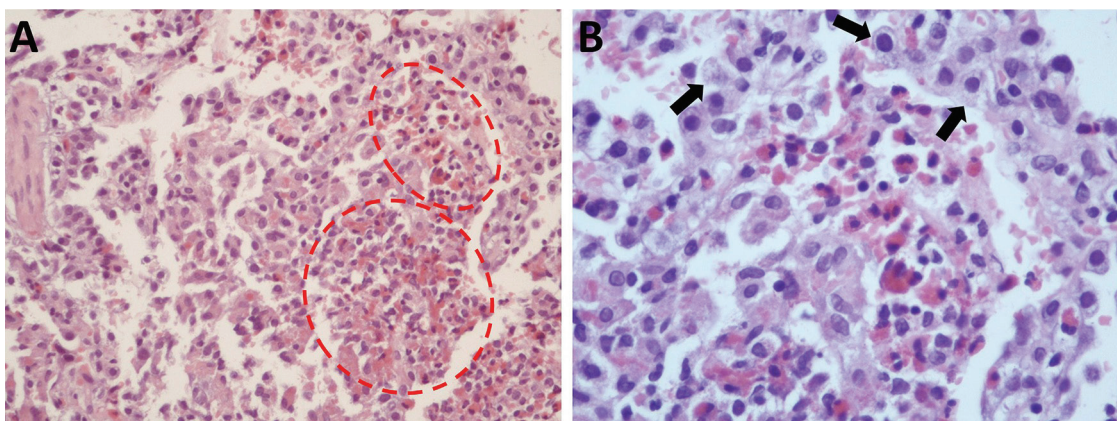


Fig. 3. Histologic sections of transbronchial biopsy showed (A) numerous eosinophil aggregations (red dashed circles) within alveolar spaces with focal thickening of the alveolar septi. (B) Lipid-laden macrophages (black arrow) and fibrinopurulent materials were also noted.

months. No recurrence of symptoms was noted. The patient had already quit smoking.

Discussion

Due to the absence of combustion, fire, ash, or smoke, the population of HNB tobacco cigarette users is increasing worldwide, especially among young people [5]. HNB tobacco cigarettes are reported to produce a lesser amount of tar, nicotine, and other toxic chemical compounds than conventional cigarettes [2, 6]. However, there is no evidence that people using HNB tobacco cigarettes will have a lower health risk.

CEP is a rare disease that is characterized by clinical symptoms persisting for weeks to months, abnormal chest radiographic findings, and pulmonary eosinophilia. Diagnosis of CEP is made by exclusion of other causes of eosinophilic pneumonia, like drug-induced eosinophilic pneumonia, parasites, allergic bronchopulmonary aspergillosis and eosinophilic granulomatosis with polyangiitis [7]. CEP is unlike acute eosinophilic pneumonia (AEP), which usually occurs within 1 month of symptoms onset and may present with acute hypoxemic respiratory failure. Instead, CEP has a gradual onset, and usually requires about 5 months until the diagnosis is confirmed. Clinical symptoms of CEP include cough, sputum, mild fever, dyspnea, and body weight loss. Acute respiratory failure is rare [8]. CEP is female-predominant and is usually correlated with asthma, allergic rhinitis and atopic dermatitis [9]. Chest computed tomography (CT) of CEP may reveal subpleural ground-glass opacities (GGO). Mediastinal lymphadenopathy may also be present. Pleural effusion is rare [7].

To our knowledge, this is the first case of

CEP associated with HNB tobacco cigarettes use. There were just 2 case reports of HNB tobacco cigarettes-induced AEP in the literature [10-11]. Kamada T, *et al.* reported the case of a 20-year-old man who had smoked HNB cigarettes for 6 months. After he double-dosed for another 2 weeks, he suffered from fever and dyspnea. Chest CT revealed bilateral infiltrations, smooth interlobular septal thickening, and bilateral pleural effusion. The patient required oxygen therapy without mechanical ventilation. BALF showed an increased eosinophil count [10]. Aokage T, *et al.* reported the case of a 16-year-old male who suffered from severe cough, fatigue, and dyspnea after smoking HNB tobacco cigarettes for only 2 weeks. Chest CT showed GGO spreading over bilateral lung fields. BALF showed slightly elevated eosinophil counts. His lung function deteriorated rapidly, and both mechanical ventilation and extracorporeal membrane oxygenation were used [11]. There was no peripheral eosinophilia, a characteristic of AEP [7], in either case. Both cases had rapid improvement after steroid therapy. As for our case, the sputum study and BALF, including cultures for bacteria, fungi, and mycobacteria, were all negative, and the patient had no asthma history or other medication exposure. An elevated eosinophil percentage in the BALF (>25%) is a characteristic of both AEP and CEP. But peripheral eosinophilia, a characteristic of CEP, was present in our case. CEP usually has more slowly progressive symptoms. Both AEP and CEP respond well to steroid therapy.

E-cigarette use attracts young people, and the prevalence of e-cigarette use among this population is increasing rapidly [12]. E-cigarettes are another form of battery-operated device that heats liquid or wax to produce vapor,

which may contain various substances, such as nicotine, cannabinoids, tetrahydrocannabinol, cannabidiol, or flavorings [13]. However, e-cigarettes, or vaping product use-associated lung injury (EVALI) has been widely reported. EVALI is a variety of acute or subacute pulmonary illness and may be life-threatening. The pathogenesis of EVALI remains unknown. The radiological features of EVALI vary, and may present as bilateral consolidation and ground-glass patches with subpleural sparing on chest CT. It has been reported that the radiological patterns of vaping-associated lung injury can mimic hypersensitivity pneumonitis, AEP, diffuse alveolar damage, lipoid pneumonia, or organizing pneumonia [14-15]. Hypersensitivity pneumonitis occurs when there is an exposure to the allergen in the environment. Chest CT may present bilateral basilar-predominant centrilobular ground-glass nodules. AEP is linked to toxin inhalation, and CT may present diffuse GGO and consolidation with interlobular septal thickening. Unlike CEP, pleural effusion may also be present. Diffuse alveolar damage is the histopathological presentation of the acute lung injury. CT may reveal diffuse consolidation and GGO in the dependent lung. Lipoid pneumonia is related to lipid materials inhalation or aspiration. In these cases, CT may reveal bilateral basilar GGO and consolidation. Focal fat attenuation within consolidation (<-30 Hounsfield unit (HU)) characterizes lipoid pneumonia, but is not seen in EVALI cases. Organizing pneumonia is associated with chronic inflammation and is characterized by fibroblast proliferation and intraluminal granulation tissue polyps involvement in alveolar ducts and surrounding alveoli. CT may present perilobular consolidation patches and GGO in bilateral lungs, and a “reversed halo” sign [15]. The BAL cell counts

tend to show an increase in neutrophils (65%, with a range of 10% to 91%). Eosinophils are minimal (0%, with range of 0% to 6%) [16]. This differs from eosinophilic pneumonia, which is characterized by eosinophils $>25\%$ in the BAL fluid. Histopathology findings are non-specific and usually reveal acute lung injury, including acute fibrinous pneumonitis, diffuse alveolar damage, or organizing pneumonia [17].

Since EVALI has been widely reported recently, the general public may choose HNB cigarette use as a safer alternative. Therefore, elucidating the risk to health with HNB tobacco cigarette use is important and urgent. To our knowledge, this is the first case of CEP induced by HNB tobacco cigarette use. Due to the diversity of HNB devices, products and user habits, determining the specific chemical compound causing lung injury requires further investigation. HNB tobacco cigarettes are not legally approved in Taiwan. However, HNB tobacco cigarettes are already marketed or are going to be marketed in more than 40 countries worldwide. HNB cigarette use could cause a public health burden, and its adverse effects need more detailed confirmation.

References

1. Caputi TL. Industry watch: heat-not-burn tobacco products are about to reach their boiling point. *Tob Control* 2016; 26(5): 609-10.
2. Auer R, Concha-Lozano N, Jacot-Sadowski I, *et al.* Heat-not-burn tobacco cigarettes: smoke by any other name. *JAMA Intern Med* 2017; 177(7):1050-2.
3. Simonavicius E, McNeill A, Shahab L, *et al.* Heat-not-burn tobacco products: a systematic literature review. *Tob Control* 2019; 28(5): 582-94.
4. Tabuchi T, Gallus S, Shinozaki T, *et al.* Heat-not-burn tobacco product use in Japan: its prevalence, predictors and perceived symptoms from exposure to secondhand

- heat-not-burn tobacco aerosol. *Tob Control* 2018; 27(e1): e25-e33.
5. Czoli CD, White CM, Reid JL, *et al.* Awareness and interest in IQOS heated tobacco products among youth in Canada, England and the USA. *Tob Control* 2020; 29(1): 89-95.
 6. Werley MS, Freelin SA, Wrenn SE, *et al.* Smoke chemistry, in vitro and in vivo toxicology evaluations of the electrically heated cigarette smoking system series K. *Regul Toxicol Pharmacol* 2008; 52(2): 122-39.
 7. Suzuki Y, Suda T. Eosinophilic pneumonia: A review of the previous literature, causes, diagnosis, and management. *Allergol Int* 2019; 68(4): 413-9.
 8. Marchand E, Reynaud-Gaubert M, Lauque D, *et al.* Idiopathic chronic eosinophilic pneumonia. A clinical and follow-up study of 62 cases. *The Groupe d'Etudes et de Recherche sur les Maladies "Orphelines" Pulmonaires (GERM"O"P)*. *Medicine (Baltimore)* 1998; 77(5): 299-312.
 9. Marchand E, Etienne-Mastroianni B, Chanez P, *et al.* Idiopathic chronic eosinophilic pneumonia and asthma: how do they influence each other? *Eur Respir J* 2003; 22(1): 8-13.
 10. Kamada T, Yamashita Y, Tomioka H. Acute eosinophilic pneumonia following heat-not-burn cigarette smoking. *Respirol Case Rep* 2016; 4(6): e00190.
 11. Aokage T, Tsukahara K, Fukuda Y, *et al.* Heat-not-burn cigarettes induce fulminant acute eosinophilic pneumonia requiring extracorporeal membrane oxygenation. *Respir Med Case Rep* 2019; 26: 87-90.
 12. Barrington-Trimis JL, Leventhal AM. Adolescents' use of "pod mod" e-cigarettes - urgent concerns. *N Engl J Med* 2018; 379(12): 1099-102.
 13. Tabuchi T, Kiyohara K, Hoshino T, *et al.* Awareness and use of electronic cigarettes and heat-not-burn tobacco products in Japan. *Addiction* 2016; 111(4): 706-13.
 14. Henry TS, Kligerman SJ, Raptis CA, *et al.* Imaging findings of vaping-associated lung injury. *AJR Am J Roentgenol* 2019; 1-8.
 15. Henry TS, Kanne JP, Kligerman SJ. Imaging of vaping-associated lung disease. *N Engl J Med* 2019; 381(15): 1486-7.
 16. Layden JE, Ghinai I, Pray I, *et al.* Pulmonary illness related to e-cigarette use in Illinois and Wisconsin - preliminary report. *N Engl J Med* 2019.
 17. Butt YM, Smith ML, Tazelaar HD, *et al.* Pathology of vaping-associated lung injury. *N Engl J Med* 2019; 381(18): 1780-1.

Influenza Pneumonia Associated with Invasive Pulmonary Aspergillosis Requiring Venovenous Extracorporeal Membrane Oxygenation Support: A Case Report and Literature Review

Tzu-Hsuan Chiu¹, Chiung-Hung Lin¹, Jia-Shiuan Ju¹, Han-Chung Hu¹

Invasive pulmonary aspergillosis (IPA) is an often underdiagnosed, lethal coinfection in critically ill patients who have influenza pneumonia. Here, we reported the case of a 49-year-old man without classic immunocompromised host factors for IPA. The patient was diagnosed with influenza and IPA coinfection complicated by acute respiratory distress syndrome. He recovered successfully after antifungal agent treatment and venovenous extracorporeal membrane oxygenation (ECMO) support. With regard to the effect of ECMO on the pharmacokinetics of voriconazole, therapeutic drug monitoring was performed to ensure an optimal antifungal agent dose. This case report highlights the importance of early diagnosis and treatment of IPA, and the role of therapeutic drug monitoring in patients receiving ECMO. (*Thorac Med* 2022; 37: 132-139)

Key words: invasive pulmonary aspergillosis, acute respiratory distress syndrome, extracorporeal membrane oxygenation, therapeutic drug monitoring

Introduction

Invasive pulmonary aspergillosis (IPA) is seen mostly in immunodeficient patients associated with high morbidity and mortality rates [1]. In the past 20 years, several studies have pointed out that IPA also affects critically ill patients in the intensive care unit (ICU) who lack a classical host factor for IPA [2-3]. Moreover, influenza infection has been identified as an independent risk factor for developing IPA [4].

Venovenous extracorporeal membrane oxy-

genation (vv-ECMO) is an effective treatment to support patients with acute respiratory distress syndrome (ARDS) unresponsive to optimal medical therapy and mechanical ventilation management [5]. Since there is considerable change in the pharmacokinetics of voriconazole during ECMO, therapeutic dose monitoring is indicated to reduce unanticipated changes in drug concentrations [6].

Here, we describe a case of coinfection with influenza and aspergillus complicated with ARDS that required vv-ECMO support.

¹Respiratory and Pulmonary Department, Linkou Chang Gung Memorial Hospital, Taoyuan, Taiwan. Address reprint requests to: Dr. Han-Chung Hu, Respiratory and Pulmonary Department, Linkou Chang Gung Memorial Hospital, No.5, Fuxing St., Guishan Dist., Taoyuan City 333423, Taiwan (R.O.C.)

Case Presentation

A 49-year-old man with type 2 diabetes mellitus and hypertension was sent to our emergency department with a 5-day history of dry cough and shortness of breath. In triage, his vital signs were blood pressure: 136/82 mmHg, HR: 102 bpm, RR: 33/min, BT: 37.2°C, and SpO₂: 92%. On physical examination, he appeared acutely ill with severe shortness of breath and accessory muscle usage. Bilateral crackles were noted on auscultation. The patient remained desaturated while using a non-rebreathing mask with 15 L/min.

Laboratory tests revealed slightly elevated aspartate transaminase (AST) (66 IU) and C-reactive protein (CRP) levels (221.5 mg/dL). Initial chest X-ray showed bilateral lung diffuse interstitial infiltration (Figure 1). Intubation was performed immediately, and empiric antibiotics including intravenous piperacillin/tazobactam, teicoplanin and oral oseltamivir were administered in their usual doses. He was admitted to the ICU subsequently.

Echocardiogram showed adequate left ventricular function with a left ventricular ejection fraction of 68% without regional wall abnormality. After intubation, arterial blood gas (ABG) analysis showed both hypercapnia and hypoxemia (pH: 7.285, PaCO₂: 64 mmHg, PaO₂: 74 mmHg, FiO₂ 0.8). The PaO₂/FiO₂ ratio (PFR) was 92.5 mmHg with a positive end expiratory pressure (PEEP) of 16 cm H₂O. The sputum Gram stain, influenza rapid test and influenza polymerase chain reaction (PCR) test were all negative, but the sputum culture yielded mold on the 4th day of admission (day 4). Meanwhile, the serum Aspergillus Galactomanan antigen (GM Ag) was 6.54. The tentative diagnosis was atypical pneumonia with severe

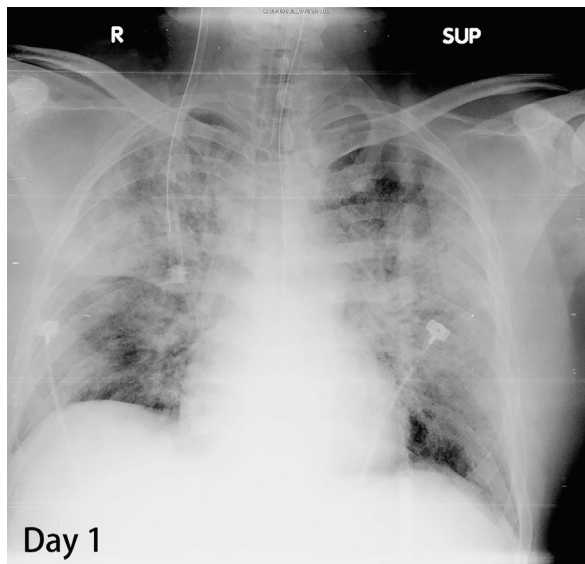


Fig. 1. Chest radiography on day 1 after admission.

ARDS. Voriconazole (4.4 mg/kg q12h IV) and peramivir were then given.

Chest CT scan showed bilateral opacity with an antero-posterior density gradient (dense consolidation in the dependent region and ground-glass attenuation in the non-dependent region) (Figure 2A-D). Microbial investigation via bronchoalveolar lavage revealed the presence of *Aspergillus flavus*, an *Aspergillus* GM Ag of 5.63 and positive SWH1N1 PCR. A diagnosis of coinfection with influenza and aspergillus was confirmed.

On day 7, deteriorating hypoxia was noted, with ABG analysis showing pH 7.44, pCO₂ 63.9 mmHg and pO₂ 56 mmHg on ventilator support using FiO₂ 100%, PEEP 16, and Vt 480 ml/min. He had a PFR of 56, oxygenation index of 25, and RESP score of 4 (estimated survival rate: 76%). VV-ECMO (2000rpm; blood flow, 3.8L/min; sweep gas flow, 4 L/min; Circuit FiO₂, 1) was established accordingly. Protective mechanical ventilator settings were used.

Therapeutic dose monitoring of serum

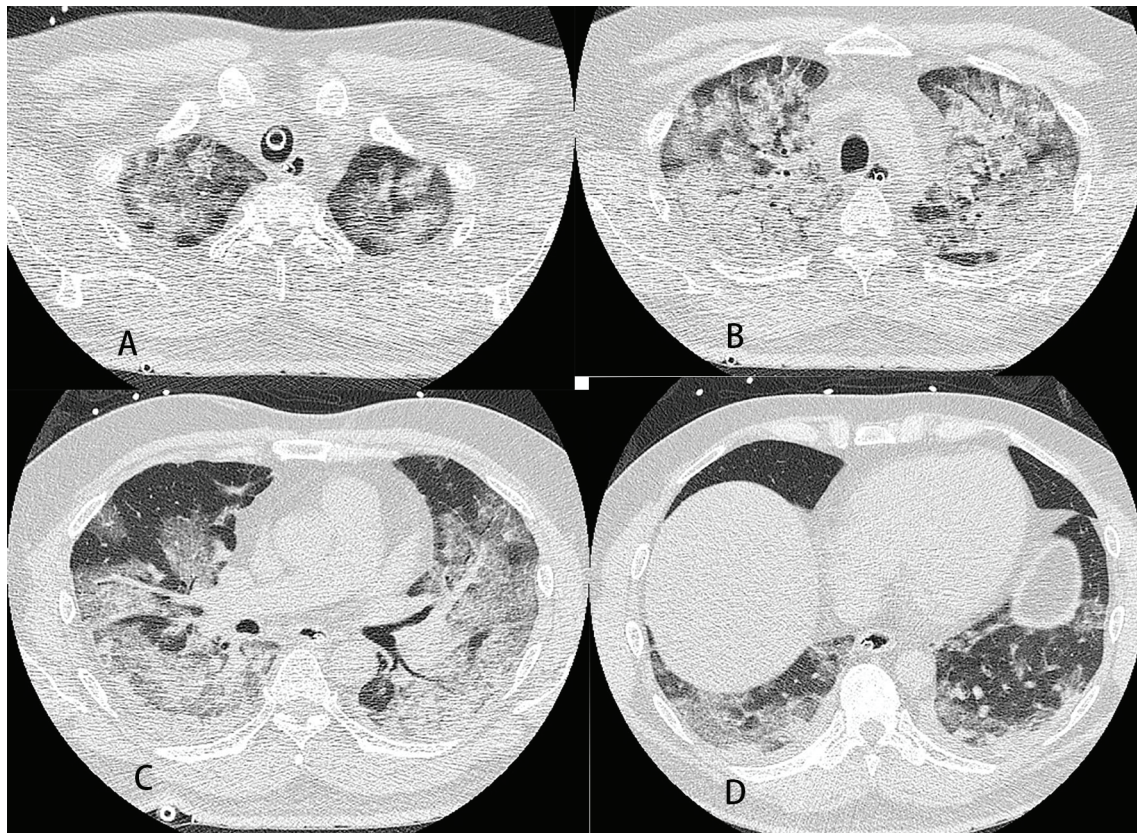


Fig. 2. A-D: Chest CT showing bilateral opacity with an antero-posterior density gradient.

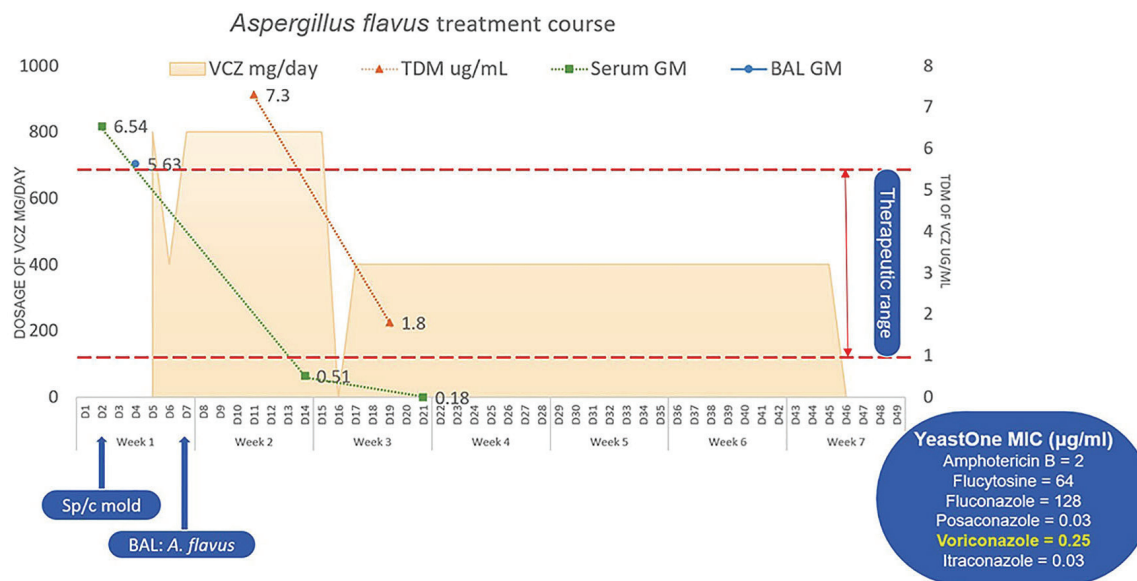


Fig. 3. Therapeutic drug monitoring of voriconazole.

voriconazole was performed on day 13, and the result was higher than the target dose (serum dose: 7.3 ug/mL; target dose: 1-5.5 ug/mL). After tapering voriconazole to 2.2 mg/kg q12h on day 19, the serum dose on day 24 was within a therapeutic range (1.8 ug/mL) (Figure 3). Serial follow-up chest radiography from day 6 to day 22 showed improvement in *Aspergillus flavus*, aspergillus GM Ag 5.63 the bilateral infiltration (Figure 4 A-F). We started to wean ECMO on day 21, since the patient was hemodynamically stable with improvement of lung function. After stepwise reduction of the ECMO blood flow to 1.5 L/min, we tapered the ECMO gas flow and increased ventilator support at the same time. VV-ECMO was shut down on day 22. The pa-

tient was weaned from the ventilator successfully on day 29, and then discharged from the ICU on day 31. Follow-up chest radiography on day 40 and day 70 (after discharge) showed complete resolution of the bilateral infiltration (Figure 5 A-B).

Discussion

According to the criteria of the European Organization for the Research and Treatment of Cancer/Mycoses Study Group (EORTC/MSG) in 2008, a diagnosis of “proven” IPA requires histopathologic confirmation [7]. In addition, “probable” or “possible” IPA is diagnosed for those who have classic immunocompromised

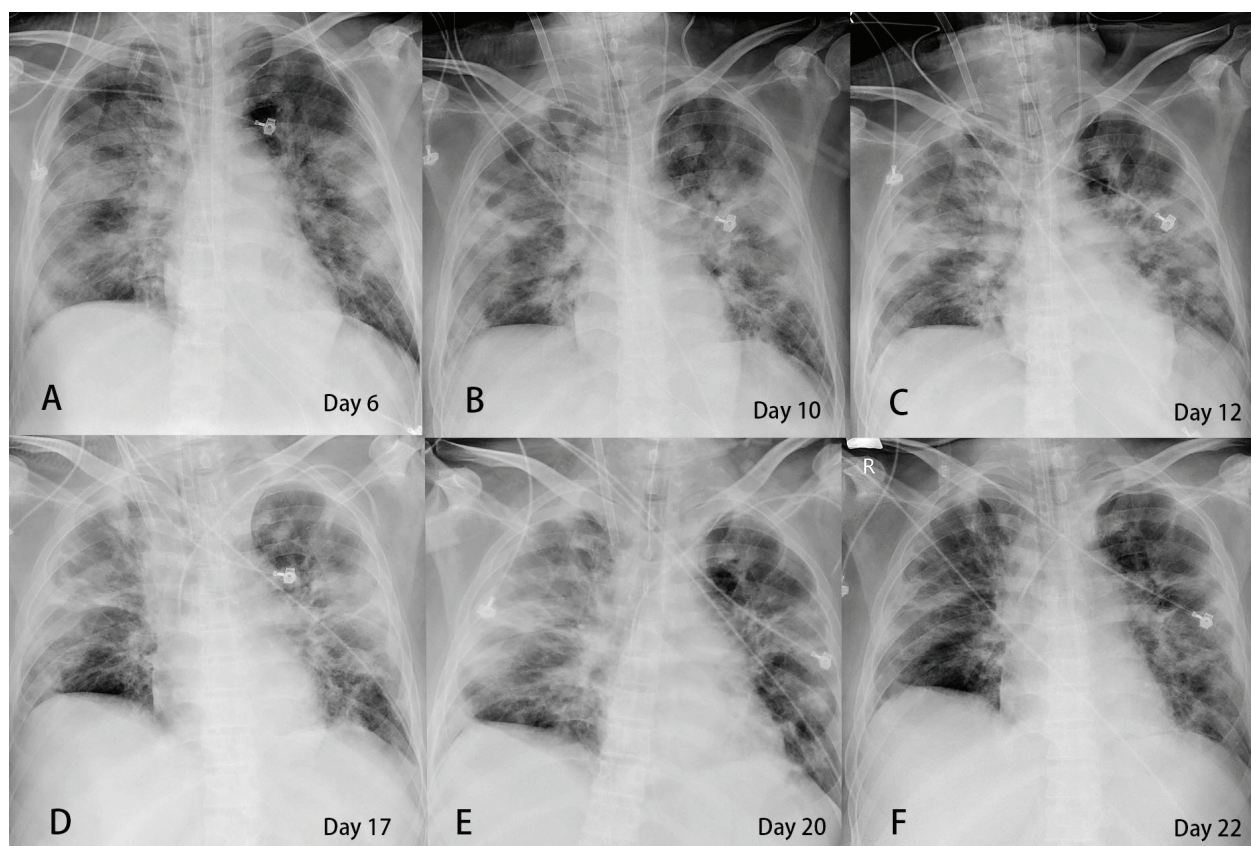


Fig. 4. A-F: Serial chest radiography from day 6 to day 22.

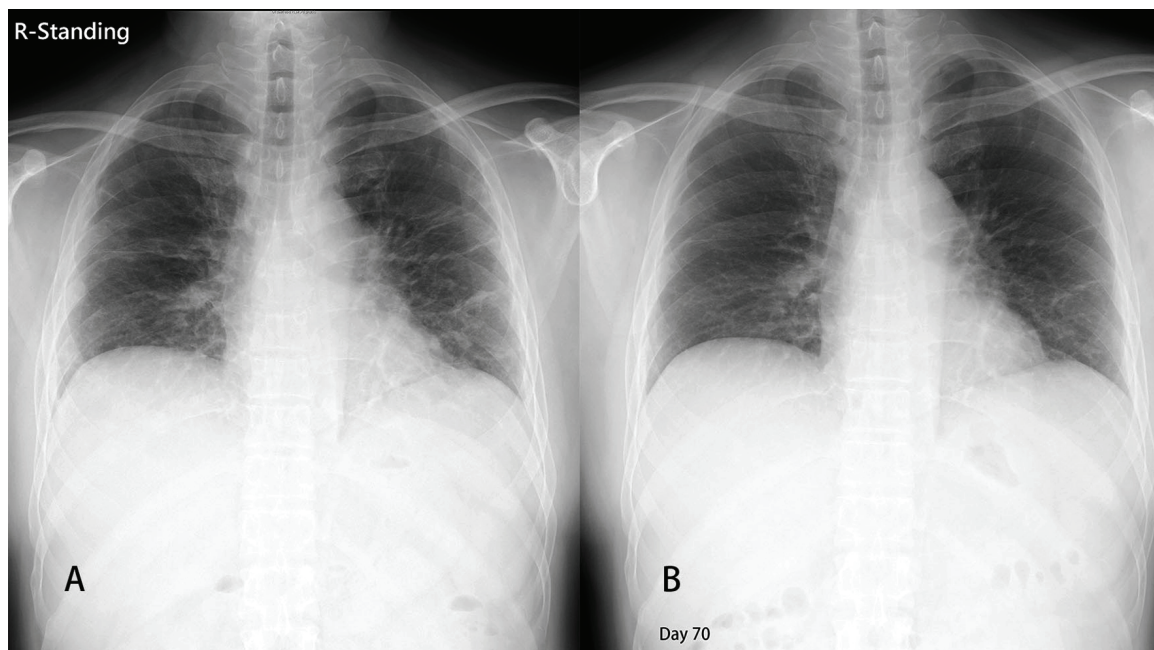


Fig. 5. A-B: Follow-up chest radiography on day 40 and day 70.

host factors. Considering that histopathology is often unfeasible in clinical practice, EORTC/MSG criteria might result in underdiagnosis of IPA. Blot SI *et al* establish an alternative clinical diagnostic algorithm via a cohort study, which discriminates aspergillus colonization from IPA in ICU patients with aspergillus-positive endotracheal aspiration culture (Table 1). The algorithm revealed a specificity of 61%, sensitivity of 92%, PPV of 61%, and a NPV of 92% [8]. In this case, the patient had no classic immunocompromised host factors nor typical signs of IPA on CT. He would be excluded using EORTC/MSG criteria, but was classified as “putative IPA” based on an alternative clinical algorithm. H1N1 infection was later proven by positive influenza PCR in a bronchoalveolar lavage specimen, and he was promptly treated with voriconazole and neuraminidase inhibitors. In 2018, Schauwvlieghe A *et al.* reported a retrospective multicenter cohort study that

found the incidence of severe influenza-related IPA was 19%, and that severe influenza was an independent risk factor for IPA with a 90-day-mortality rate of 51% [9]. Rodriguez-Goncer I *et al.* found that patients with IPA receiving vv-ECMO had a higher 6-month mortality rate than those who used vv-ECMO with other diagnoses (80% vs 11%) [10]. Our patient successfully recovered from ARDS without obvious complications, probably due to the early diagnosis and intervention. A clinical algorithm is useful and more practical than the EORTC/MSG algorithm for critically ill patients in the ICU.

According to the 2016 Infectious Diseases Society of America (IDSA) guidelines for the diagnosis and management of aspergillosis, voriconazole was recommended for primary treatment of IPA with a minimum duration of 6-12 weeks. Alternative therapies include liposomal amphotericin B (AmB), isavuconazole, or other lipid formulations of AmB. A primary

Table 1. Comparison of Differences Between Pulmonary Parenchymal Calcification and Ossification

1. Aspergillus (+) lower respiratory tract specimen culture (entry criterion)
2. Compatible signs and symptoms (1 of the following)
◆ Fever refractory to at least 3 days of appropriate antibiotic therapy
◆ Recrudescence fever after a period of defervescence of at least 48 h while still on antibiotics and without other apparent cause
◆ Pleuritic chest pain
◆ Pleuritic rub
◆ Dyspnea
◆ Hemoptysis
◆ Worsening respiratory insufficiency in spite of appropriate antibiotic therapy and ventilatory support
3. Abnormal medical imaging by portable chest X-ray or CT scan of the lungs
4. Either
4a. Host risk factors (1 of the following conditions)
◆ Neutropenia (absolute neutrophil count less than 500/mm ³) preceding or at the time of ICU admission
◆ Underlying hematological or oncological malignancy treated with cytotoxic agents
◆ Glucocorticoid treatment (prednisone or equivalent, >20 mg/day)
◆ Congenital or acquired immunodeficiency
OR
4b. Semiquantitative Aspergillus-positive
◆ Culture of BAL fluid (+ or ++) without bacterial growth together with a positive cytological smear showing branching hyphae
Probable IPA: 1 + 2 + 3 + either 4a or 4b
Aspergillus colonization: when ≥1 criterion is not met

combination therapy (a combination of polyenes or azoles with echinocandins) is not routinely recommended, while it may be considered as a salvage therapy for refractory IPA [11].

Voriconazole exhibits highly variable inter-individual pharmacokinetics, especially for those who are critically ill. The pharmacokinetics of voriconazole is affected by body weight, gastrointestinal absorptive function, drug-drug interaction and the cytochrome P450 2C19 (CYP2C19) polymorphism [12]. All patients in the ICU receiving voriconazole therapy are

indicated for TDM, and the target steady-state trough blood concentration is 1-5.5 mg/L [13]. Winiszewski H *et al.* reported an IPA patient with episodic decreased voriconazole concentrations each time the ECMO membrane was changed, possibly resulting from drug sequestration on the ECMO membrane [14]. Thus, therapeutic drug monitoring TDM is highly recommended for patients receiving ECMO. In our case, the patient's serum voriconazole concentration was supratherapeutic and toxic (7.3 ug/mL), even though we administered a

standard adult dose (4 mg/kg Q12H IV, using actual body weight). Five days after decreasing the voriconazole dose by 50%, the serum concentration was within therapeutic range (1.8 ug/mL). The patient did not receive any medication that would induce drug-drug interaction with voriconazole. The high voriconazole concentration might have resulted from his obesity. The patient was 81.1 kg in weight and 175 cm in height. His body mass index (BMI) was 26.5, and his ideal body weight (IBW) and adjusted body weight (AJBW) were 70.47 kg and 74.7 kg, respectively. Though the evidence was limited, several retrospective studies found that using actual body weight to dose voriconazole in obese patients resulted in overdose, and IBW or AJBW is suggested for dosing adjustment [15-16].

To reduce the risk of IPA, antifungal prophylaxis with posaconazole or voriconazole is recommended for those who are at high risk of IPA (including patients who are expected to experience prolonged severe neutropenia for >7 days, those who are allogeneic hematopoietic stem cell transplant recipients with Graft-Versus-Host Disease, and those who received a lung transplant within the previous 3 months) [11]. Since our patient had none of the traditional risk factors, antifungal prophylaxis played no role in his condition.

In our case, we noted that IPA is a lethal infection in ICU patients even without classic immunocompromise host factors. Early clinical suspicion and prompt initiation of anti-fungal therapy for these patients is crucial and may result in a better outcome. We also highlight the role of voriconazole dose adjustment via body weight and TDM for obese patients receiving vv-ECMO.

References

1. Patterson, T. F., et al. Practice guidelines for the diagnosis and management of aspergillosis: 2016 update by the Infectious Diseases Society of America. *Clin Infect Dis* 2016; 63(4): e1-e60.
2. Bassetti M, Bouza E. Invasive mold infections in the ICU setting: complexities and solutions. *J Antimicrob Chemother* 2017; 72: i39-i47.
3. Danion F, Rouzaud C, Duréault A, *et al.* Why are so many cases of invasive aspergillosis missed? *Med Mycol* 2019; 57: S94-s103.
4. Crum-Cianflone NF. Invasive aspergillosis associated with severe influenza infections. *Open Forum Infect Dis* 2016; 3: ofw171.
5. Peek GJ, Mugford M, Tiruvoipati R, *et al.* Efficacy and economic assessment of conventional ventilatory support versus extracorporeal membrane oxygenation for severe adult respiratory failure (CESAR): a multicentre randomised controlled trial. *Lancet* 2009; 374: 1351-1363.
6. Hahn J, Choi JH, Chang MJ. Pharmacokinetic changes of antibiotic, antiviral, antituberculosis and antifungal agents during extracorporeal membrane oxygenation in critically ill adult patients. *J Clin Pharm Ther* 2017; 42: 661-671.
7. Revised definitions of invasive fungal disease from the European Organization for Research and Treatment of Cancer/Invasive Fungal Infections Cooperative Group and the National Institute of Allergy and Infectious Diseases Mycoses Study Group (EORTC/MSG) consensus group. *Clin Infect Dis* 2008 Jun 15; 46(12): 1813-21.
8. Blot SI, Taccone FS, Van den Abeele AM, *et al.* A clinical algorithm to diagnose invasive pulmonary aspergillosis in critically ill patients. *Am J Respir Crit Care Med* 2012; 186:56-64.
9. Schauvlieghe A, Rijnders BJA, Philips N, *et al.* Invasive aspergillosis in patients admitted to the intensive care unit with severe influenza: a retrospective cohort study. *Lancet Respir Med* 2018; 6: 782-792.
10. Rodriguez-Goncer I, Thomas S, Foden P, *et al.* Invasive pulmonary aspergillosis is associated with adverse clinical outcomes in critically ill patients receiving veno-venous extracorporeal membrane oxygenation. *Eur J Clin Microbiol Infect Dis* 2018; 37: 1251-1257.

11. Patterson TF, Thompson GR 3rd, Denning DW, *et al.* Practice Guidelines for the Diagnosis and Management of Aspergillosis: 2016 Update by the Infectious Diseases Society of America. *Clin Infect Dis.* 2016; 63(4):e1. Epub 2016 Jun 29.
12. Hope WW. Population pharmacokinetics of voriconazole in adults. *Antimicrob Agents Chemother* 2012; 56: 526-531.
13. Ashbee HR, Barnes RA, Johnson EM *et al.* Therapeutic drug monitoring (TDM) of antifungal agents: guidelines from the British Society for Medical Mycology. *J Antimicrob Chemother* 2014; 69: 1162-76.
14. Winiszewski H, Rougny AC, Lagoutte-Renosi J, *et al.* The pharmacokinetic challenge of treating invasive aspergillosis complicating severe influenzae assisted by extracorporeal membrane oxygenation. *Crit Care* 2018; 22: 355.
15. Davies-Vorbrodt S, Ito JI, Tegtmeyer BR, *et al.* Voriconazole serum concentrations in obese and overweight immunocompromised patients: a retrospective review. *Pharmacotherapy* 2013; 33: 22-30.
16. Eljaaly K, Nix DE. Voriconazole dosing in obese patients. *Clin Infect Dis* 2016; 63: 286-287.

Pulmonary Arteriovenous Malformation in a Woman with Chronic Obstructive Pulmonary Disease and Recurrent Stroke: A Case Report

Ting-Chia Chang¹, Shian-Chin Ko²

Pulmonary arteriovenous malformation (PAVM) is a rare cardiovascular anomaly that can cause serious complications, such as stroke and cerebral abscess. We present the case of a 55-year-old woman with old stroke, who presented with dyspnea and severe hypoxia refractory to high-concentration oxygen therapy. A large mass-like opacity in the right lower lung field was noted on the chest radiograph. Diagnosis of PAVM was considered based on the clinical and radiological findings. Spiral computed tomography pulmonary angiogram showed 2 arteriovenous malformations with right-to-left shunts, a large one in the right lower lobe and a smaller one in the left lingula. After successful embolization, her hypoxemia was corrected and there were no embolic stroke episodes thereafter. (*Thorac Med* 2022; 37: 140-146)

Key words: pulmonary arteriovenous malformation, refractory hypoxemia, paradoxical embolism

Introduction

Pulmonary arteriovenous malformation (PAVM) is a rare clinical condition involving abnormal communication between pulmonary arteries and pulmonary veins without interposition of a capillary bed. The first reported PAVM in a living patient was in 1939. Asymptomatic hypoxemia is a common clinical presentation, with resting oxygen saturation of 80% to 96% [1]. A retrospective series found that only half

of patients with PAVMs presented because of dyspnea [2]. Dyspnea was more likely to be reported if the patient had coexisting cardiopulmonary disease, such as airflow obstruction and/or elevated pulmonary artery pressure [3]. Higher-grade contrast echocardiography shunts have been linked to an increased rate of cerebral complications [4]. Therefore, PAVMs are an important consideration in the differential diagnosis of recurrent stroke refractory to medical therapy. In this report, we describe a case of

¹Department of Internal Medicine, Chi Mei Hospital, Tainan City, Taiwan, ²Division of Chest Medicine, Chi Mei Hospital, Tainan City, Taiwan.

Address reprint requests to: Dr. Shian-Chin Ko, Division of Chest Medicine, Department of Internal Medicine, Chi Mei Hospital, No.901, Zhonghua Rd., Yongkang Dist., Tainan City 710, Taiwan (R.O.C.)

PAVM diagnosed in a 55-year-old woman with chronic obstructive pulmonary disease (COPD) and recurrent stroke.

Case Report

This 55-year-old woman presented at our emergency department with the chief complaint of progressive dyspnea for 1 day. She was an ever-smoker and had quit smoking 6 years before this presentation. Her past medical history was significant for hypertension, dyslipidemia and iron deficiency anemia. She had experienced 2 episodes of ischemic stroke, once when she was 35 and once when she was 46 years old. She underwent salpingo-oophorectomy because of a serous papillary cystic ovarian borderline tumor at 38 years of age. She denied fever, productive cough, chest pain, hemopty-

sis, epistaxis or a history of asthma. Chest X-ray revealed a lobulated soft tissue opacity in the anterobasal segment of the right lower lobe (Figure 1).

The patient's vital signs were afebrile, with a pulse rate of 58 beats/min regularly, respiratory rate of 30 breaths/min, blood pressure of 152/102 mm Hg, and pulse oximetry saturation of 83% to 90% on nearly 100% inspired oxygen via a non-rebreather mask. Her lips were cyanotic and she had clubbing fingers on both hands. She also had telangiectasia on her lips and tongue. Breathing sounds revealed bilateral diffuse expiratory wheezes on auscultation. Laboratory examinations showed hemoglobin of 12.8 g/dL and a normal coagulation panel. Her arterial blood gas (ABG) (under 100% oxygen through a non-rebreather mask) revealed a pH of 7.368, PaCO₂ of 49.9 mm Hg, PaO₂ of

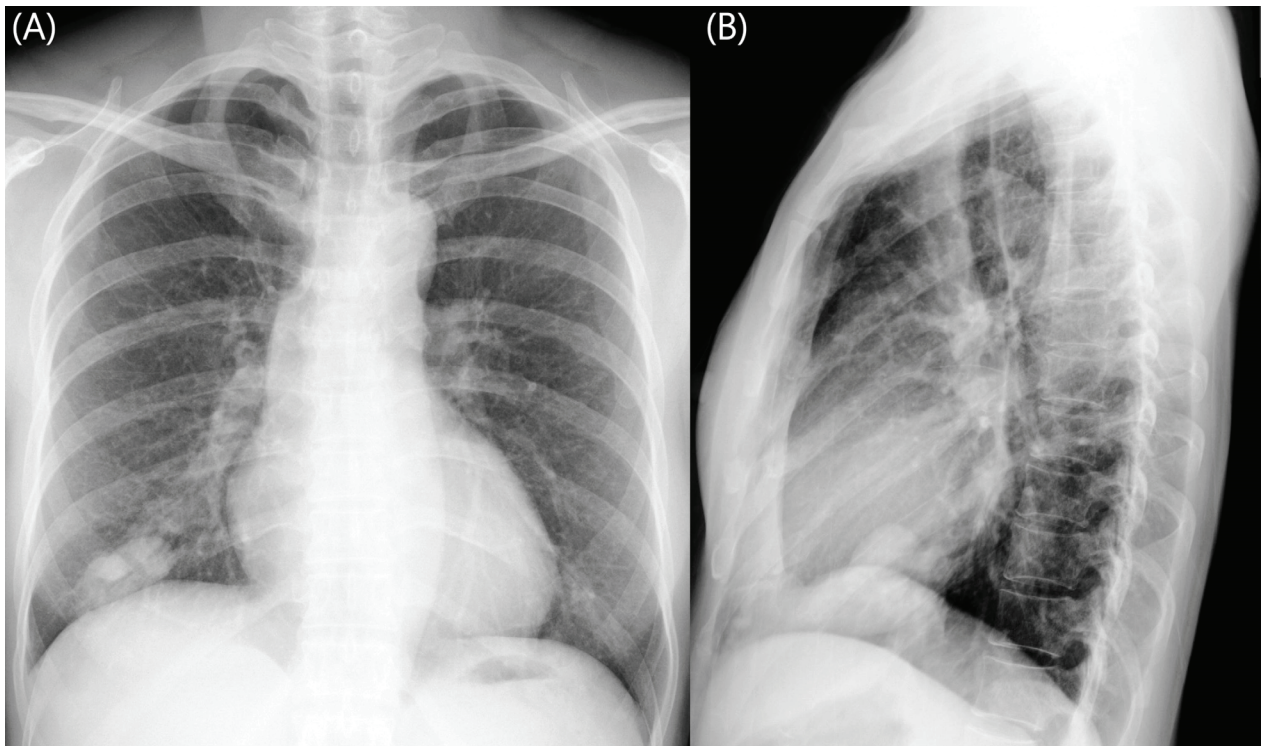


Fig. 1. Chest radiography. Posteroanterior (A) and lateral (B) views showed a lobulated soft tissue opacity in the anterobasal segment of the right lower lobe.

45.7 mm Hg, and O₂ saturation of 77%. She did not demonstrate platypnea or orthodeoxia. Pulmonary function tests from 6 years previous revealed mild restriction and moderate obstruction (FVC, FEV₁, and PEF of 56%, 54%, and 55% predicted, respectively). Carbon monoxide diffusion capacity was not done.

The initial impression was COPD, but the arterial oxygen levels were unusually low, even under oxygen supplementation. Chest computed tomography (CT) with contrast-enhancement revealed 2 entangled vascular lesions, a small one in the left lingular lobe and a large one in

the right lower lobe (4.4 cm in diameter), consistent with PAVMs (Figure 2). Neither mediastinal lymphadenopathy nor other pulmonary nodule was observed. The diagnosis of major pulmonary embolism or neoplasm was excluded on chest CT images. Subtle inhomogeneous myometrial tubular structures were also detected in the uterus, compatible with uterine AVM and suggestive of Osler-Weber-Rendu Disease.

Pulmonary angiography revealed a large AVM in the anterobasal segment of the right lower lobe with 2 arterial feeders from a single segmental artery, and a smaller AVM in the me-

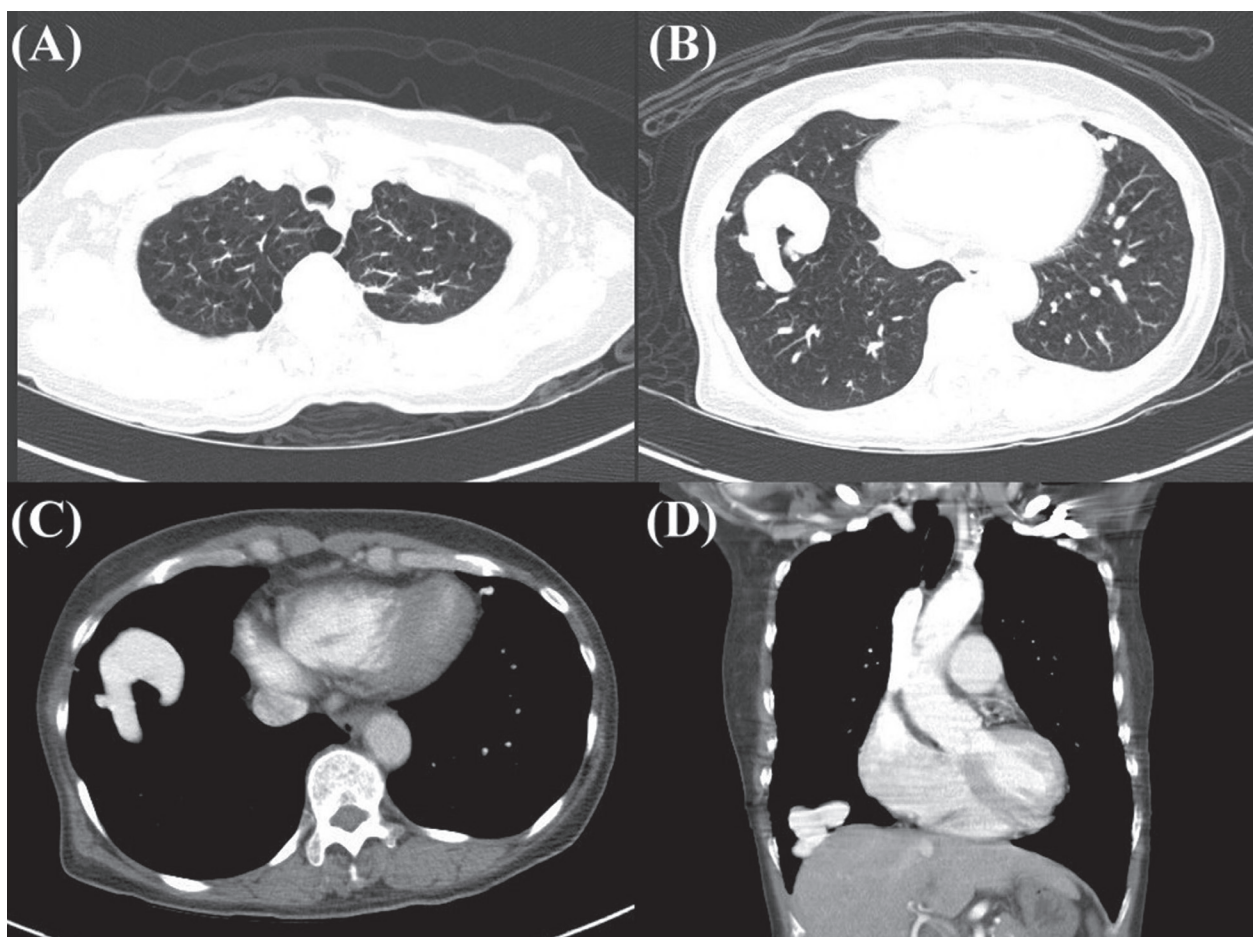


Fig. 2. Chest computed tomography scan. (A) Lung window showed emphysematous changes in the bilateral upper lobes and a fibrotic nodule at the left apex, up to 1.2 cm in size, suspected of being sequelae of a previous inflammatory process. (B) In the lung window, pulmonary arteriovenous malformations were found at the anterobasal segment of the right lower lobe and medial segment of the left lingular lobe. (C,D) Transverse and frontal views of the soft tissue window after contrast enhancement.

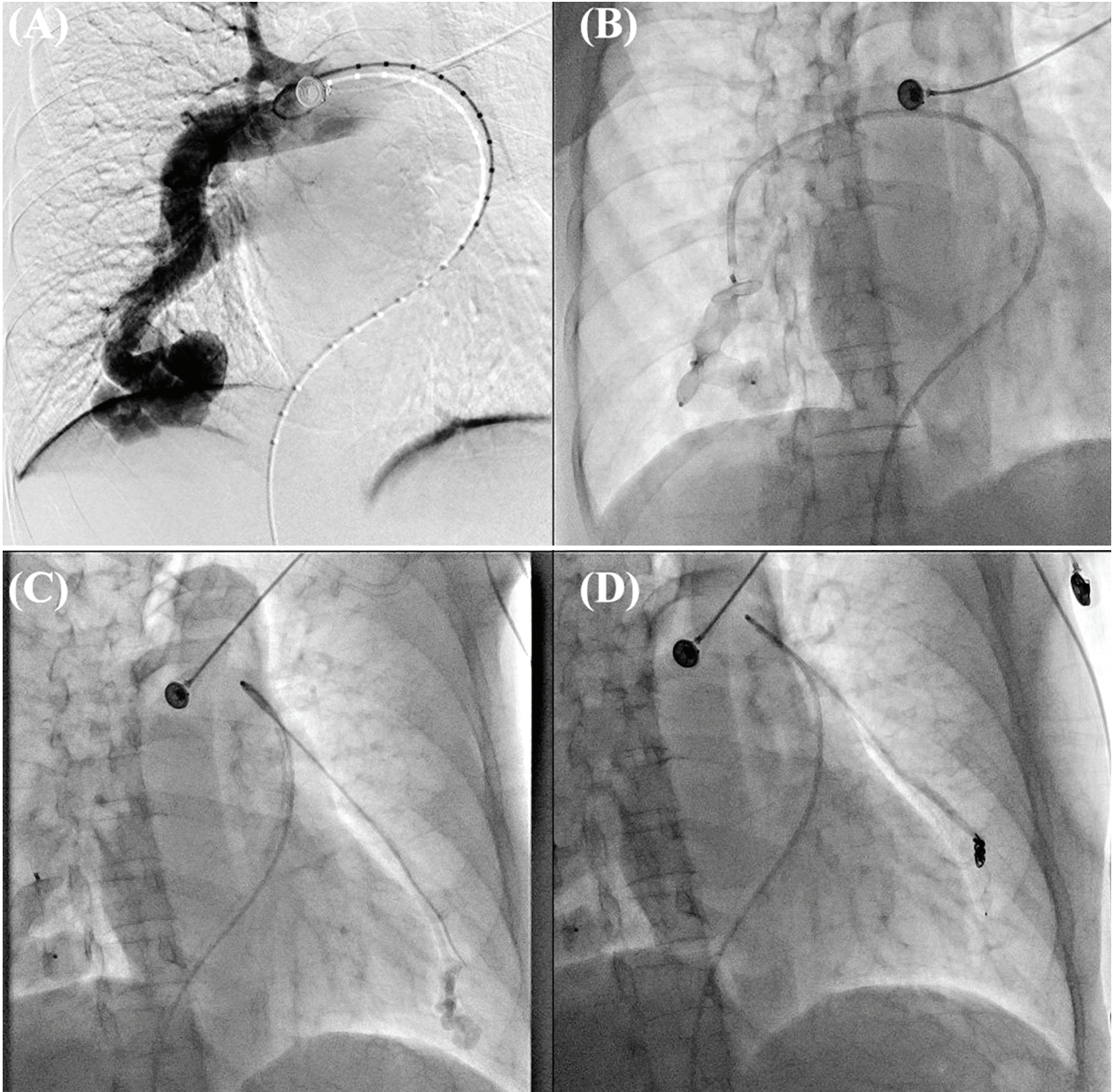


Fig. 3. Pulmonary angiography. (A) A large arteriovenous malformation (AVM) in the anterobasal segment of the right lower lobe with 2 arterial feeders from a single segmental artery was found. (B) Two Amplatzer® Vascular Plug II devices were deployed, respectively, in the large AVM. (C) A smaller AVM in the medial segment of the left lingular lobe with a single segmental arterial feeder was found on the left-side pulmonary angiography. (D) One Amplatzer® Vascular Plug IV followed by a pushable coil (MWCE-35-14-4-Nester®) was placed in the arterial feeder of the lingular AVM.

dial segment of the left lingular lobe with a single segmental arterial feeder. Two Amplatzer® Vascular Plug II devices (16×12 mm and 20×16 mm) were deployed, respectively, in the large

AVM, and 1 Amplatzer® Vascular Plug IV followed by a pushable coil (MWCE-35-14-4-Nester®) was placed in the arterial feeder of the lingular AVM (Figure 3).

Oxygen saturation improved significantly and promptly after successful vascular embolization. The patient had an uncomplicated course subsequently and was discharged home 2 days later. DNA testing for hereditary hemorrhagic telangiectasia (HHT) was not performed during this hospitalization. A follow-up chest radiograph 1 month later showed marked reduction of the lung lesion in the right lower lung field (Figure 4). There were no embolic events after discharge.

Discussion

Pulmonary arteriovenous malformations (PAVMs) are rare anomalies caused by abnormal direct connections between a pulmonary artery and a pulmonary vein. PAVMs provide an anatomic right-to-left shunt, allowing deoxygenated systemic venous blood to bypass the lungs and return to the body. Dyspnea is the most common symptom (34%), followed by hemoptysis (12%), but the majority of patients remain asymptomatic.

Most (50-90%) PAVMs are associated with HHT, also called Osler-Weber-Rendu syndrome [5]. HHT is an autosomal-dominant genetic disorder caused by mutations of endoglin at chromosome 9q34.1 and activin A receptor type II-like 1 (ACVRL1) at chromosome 12q31, known to produce HHT1 and HHT2, respectively. The genetic disorder leads to AVM and smaller telangiectatic vessels formation at multiple sites, including the skin, mucous membranes, lung, liver, and brain. Idiopathic PAVM is the second leading etiology of single PAVMs. More sporadic PAVMs are detected in the general population especially given the increasing use of CT scans in medical practice. In the present study, the lower lobes were the most com-



Fig. 4. Chest radiograph 1 month after transcatheter embolization showing multiple plugs and coils.

mon location of PAVMs [2].

Hypoxemia due to right-to-left shunting can be severe. It is of note that significantly hypoxemic patients were mildly symptomatic and had dyspnea on exertion only when a compensatory mechanism (such as polycythemia and/or an increase in cardiac work) began acting to preserve oxygen delivery to the tissues and avoid hypoxic end-organ dysfunction [6-7]. An increase in hemoglobin concentration was enough to maintain an unchanged arterial oxygen content (CaO_2) [6]. A compensatory increase in stroke volume is responsible for rise in the cardiac output during exercise among patients with PAVM [5]. An obvious increase in heart rate when standing could be observed, and this compensation is sufficient to balance the orthostatic fall in arterial oxygen saturation and content (SaO_2/CaO_2) [8].

Neurologic symptoms have been reported in up to 40% of patients [9]. Direct right-to-left shunting through pulmonary AVMs bypassing the pulmonary capillary bed may result in paradoxical emboli to the brain. Paradoxical emboli lead to strokes and brain abscesses. The risk of stroke from paradoxical emboli in patients with PAVM is higher in those with a larger shunt size [4].

Transcatheter embolization is a minimally invasive procedure, most commonly performed with high treatment success (83.3%-100% of cases) [10]. Higher-grade contrast echocardiography shunts can predict the size of PAVMs that are associated with detectable PAVMs on a thoracic CT angiogram, and may be a reliable indicator for the necessity of embolization. The risk of stroke is reduced after successful embolization. Surgical resection is reserved for cases of massive hemoptysis or hemothorax. The most recent comprehensive study recommended follow-up pulmonary CT scans 6-12 months after embolization to confirm successful occlusion and evaluate the existence of any residual or new PAVM, and then every 3-5 years thereafter [11].

Going back to our patient, her dyspnea and hypoxemia may have been associated with PAVM and COPD exacerbation. ABG measurements taken before the acute episode were consistent with marked hypoxemia and hyperventilation: pO_2 , 55.3 mmHg; pCO_2 , 30.3 mmHg, and SaO_2 , 90.4%. After applying high-flow oxygen via a non-rebreather mask, ABG revealed pH of 7.432, pCO_2 of 42.6 mmHg, pO_2 of 36.4 mmHg, and SaO_2 67% during exacerbation of COPD. ABGs in patients with mild-to-moderate COPD are near-normocapnic, with increased respiratory effort as compensation. As COPD progresses to a severe stage, the hy-

poxemia becomes more severe and hypercapnia may develop due to an increasing expiratory flow limitation and dynamic lung hyperinflation. In a study of stable severe COPD patients (FEV_1 $35\pm 12\%$ $PaCO_2$ 42 ± 5 mmHg) using nasal high-flow therapy, the average PaO_2 was 73 ± 13 mmHg [12]. Our patient's lower-than-expected PaO_2 in the emergency room was consistent with the clinical scenario of mixed COPD and PAVM. The physical finding of wheezing also indicated that her dyspnea was attributed not only to PAVM, but also to COPD. Her central cyanosis and hypoxemia refractory to supplemental oxygen administration were indicative of a right-to-left shunt. After correction of the hypoxemia by PAVM embolization, the cyanosis improved significantly.

In conclusion, recurrent stroke-like events, especially when the patient is undergoing proper medical treatment, raises the clinical suspicion of an alternative diagnosis. Therefore, it is imperative to investigate the lung mass, which would lead to early diagnosis. Embolization is mandatory for clinically significant PAVMs and may prevent severe complications. PAVMs grow over time, so regular follow-up appointments every 5 years, even after embolization, are a must to detect the growth of small PAVMs that may reach a size large enough to cause paradoxical embolization and stroke.

References

1. Howard LS, Santhirapala V, Murphy K, *et al.* Cardiopulmonary exercise testing demonstrates maintenance of exercise capacity in patients with hypoxemia and pulmonary arteriovenous malformations. *Chest* 2014; 136: 709-18.
2. Wong HH, Chan RP, Klatt R, *et al.* Idiopathic pulmonary arteriovenous malformations: clinical and imaging characteristics. *Eur Respir J* 2011; 38(2): 368-75.

3. Shovlin CL, Chamali B, Santhirapala V, *et al.* Ischaemic strokes in patients with pulmonary arteriovenous malformations and hereditary hemorrhagic telangiectasia: associations with iron deficiency and platelets. *PLoS One* 2014; 9: e88812.
4. Velthuis S, Buscarini E, van Gent MWF, *et al.* Grade of pulmonary right-to-left shunt on contrast echocardiography and cerebral complications: a striking association. *Chest* 2013; 144: 542-8.
5. Shovlin CL, Guttmacher AE, Buscarini E, *et al.* Diagnostic criteria for hereditary hemorrhagic telangiectasia (Rendu-Osler-Weber syndrome). *Am J Med* 2000; 91: 66-7.
6. Santhirapala V, Williams LC, Tighe HC, *et al.* Arterial oxygen content is precisely maintained by graded erythrocytotic responses in settings of high/normal serum iron levels, and predicts exercise capacity: an observational study of hypoxaemic patients with pulmonary arteriovenous malformations. *PLoS One* 2014; 9(3): e90777.
7. Grocott MP, Martin DS, Levett DZ, *et al.* Arterial blood gases and oxygen content in climbers on Mount Everest. *N Engl J Med* 2009; 360(2): 140-9.
8. Santhirapala V, Chamali B, McKernan H, *et al.* Orthodeoxia and postural orthostatic tachycardia in patients with pulmonary arteriovenous malformations: a prospective 8-year series. *Thorax* 2014; 69: 1046-7.
9. Lacombe P, Lagrange C, Beauchet A, *et al.* Diffuse pulmonary arteriovenous malformations in hereditary hemorrhagic telangiectasia: long-term results of embolization according to the extent of lung involvement. *Chest* 2009; 135: 1031-7.
10. Adachi A, Ohta K, Jahangiri Y, *et al.* Treatment of pulmonary arteriovenous malformations: clinical experience using different embolization strategies. *Jpn J Radiol* 2020 Apr; 38(4):382-386.
11. Majumdar S, McWilliams JP. Approach to pulmonary arteriovenous malformations: a comprehensive update. *J Clin Med* 2020 Jun 19;9(6): 1927.
12. Cirio S, Piran M, Vitacca M, *et al.* Effects of heated and humidified high-flow gases during high-intensity constant-load exercise on severe COPD patients with ventilatory limitation. *Respir Med* 2016 Sep; 118: 128-32.

Bilateral *Cunninghamella Bertholletiae* Empyema and Pneumothorax: A Case Report and Literature Review

Wei-Cheng Hong¹, Chien-Wei Hsu^{1,2}, David-Lin Lee^{1,2}

Pulmonary mucormycosis is a rare fungal infection that is difficult to diagnose and causes high mortality in immunocompromised patients. *Cunninghamella bertholletiae* accounts for only 7% of mucormycosis infections. Due to its angioinvasive characteristic and the narrow spectrum of antifungal therapy, *Cunninghamella* species infection has a poor prognosis and a high mortality rate. Pulmonary infection is a common outcome of *C. bertholletiae*. *C. bertholletiae* results in high mortality, and most surviving patients undergo early anti-fungal therapy with amphotericin B or liposomal amphotericin B along with aggressive surgical intervention. Thus, early recognition is essential and aggressive surgery should be considered for these patients. (*Thorac Med* 2022; 37: 147-153)

Key words: *Cunninghamella bertholletiae*, empyema, pulmonary mucormycosis

Introduction

Pulmonary mucormycosis infection most often occurs in immunocompromised patients, especially in those with hematological disorders and transplant recipients [1].

Cunninghamella species, an unusual mucormycosis, are a saprobic fungus commonly found in the soil of temperate climates [2]. The predominant mode of acquisition of *C. bertholletiae* infection is presumed to be via the respiratory tract [3]. Pulmonary infection was

reported in 30.2% of proven *C. bertholletiae* infections [3].

Management of mucormycosis infection depends on recognizing disease patterns and on early diagnosis [4]. An early complete surgical treatment for mucormycosis is recommended whenever possible, in addition to systemic anti-fungal treatment [5]. Herein, we reported a rare case of mucormycosis empyema with pneumothorax caused by *C. bertholletiae* that was diagnosed postmortem.

¹Division of Pulmonary Medicine, Kaohsiung Veterans General Hospital, ²School of Medicine, National Yang-Ming University, Taipei, Taiwan.

Address reprint requests to: Dr. Chien-Wei Hsu, Division of Pulmonary Medicine, Kaohsiung Veterans General Hospital, No. 386, Dazhong 1st Rd., Zuoying Dist., Kaohsiung City 813, Taiwan (R.O.C.)

Case Description

A 73-year-old healthy Taiwanese non-smoker was admitted in February, 2018 with the initial presentation of hemoptysis for a month and progressive shortness of breath for a day. Chest CT (Figure .1) showed mixed consolidation and ground-glass infiltration in both lung fields. In addition to antimicrobials, high- dose steroids were given for suspected interstitial pneumonia. The patient was discharged on day 14.

However, fever and a progressive cough with hemoptysis occurred on the day the patient was discharged. A rapid influenza test was positive for influenza B. The patient was readmitted again, and Tamiflu was administered for influenza B. Chest radiography showed progressive bilateral infiltration (Figure .2), despite the broad-spectrum antibiotics. Hypoxic respiratory failure, septic shock, and multi-organ failure occurred on day 16. The patient then was intubated with mechanical ventilator support. Chest radiography showed bilateral pleural effusion.

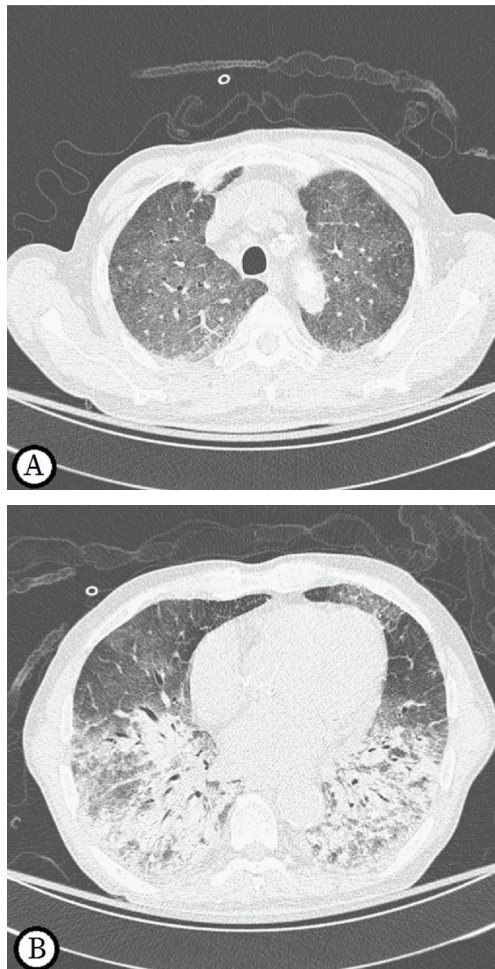


Fig. 1. Chest CT showed mixed (A) ground-glass opacity and (B) consolidation infiltration in both lung fields.

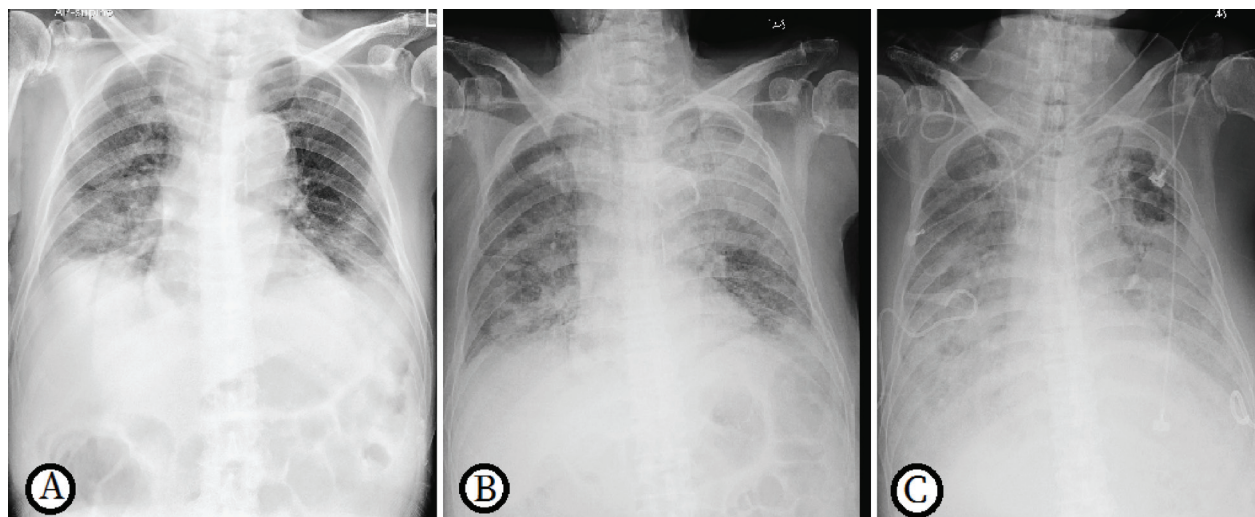


Fig. 2. Serial follow- up CXR during admission, (A) Day 5, (B) Day 12, (C) Day 19, showed progressive bilateral infiltration and CP angle blunting, indicating pleural effusion.

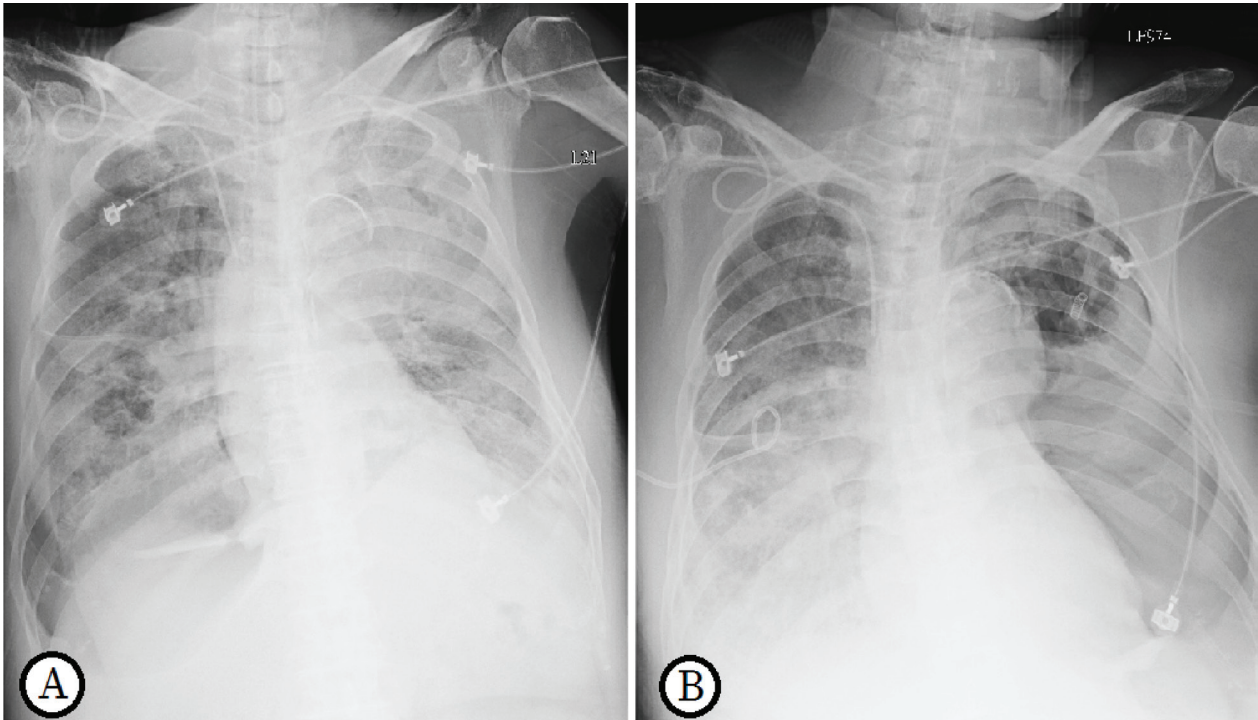


Fig. 3. (A) Right pneumothorax, (B) left pneumothorax.

fusion and spontaneous pneumothorax (Figure .3). Pigtailed drainage was performed for the bilateral pleural effusion, revealing exudative effusion. The pneumothorax improved soon after pigtailed drainage. The patient died on day 20 post- admission, and the pleural effusion culture revealed *C. bertholletiae* 2 days postmortem.

Discussion

Pulmonary mucormycosis infection is an uncommon pathogen that results in high mortality in immunocompromised patients, especially in those with hematological disorders and in transplant recipients [1]. Hematological malignancy was a major risk factor (32–40%) in pulmonary mucormycosis, followed by diabetes mellitus (32–56%), hematopoietic stem cell transplant (1–9.8%), solid organ transplant

(6.5–9%), and renal disease (13–18%) [1].

In a global review of more than 900 reported cases of mucormycosis, *Rhizopus* species (47%) were the most common cause of culture-confirmed mucormycosis, followed by *Mucor* species (18%), *C. bertholletiae* (7%), *Apophysomyces elegans* (5%), *Lichtheimia* (*Absidia*) species (5%), *Saksenaia* species (5%), and *Rhizomucor pusillus* (4%) [6]. However, *Cunninghamella* species had angioinvasion and a narrow spectrum of antifungal therapy, which contributed to a poor outcome and high mortality [7]. Mucormycosis caused by *Cunninghamella*, following a fulminant course, had an overall mortality rate approaching 80% [8].

The diagnosis of pulmonary mucormycosis is challenging. Clinical manifestations of pulmonary mucormycosis are nonspecific. Common symptoms include fever, cough, sputum

production, hemoptysis, shortness of breath, chest pain, and weakness [9]. In radiological exams, multiple (≥ 10) nodules and pleural effusion were reportedly more common in mucormycosis [10]. In additional finding of the computerized tomography (CT) scans was the reverse halo sign (RHS), which seemed to indicate the presence of mucormycosis [10]. Microscopy (direct and histopathology) and cultures of the various clinical specimens are the cornerstones of a correctly diagnosis of mucormycosis. Molecular assays (conventional polymerase chain reaction [PCR], restriction fragment length polymorphism analyses [RFLP], 53, 54 DNA sequencing of defined gene regions, 55, 56, and melt curve analysis of PCR products) can be used either for detection or identification of mucormycetes and can be recommended as valuable add-on tools to complement conventional diagnostic procedures [10].

Polyene-based antifungal agents, such as amphotericin B or liposomal amphotericin B, are more active drugs for managing *C. bertholletiae* [11]. Posaconazole is a second-generation triazole that is highly lipophilic, is orally absorbed, and is extensively distributed in tissues. Garbino reported the successful treatment case of a pediatric patient with graft versus host disease (GVHD) and pulmonary infection caused by *C. bertholletiae* in whom therapy with surgery and liposomal amphotericin B was followed by treatment with posaconazole [12].

In a search for previous reports of *C. bertholletiae* infection, we found in a total of 20 cases from 1959 to 2019 (Table 1) [2, 12-27]. Only 2 (10%) (2 patients) of the patients were immunocompetent [21, 23]. Among these patients, 18 had pulmonary involvement infection and only 6 survived [12, 13, 17, 19, 20, 24].

Pulmonary involvement was the most common result of *C. bertholletiae* infection, at 90% (18/20), which was higher than that in a previous study [3]. The mortality rate was very high, at 67% (12/18), for pulmonary *C. bertholletiae* infection. Of those that survived, 2 patients did not undergo operation [17, 20]. Koyama *et al.* reported the successful non-surgical treatment of a case of pulmonary *C. bertholletiae* infection, complicated with bilateral pneumothorax and empyema, without surgical intervention [17]. Chest tube drainage may have contributed to debridement of the lesion [17]. In 2 successful non-surgical successful cases, the glucocorticoid dose was tapered to reduce suppression of the host defense against fungi in 1 patient [17], and granulocyte and granulocyte-macrophage colony-stimulating factors were used to aid recovery from neutropenia in another patient [20]. These cases suggest that both the rapid reversal of immunosuppression and the initiation of amphotericin B therapy may eradicate pulmonary *C. bertholletiae* infection, even if surgical intervention is not contraindicated [17]. However, further studies are needed to confirm this.

We presented a rare case of *C. bertholletiae* empyema with pneumothorax in a previously healthy patient who had been prescribed with high-dose steroids and who had post-influenza infection. The patient died of respiratory failure and multiple organ failure. The postmortem pleural effusion culture revealed *C. bertholletiae* infection, and effective anti-fungal agents had not been used. Therefore, we need to be aware that not only that hematologic disease and immunocompromise may lead to invasive fungal infections, but that prolonged high-dose steroids may also be risk factors. Chest CT and microbiology examinations are key in diagnosing pulmonary mucormycosis. In previ-

Table 1. Reported Cases of *Cunninghamella Bertholletiae* Infection

Studies	Organ involvement	Organ involvement	Survival status	Surgical lung intervention of lung
Rickerts V, <i>et al.</i> (2000)	ALL	Lung	Died	N
	ALL	Lung	Died	N
	Renal transplant	Lung	Died	N
	Lymphoma	Lung	Survived	Y
Garey KW, <i>et al.</i> (2001)	Allogeneic BMT	Lung	Died	Y
Zhang R, <i>et al.</i> (2002)	Kidney transplant	Lung	Died	N
Kobayashi M, <i>et al.</i> (2004)	ALL	Lung	Died	N
Bibashi E, <i>et al.</i> (2008)	ALL	Lung	Died	N
Koyama N, <i>et al.</i> (2008)	Scleroderma, MPA	Lung	Survived	N
Garbino J, <i>et al.</i> (2010)	AML s/p allogenic BMT, with GvHD	Lung	Survived	Y
Hsieh TT, <i>et al.</i> (2013)	AML	Lung	Died	N
Malkan AD, <i>et al.</i> (2014)	ALL	Lung	Survived	Y
Tadepalli K, <i>et al.</i> (2015)	Immunocompetent	Onychomycosis	Survived	N (toe)
Su YY, <i>et al.</i> (2016)	ALL	Lung	Died	Y
Hirano T, <i>et al.</i> (2017)	ACOS, ruptured abdominal aortic aneurysm, steroid	Lung	Died	N
Ota H, <i>et al.</i> (2017)	Cord bBlood tTransplant	Lung	Survived	Y
Bellanger AP, <i>et al.</i> (2018)	CLL	Lung	Died	N
Margoles L, <i>et al.</i> (2018)	Heart transplant recipient	Disseminated + Lung	Died	N
Liu YC, <i>et al.</i> (2019)	AML	Rhinosinusitis	Survived	N (Sinus endoscopic surgery)

ALL: acute lymphoblastic leukemia, BMT: bone marrow transplantation, AML: acute myeloblastic leukemia, MPA: microscopic polyangiitis, GvHD: graft versus host disease, ACOS: asthma COPD overlap syndrome, CLL: chronic lymphocytic leukemia.

ous research and case reports, *C. bertholletiae* resulted in high mortality, and most surviving patients underwent early anti-fungal therapy with either amphotericin B or liposomal amphotericin B, along with aggressive surgical intervention [19]. We should have been more alert and performed a second chest CT, sampled to detect *C. bertholletiae* infection early, administered amphotericin B immediately, performed video-assisted thoracoscopic surgical decortications, and performed chest tube drainage for empyema or even lobectomy if evidence of pulmonary parenchyma involvement was present.

References

- Prakash H, Chakrabarti A. Global epidemiology of mucormycosis. *J Fungi (Basel)* 2019; 5(1): 26.
- Bibashi E, Sidi V, Kotsiou M, *et al.* Pulmonary zygomycosis caused by *Cunninghamella bertholletiae* in a child with acute lymphoblastic leukemia. *Hippokratia* 2008; 12(1): 43-5.
- Gomes MZR, Lewis RE, Kontoyiannis DP. Mucormycosis caused by unusual mucormycetes, non-*Rhizopus*, -*Mucor*, and -*Lichtheimia* species. *Clin Microbiol Rev* 2011; 24(2): 411-445.
- Cornely OA, Alastruey-Izquierdo A, Arenz D, *et al.* Global guideline for the diagnosis and management of mucormycosis: an initiative of the European Confederation of Medical Mycology in cooperation with the Mycoses Study Group Education and Research Consortium. *Lancet Infect Dis* 2019; 19(12): e405-e421.
- Pilmis B, Alanio A, Lortholary O, *et al.* Recent advances in the understanding and management of mucormycosis. *F1000Res* 2018; 7: F1000 Faculty Rev-1429.
- Bennett JE, Dolin R, Blaser MJ. Mandell, Douglas, and Bennett's Principles and Practice of Infectious Diseases. Philadelphia, PA: Elsevier/Saunders, 2015; p.2909.
- Roden MM, Zaoutis TE, Buchanan WL, *et al.* Epidemiology and outcome of zygomycosis: a review of 929 reported cases. *Clinical Infectious Diseases* 2005; 41(5): 634-53.
- Ribes JA, Vanover-Sams CL, Baker DJ. Zygomycetes in human disease. *Clinical Microbiology Rev* 2000; 13(2): 236-301.
- Peng M, Meng H, Sun Y, *et al.* Clinical features of pulmonary mucormycosis in patients with different immune status. *J Thorac Dis* 2019; 11(12): 5042-5052.
- Skiada A, Lass-Floerl C, Klimko N, *et al.* Challenges in the diagnosis and treatment of mucormycosis. *Med Mycol* 2018; 56(suppl_1): 93-101.
- Simitsopoulou M, Georgiadou E, Walsh TJ, *et al.* *Cunninghamella bertholletiae* exhibits increased resistance to human neutrophils with or without antifungal agents as compared to *Rhizopus* spp. *Med Mycol* 2010; 48(5): 720-4.
- Garbino J, Myers C, Ambrosioni J, *et al.* Report of a successful treatment of pulmonary *Cunninghamella bertholletiae* infection with liposomal amphotericin and posaconazole in a child with GVHD and review of the literature. *J Pediatr Hematol Oncol* 2010; 32(2): 85-7.
- Rickerts V, Böhme A, Viertel A, *et al.* Cluster of pulmonary infections caused by *Cunninghamella bertholletiae* in immunocompromised patients. *Clinical Infectious Diseases* 2000; 31(4): 910-13.
- Garey KW, Pendland SL, Huynh VT, *et al.* *Cunninghamella bertholletiae* infection in a bone marrow transplant patient: amphotericin lung penetration, MIC determinations, and review of the literature. *Pharmacotherapy* 2001; 21(7): 855-60.
- Zhang R, Zhang JW, Szerlip HM. Endocarditis and hemorrhagic stroke caused by *Cunninghamella bertholletiae* infection after kidney transplantation. *Am J Kidney Dis* 2002; 40(4): 842-6.
- Kobayashi M, Togitani K, Machida H, *et al.* Molecular polymerase chain reaction diagnosis of pulmonary mucormycosis caused by *Cunninghamella bertholletiae*. *Respirology* 2004; 9(3): 397-401.
- Koyama N, Nagata M, Hagiwara K, *et al.* Survival of a patient with pulmonary *Cunninghamella bertholletiae* infection without surgical intervention. *Respirology* 2008; 13(2): 309-11.
- Hsieh TT, Tseng HK, Sun PL, *et al.* Disseminated zygomycosis caused by *Cunninghamella bertholletiae* in patient with hematological malignancy and review of published case reports. *Mycopathologia* 2013; 175(1-2): 99-106.
- Malkan AD, Wahid FN, Rao BN, *et al.* Aggressive

- Cunninghamella pneumonia in an adolescent. *J Pediatr Hematol Oncol* 2014; 36(7): 581-2.
20. Navanukroh O, Jitmuang A, Chayakulkeeree M, *et al.* Disseminated *Cunninghamella bertholletiae* infection with spinal epidural abscess in a kidney transplant patient: case report and literature review. *Transpl Infect Dis* 2014; 16(4): 658-65.
 21. Tadepalli K, Gupta PK, Asati DP, *et al.* Onychomycosis due to *Cunninghamella bertholletiae* in an immunocompetent male from central India. *Case Reports in Infectious Diseases* 2015.
 22. Su YY, Chang TY, Wang CJ, *et al.* Disseminated *Cunninghamella bertholletiae* infection during induction chemotherapy in a girl with high-risk acute lymphoblastic leukemia. *Pediatr Neonatol* 2016; 57(6): 531-534.
 23. Hirano T, Yamada M, Sato K, *et al.* Invasive pulmonary mucormycosis: rare presentation with pulmonary eosinophilia. *BMC Pulm Med* 2017; 17: 76.
 24. Ota H, Yamamoto H, Kimura M, *et al.* Successful treatment of pulmonary mucormycosis caused by *Cunninghamella bertholletiae* with high-dose liposomal amphotericin B (10 mg/kg/day) followed by a lobectomy in cord blood transplant recipients. *Mycopathologia* 2017; 182(9-10): 847-853.
 25. Bellanger AP, Berceanu A, Rocchi S, *et al.* Development of a quantitative PCR detecting *Cunninghamella bertholletiae* to help in diagnosing this rare and aggressive mucormycosis. *Bone Marrow Transplant* 2018; 53: 1180-1183.
 26. Margoles L, DeNofrio D, Patel AR, *et al.* Disseminated mucormycosis masquerading as rejection early after orthotopic heart transplantation. *Transpl Infect Dis* 2018; 20(1): 10.1111.
 27. Liu YC, Zhou ML, Cheng KJ, *et al.* Successful treatment of invasive fungal rhinosinusitis caused by *Cunninghamella*: a case report and review of the literature. *World J Clin Cases* 2019; 7(2): 228-235.